

**ANALYSIS OF AXIAL AND LATERAL DRILLED SHAFT SOCKET LOAD
TESTS AND AXIAL PILE LOAD TESTS FOR FOUNDATION FOR T-36
BRIDGE OVER THE ST. CROIX RIVER, STILLWATER, MINNESOTA**

a report to the

**Minnesota Department of Transportation
St. Paul, Minnesota**

by

Michael W. O'Neill, Ph. D and
Reniere E. Majano, Ph. D.

December, 1995

Michael W. O'Neill, Consulting Engineer
2922 Kevin Lane
Houston, Texas 77043

Table of Contents

	Page
Authorization	1
Purpose and Scope	1
General Qualifications	2
Construction of Drilled Shaft Test Sockets	2
Drilled Shaft Test Elements	5
Axial Drilled Shaft Socket Test Results and Scaling to Conditions in St. Croix River	8
General	8
Load Test Results	8
Scaling of Side Resistance to Axial Loading ("Skin Friction") for Franconia Sandstone	10
ROCKET Analysis	11
FHWA Method Analysis	13
Scaling to Prototype Conditions Using ROCKET	14
Scaling of End-Bearing Resistance to Axial Loading for Franconia Sandstone	17
Qualifications for Axial Loading	18
Lateral Split Cylinder Socket Test Results	19
Development and Scaling of p-y Curves for Franconia Sandstone	20
Model of Loading	21
Depth and Diameter of Socket	22
Scaling of p_u	23
Scaling of E_s	24
Qualifications for Lateral Loading	25
Pile Load Test in St. Croix River	26
Load Test Results	26
Analysis for Buckling	28
Summary	30
References	34
Figures and Tables	Following p. 35
Appendix	Following Figures and Tables

**ANALYSIS OF AXIAL AND LATERAL DRILLED SHAFT SOCKET LOAD
TESTS AND AXIAL PILE LOAD TESTS FOR FOUNDATION FOR T-36
BRIDGE OVER THE ST. CROIX RIVER, STILLWATER, MINNESOTA**

by

**Michael W. O'Neill
Reniere E. Majano**

AUTHORIZATION

The engineering study documented in this report is one task authorized in Mn/DOT Agreement No. 73415, Design Assistance, S. P. 8217-12 (T. H. 36), Stillwater Bridge, dated July 5, 1995.

PURPOSE AND SCOPE

The purpose of this report is to document and interpret the installation and load testing of two drilled shaft test sockets and one driven pipe pile, respectively located along the bank and within the St. Croix River. The drilled shaft test sockets and the driven pile were installed and tested by a constructor under contract to the Minnesota DOT. The authors of this report are acting as consultants to the Minnesota DOT to help develop construction specifications for the test elements and to assist in interpreting the constructor's test results.

The test sockets and were constructed for the purpose of determining unit side shear resistance and unit lateral resistance in a formation of friable sandstone for purposes of developing design parameters for compression and lateral loading of drilled shafts within the same formation within the St. Croix River. The apparent frictional nature of the friable sandstone and the difference in geomaterial confining pressures at the test site and within the river made it necessary to scale the results of the drilled shaft socket tests to confinement conditions within the river for prototype drilled shafts. The scaling procedures are documented in this report. It was not within the scope of this study to determine whether the rock at the test site was representative of the potential founding stratum for drilled shafts in the St. Croix River. In order to apply these results presented in this report, such a determination should be made by Minnesota DOT personnel.

The test pile was driven and tested to determine factors for the analysis of buckling of prototype piles having the same properties and water and geomaterial layer penetrations as the test pile and to determine the pullout resistance of the test pile.

Although the authors were present for the construction and load testing of the drilled shaft sockets and for the load testing of the driven pile in compression, all

construction and test data for both the pile and the drilled shaft sockets were obtained by others.

GENERAL QUALIFICATIONS

The general qualifications of the results reported here are explicitly listed below.

1. All data used in the analyses reported here were obtained from others. The assumption was made that all such data were true and correct; however, the authors make no representation that any data are valid. Where no data existed, assumptions were made about values of parameters necessary to perform the analyses. The authors also make no representation that such assumptions are correct.
2. Any application of the test results, scaled or unscaled, to design conditions for drilled shafts sockets depends upon the properties (density, internal friction and cohesion) of the friable sandstone being equivalent at the site of the prototype drilled shaft socket and at the test site. The authors make no representation that such is the case anywhere on the bridge site.
3. Furthermore, since no load tests were conducted in other than friable sandstone in the Franconia formation, no representation is made that any application of the test results, scaled or unscaled, to design of drilled shaft sockets in non-friable sandstone (e. g., glauconitic sandstone, which is reported in boring logs for the project to interbed with the friable sandstone in the St. Croix River) is valid.
4. This document contains information on subsurface soil and rock profiles. In some cases such information is presented in an idealized form for the purpose of analyzing load transfer and buckling. The information on subsurface profiles is therefore not appropriate for construction purposes and should not be used by any potential contractor to assess construction procedures or costs.

CONSTRUCTION OF DRILLED SHAFT TEST SOCKETS

The test sockets were constructed by the constructor for the project, Case Foundation Company, Inc., of Roselle, Illinois, using a crane-mounted drilling rig. Excavation for the test sockets began on October 16, 1995, at the locations shown in Figs. 1 and 2. The location of the test pile, described later, is shown in Fig. 3. Profiles of the test elements, including the depths of the test sockets, and the general soil and rock conditions at the drilled shaft and pile test sites and at two locations in the river is shown in Fig. 4. General information on rock recovery from cores is given in Table A-1 in the Appendix.

One borehole nominally 60 inches in diameter was excavated for both an axial and a lateral test socket to a depth of approximately 47 feet, after which a surface steel casing 60 inches in outside diameter was set in place in each borehole. Excavation then

proceeded below the bottoms of the casings in sequence on each of the two boreholes, which had 48-inch nominal diameters. While the boreholes were reported to be stable during drilling, water intruded below the casings, so that all excavation, including the excavation of the test sockets, was made under water. The water level rose to approximately one foot below the ground surface during excavation. The test sockets themselves were not excavated until October 25. An undersized rock core barrel was used to excavate a pilot hole for each socket, and each socket was then enlarged to a 48-inch nominal diameter using a rock auger.

On October 26, each of the test sockets, up to the bottoms of the surface casings, was calipered by Western-Atlas, Inc., using a four-arm electronic caliper with a resolution of approximately 1/4 on average diameter. The results of this caliper logging process are shown on Figs. 5 and 7. In those figures, the depth below the top of the casing (about three feet above ground surface) is shown in feet on the vertical axis, and the diameter in excess of 44 inches is shown on the horizontal axis. The two relations shown in each figure are average diameters in two orthogonal directions versus depth. Each grid line in the horizontal direction is one inch. Neither socket was very rough, although the axial socket was tapered slightly outward from bottom to top, and the lateral socket was virtually cylindrical.

The original schedule for construction called for the sockets to be concreted on October 26, but instrument placement and concreting were delayed. During the day on October 26 and during the following night several feet of sediment accumulated in each of the sockets. The primary source of this sediment appeared to be high up the borehole. In the range of 30 to 40 feet below the bottom of the casing the axial borehole is very ragged, at some locations more than six inches larger in diameter than intended, suggesting that this is the zone from which most of the sediment sloughed. In the axial borehole, about seven feet of loose sediment was measured on the morning of October 27, after the borehole had been cleaned on October 26. Less enlargement in the borehole below the casing is observed in the lateral test borehole, and less sediment (about three feet of loose material) accumulated in the socket in this borehole between October 26 and October 27. On the morning of October 27, both sockets were cleaned again using a cleanout bucket and recaliper to a larger vertical scale. The second set of caliper logs is shown in Figs. 6 and 8, respectively. Note that the vertical scale for Figs. 6 and 8 is larger than that for Figs. 5 and 7. Comparing Figs. 5 and 6, there is no evidence of any significant geometry change in the axial test socket between October 26 and October 27 (i. e., no sloughing within the test socket). Similarly, comparing Figs. 7 and 8, there is no evidence of geometry changes (sloughing) in the lateral test socket between October 26 and October 27. Shaft diameters in the axial test socket varied from about 47.5 to about 49.5 inches, generally becoming larger at higher elevations within the sockets. The shaft diameter in the lateral test socket was 48.0 to 48.75 inches. The planned diameters in both cases were 48.0 inches. The diameter resolution on the caliper was about 0.25 inches.

After the second caliper of the boreholes on October 27, samples of the borehole drilling water were recovered from the bottoms of both boreholes by GME, Inc., personnel and subjected to standard field specific gravity, viscosity and sand content tests. Note that no drilling slurry was used. The results of the tests were reported to be as follows.

Property	Axial Test Socket	Lateral Test Socket
Specific gravity	1.01	1.02
Marsh funnel viscosity	27.0 sec/quart	27.5 sec/quart
API sand content	<0.25 %	< 0.25 %

Plans were modified to install the test sockets on October 27, immediately after the second round of caliper. Once the unit consisting of the instrumented cages for the test and reaction sockets, the Osterberg Cell and the carrier frame for the lead wire and hydraulic hoses was set in the axial test borehole (most easterly location in Fig. 2), the contractor attempted to lower the tremie line alongside the carrier frame and through a slot in the loading plates to the bottom of the borehole. After many hours of attempting to get the tremie past the top loading plate, the contractor abandoned the attempt to concrete either socket on October 27. The carrier frame, Osterberg Cell and cages were removed from the axial test socket. [Details of the axial test socket loading and instrumentation system are described in the following section.]

During the next several days, both test sockets remained open with the surface casings in place as the contractor resolved the problem of concrete placement. The sockets and boreholes remained full of water to within about one foot of the ground surface during this time. Several feet of debris had accumulated by November 3 on the borehole bases while the holes had remained open. On November 3, 1995, the contractor cleaned the base of the axial test socket with a cleanout bucket. No overreaming or other means were used to clean or scarify the sides of the socket. The contractor then lowered the carrier frame, Osterberg Cell and cages as a unit. However, this time the tremie (four-inch steel pipe) was affixed to the side of the carrier frame before lowering. A pig was inserted in the tremie to separate concrete from water, and the concrete was pumped into the bottom of the reaction socket through the tremie, presumably displacing the water in the borehole and flowing up to the top of the test socket. [There is evidence that some sediment may have been trapped at the bottom of the borehole at the time of concreting. This point will be discussed when the test results are analyzed.] At that point pumping was stopped, and the flow of concrete stopped. However, the contractor then extracted the tremie, allowing about two feet of concrete to fall out of the tremie onto the top of the test socket. This extra concrete is considered part of the test socket for purposes of analysis.

Immediately after concreting the axial test socket, on November 3, 1995, the lateral test socket was cleaned in a manner identical to that for the axial test socket except that after cleanout the bottom of the cleanout bucket was coated with a heavy layer of grease. The bucket was then lowered to the bottom of the borehole and turned a quarter turn with the crowd of the kelly bar to grease the bottom of the borehole and thus destroy bond between the concrete in the socket and the bottom of the borehole. The Osterberg Cell and loading plates were lowered to the bottom of the borehole and the socket was concreted by using the four-inch tremie. Again, as the tremie was removed, about two feet of excess concrete fell out of the tremie onto the top of the test socket. [Details of the axial test socket loading and instrumentation system are described in the following section.]

The concrete had a maximum coarse aggregate size of 3/4 inch. Slump tests taken during placement of the concrete in the test sockets indicated slump values between 8.5 and 9.0 inches. The time required to place the concrete in each socket was less than one hour. Details of concrete strength tests are shown in Table 1 and Fig. 9.

For economic reasons, the boreholes were not recalipered on November 3 prior to placement of the concrete. Since no measurable changes in geometry of the test sockets occurred between October 26 and October 27, it is assumed that the caliper logs in Figs. 5 - 8 are representative of the socket geometry at the time of concrete placement on November 3.

The axial test shaft socket was load-tested on November 7 and 8, 1995, and the lateral split cylinder socket was load-tested on November 8, 1995. Details of the load tests themselves are contained in a report from Loadtest, Inc., to the Minnesota DOT (Loadtest, 1995).

The following section describes the test elements and a few pertinent testing details.

DRILLED SHAFT TEST ELEMENTS

Schematic views of the axial and lateral test sockets are shown in Figs. 10 - 14. Load was applied in both axial and lateral socket tests every five minutes in increments of approximately 50 tons (US). [Note, where the unit "ton" is mentioned in this report, it will always be understood to be U. S. tons, not metric tons.] The load was applied in each test socket by means of 3000-ton-capacity Osterberg Cells, provided by Loadtest, Inc., situated horizontally atop a reaction socket in the axial load test and vertically between the two halves of the cylindrical shaft in the lateral load test.

Strain gages, which were provided, installed and read by Loadtest, Inc., were affixed to the rebar cages for the axial test, as shown in Figs. 10 and 11. These gages were Geokon Model 4911 vibrating wire strain meters coupled to 48-inch long segments of No. 4 deformed rebar (also known as "sister bars"). These instruments were all read each time the Osterberg Cell, LVDT's and dial gages were read, one, two and four minutes after the

application of each load. Four sister bars were placed at each level to eliminate the effects of bending, to minimize the effects of minor flaws in the concrete and for redundancy. The objective of using the sister bars was to determine the distribution of unit side shear resistance along the test socket as the test progressed by converting the strain to stress and the stress to load, as explained in the section on test data interpretation. One level of sister bars was placed 24 inches above the base of the reaction socket to obtain some indication of the base resistance being developed in the reaction socket. With this system of load measurement, gages could not be placed closer to the base than 24 inches because of the need to provide 24 inches of development length in the 48-inch-long sister bar on either side of the vibrating-wire sensor.

The load was applied to the test socket, located above the Osterberg Cell, which was expanded using hydraulic pressure, through a two-inch-thick steel loading plate situated between the Osterberg Cell and the test socket. Similarly, a steel loading plate was placed between the bottom of the Osterberg Cell and the top of the reaction socket. All of the sister bars appeared to perform well except for Gage No. 9776 situated 30 inches above the top of the top plate of the Osterberg Cell, which stopped reading during the test. That gage was not used in the reduction of the data in this report.

The movement of the top plate during the axial load test was measured by two displacement gages attached to the casing of the drilled shaft at the ground surface, whose feet rested on either side of the carrier frame, which was welded to the top loading plate. The carrier frame was completely immersed in water during the test, except for the top four feet. The exposed portion of the carrier frame was not exposed to direct sunlight, and the air temperature did not vary more than 6 degrees C during the test. Therefore, no corrections were made for thermal strains in the carrier frame. The compression in the test socket was measured by means of two telltales on opposite sides of the rebar cage. The top of the telltales was at an elevation of 10 feet (120 in.) above the top loading plate, and the feet of the telltales were attached to the top loading plate. Movements of the loading plate relative to the reference point 120 in. above the loading plate were measured by means of vibrating wire LVDT's (Geokon Model 4450). Expansion of the Osterberg Cell was measured by means of two similar LVDT's spanning between the top and bottom loading plates. The LVDT's and displacement gages were all read by Loadtest, Inc., at the same time the sister bars and Osterberg Cell load were read.

The Osterberg Cell and cages for the reaction and test sockets for the axial test, along with attendant instrumentation, were welded together to form a single unit, and the steel carrier frame used to support the instrumentation lead wires and hydraulic lines to the ground surface was welded to the top plate of the Cell. A four-inch-diameter steel tremie was then placed along side the carrier frame and through a cutout in the steel loading plates to the level of the bottom of the reaction socket, and the entire unit was lowered into the borehole. One splice had to be made in the carrier frame and tremie after the base of the reaction socket cage was about 100 feet below the ground surface because the boom on the construction crane was not long enough to handle the entire carrier frame and tremie in one piece. Once the reaction cage was resting on the base of the borehole,

the reaction and test sockets were concreted through the tremie. The water in the water-filled borehole was separated from the fluid concrete by means of a plug ("pig"). Once the concrete was brought to the desired elevation at the top of the test socket, the tremie was removed, which allowed about two feet of fluid concrete to fall out of the tremie on to the top of the test socket, making the test socket 12 ft long instead of the planned 10 ft long.

The load applied to the test and reaction sockets in the axial test by the Osterberg Cell was obtained by Loadtest, Inc. by measuring the pressure applied to the hydraulic fluid in the Cell by a pneumatic pump, using a Bourdon-type pressure gage. Loadtest, Inc., represents that the Osterberg Cells and pressure gage had been calibrated prior to the load tests, and these calibrations (of registered pressure to load) were used in the data analysis. The axial test was terminated when leakage of liquid from the Osterberg Cell became excessive as evidenced by the fact that the pump operating at full speed could not produce any increase in pressure in the Osterberg Cell pressure gage.

The objective of the lateral test was to jack apart a cylinder of concrete using the Osterberg Cell to split the concrete and thereby simulate the behavior of a laterally loaded drilled shaft, except for effects of rotation of the shaft. For the lateral test, the Osterberg Cell was used in a vertical orientation with two loading plates 44 inches wide by 60 inches high located vertically on either side of the Cell. The Cell and plates were lowered into the borehole as a unit, after cleaning and greasing the bottom of the borehole and the inside surfaces of the plates and placing about two feet of concrete in the borehole. Final concreting was accomplished through a 4-inch-diameter tremie. Unfortunately, the tremie was withdrawn from the concrete, as in the axial socket construction, which allowed about two feet of concrete to fall out of the tremie onto the top of the test socket. The quality of this concrete is unknown, but it was assumed that this "spoiled" concrete did not carry any significant lateral load.

Movement of the two sides of the split cylinder relative to each other were measured by two Geokon LVDT's in a manner similar to measurement of the expansion of the Osterberg Cell in the axial test. One of these LVDT's was located above the Cell, and one was located below the Cell.

Loads in the lateral split cylinder test were applied and measured as per the axial test. However, two series of 3 unloading-reloading loops were performed to assess the effects of one-way cyclic loading. The test was terminated when the loading plates rotated (the bottom LVDT moving more than the top LVDT) to the extent that accurate measurements of lateral movements could not be made.

Further details of the drilled shaft test elements can be found in the report by Loadtest, Inc. (1995).

AXIAL DRILLED SHAFT SOCKET TEST RESULTS AND SCALING TO CONDITIONS IN THE ST. CROIX RIVER

General

For reasons of economics, it was decided to conduct the drilled shaft socket tests onshore. It was also decided to conduct the socket tests in the same friable member of the Franconia formation at the onshore test site that is found in the St. Croix River because it was assumed that the friable sandstone would be the weakest of the sandstone members encountered at the founding level for the bridge piers in the river. Identifications of these strata were made by Minnesota DOT personnel. The location of the onshore test site relative to the river, shown in Fig. 1, is about 200 m west of the Minnesota bank along the alignment of the T. H. 36 Stillwater Bridge. As shown schematically in Fig. 4¹, the stratigraphy, and therefore the geomaterial stress conditions, is different at the test site location from the stratigraphy in the river. At the test site, approximately 155 ft of rock and overburden soil overlaid the axial test socket, and approximately 175 ft of rock and overburden soil overlaid the lateral test socket. In the river, two typical conditions were assumed relative to the stratigraphy, also depicted in Fig. 4. Near the Minnesota side (Boring T-43, Appendix), the sandstone is encountered at a higher elevation than at the onshore test site. The sandstone is overlain by about 25 ft of water, 50 ft of muck and 3 to 5 ft of sand and gravel. This condition results in lower effective stresses in the rock than occurs at the test site. It will be demonstrated that the friable sandstone behaves much as a granular material with only a small amount of cohesion. Thus, effective stresses must be considered in scaling the results of the load tests to the stratigraphic conditions in the river. A similar situation exists near the Wisconsin side (Boring T-48, Appendix); however, there the muck is slightly thicker and the sand and gravel is much thicker, leaving the highest position of the friable sandstone at near the same elevation as that at the test site. See Fig. 4. However, because of the much lower elevation of the soil surface at Boring T-48 (bottom of the river) than at the test site (ground surface, about 20 ft above the water surface in the river) and the considerably lower unit weights of the muck than those of the overlying geomaterials at the test site, effective stress scaling is still necessary on the Wisconsin side.

It was reported by Minnesota DOT personnel that it is anticipated that the drilled shafts for the bridge piers will be approximately eight (8) ft in diameter. For reasons of economics, the test shaft sockets were nominally four (4) ft in diameter. Therefore, some consideration of the effects of diameter will also be necessary when scaling the test results.

Load Test Results

The axial load test was conducted on November 7 and 8, 1995, by applying increments of load to the Osterberg Cell of about 50 tons very five minutes. The test

¹ The information given on Fig. 4 and the subsurface idealizations indicated in this report are for purposes of developing design parameters only. This information is not to be used for construction.

results are documented in Figs. 15 - 21; however, much more complete documentation is provided by Loadtest, Inc. (1995) in a separate report.

Fig. 15 shows the plot of the net load on the Osterberg Cell (load measured from calibrated pressure gage less the computed buoyant weight of the test socket) versus the average measured upward displacement of the top plate, located at the bottom of the test socket (displacement of the carrier frame). The load and movement readings on this figure and on all other figures relating to the axial load test on the drilled shaft socket in this report showing load and movement or stress and movement are derived from the readings taken four minutes after each load application. Fig. 15 also shows the gross load (no correction for the buoyant weight of the test socket) versus average measured downward displacement of the bottom plate (top of the reaction socket, obtained by adding algebraically the average measured displacement of the top plate to the average measured expansion of the plates). The major unload cycle at a load of about 1500 tons occurred at the end of the first day of testing, at which time the hydraulic system was found to be leaking. After repairs, the test was continued the next day until the load reached approximately 2300 tons, at which time the leak reappeared and caused termination of the test.

The load-movement relations for both the test and reaction sockets are remarkably linear, to a deflection of greater than 1.3 inches for the test socket ("top plate"), which is a side shear socket. This behavior is unusual in the sense that side shear linearity in rock sockets to such large displacements have not been reported often. The lack of displacement recovery in the unloading cycle at 1500 tons indicates that most of the side shear resistance was developed through plastic shearing and not through elastic stresses in the rock. The fact that the original trend was recovered after reloading from 1500 tons indicates that there is little cyclic degradation under one-way cyclic axial loading.

Fig. 16 shows the compression of the test socket between the top loading plate and a point on the top of the test socket cage, 10 feet above the top plate. The compression of the test socket can be seen to be relatively small in comparison with displacement of the bottom plate. Fig. 16 also shows the separate LVDT readings at the top of the carrier frame, which measured the top plate movement. At large loads there was some tilting of the carrier frame, perhaps reflecting eccentric bearing at the base of the reaction socket, described later.

On Fig. 17 is shown a series of plots of indicated load in the test socket versus distance from the top plate (distance above the bottom of the test socket). These loads were computed from the strain gage data for which stable readings existed throughout the entire test. The strain for each gage was multiplied times the modulus of elasticity, E, of the concrete in the socket times the cross-sectional area of the concrete and times the cross-sectional area of steel times $E = 29,000,000$ psi. The results were added to give the value of load in the socket, and the loads so computed from the strain gage readings at each level were averaged to give the interpreted load at that level. Values of $E(\text{concrete})$ were computed by the ACI formula for concrete modulus using the value of f'_c for the day

of testing given in Fig. 9. The indicated load at the bottom of the socket is the net load registered by the Osterberg Cell.

It is observed that the unit side shear, which is proportional to the slopes of the line segments connecting the values of load in Fig. 17, varies with depth in the socket. This phenomenon can be seen clearly in Fig. 18, which shows the unit side resistance (f) vs. displacement of the top of the carrier frame (assumed equal to movement of the bottom of the socket) (w). f is determined from a given segment of a load-depth relation in Fig. 17 by dividing the difference in load between two depths by the perimeter area of the shaft between those two depths. The resulting variation in f appears generally random with depth. The depthwise pattern of variation may be associated with variable concrete modulus not reflected in the calculations using the laboratory specimens to determine f_c , or it may be associated with local rock features that are not random but that are also not known. However, the caliper logs (Figs. 5 and 6) suggest that the variation is not associated with any major changes in the cross-sectional area of the socket. Since there is no rational basis for relating the different local values of f that occur at various locations to any rock or socket feature, all analyses will be made with the average values of f developed along the socket and the corresponding average movement (w) of the entire socket.

Also shown on Fig. 17 is the average of the f -values in each of the four segments along the socket plotted against w . These average values are shown only to provide a sense of variation. The actual average values of f are slightly different from (less than) the average of the f values in the segments, because the segments are of different length. It is those averages (total net load applied to the socket divided by the perimeter area of a 12-ft-high socket) that will be used in the analysis documented below.

The significance of Figs. 19 - 21 will be covered later.

Scaling of Side Resistance to Axial Loading ("Skin Friction") for Franconia Sandstone

The net load-movement curve measured for the axial test socket is shown in Fig. 15. The net load (measured load minus buoyant weight of test socket) is assumed to be equal to the side shear resistance of the test socket. No asymptote for side shear failure was achieved, despite the fact that the socket moved in excess of 1.3 inches. It is also observed that upon unloading almost no recovery occurred, indicating that the development of side shear was inelastic (occurring by shearing the geomaterial at the socket-rock interface plastically). This behavior is not typical behavior for a cohesive geomaterial; therefore, the mechanism of the development of shearing resistance was analyzed using a fundamental method in order to determine the values of the basic parameters that would produce the measured behavior in the test socket. Those parameters were then scaled to their appropriate values for the conditions in the river, which then allowed for the determination, through a computational model, of the unit side

resistance - movement relations for prototype sockets in the river, assuming that the rock in the river had the same properties as the rock at the location of the test sockets.

Two analyses were conducted. The first used a direct computer simulation developed recently in Australia (ROCK sockET, or "ROCKET") (Seidel, 1994), and the second used a computer approximation of a finite element parametric study of cohesive soft rock developed for the FHWA (O'Neill et al., 1995). A list of the principal input parameters for both analyses is given in Table 2.

ROCKET Analysis. ROCKET was used to simulate the shearing behavior of a rough interface between concrete and soft rock under conditions of constant normal interface stiffness. When relative displacement occurs between the concrete and the rock, the interface dilates. Since the rock is modeled with constant stiffness (not constant stress, as is normally done in the direct shear test), the normal stresses increase on the interface. The interface and the rock itself are modeled with drained shear strength parameters; therefore, the resistance to shearing increases as the displacement increases and the interface dilates. A triangular joint pattern is used to model the interface, so that as sliding progresses the lengths of the shearing surfaces in the rock asperities decrease, finally allowing shearing failure to occur through the rock asperities.

The shearing resistance-deformation behavior is dependent upon the pattern of interface roughness, the Young's modulus of the rock, the value of the normal stiffness, the angle of internal friction of the rock and the angle of sliding friction along the interface, the cohesion of the rock, the Poisson's ratio of the rock, and the initial normal stress at the interface (which is assumed to be equal to the initial fluid pressure in the concrete).

Principles of fractal mathematics are used to simulate an interface roughness pattern. A basic fractal pattern is assumed and is scaled to a distance between troughs and peaks in the triangular joint pattern specified by the user. Fig. 22 shows three standard interface joint patterns that were used in this study, denoted "Fractal 1b, 1c and 1d." Fractal patterns 1b and 1c represent relatively smooth interfaces with mean double amplitude asperity amplitudes of less than 0.25 in. These values are smaller than the resolution available in the electronic tools used to caliper the test sockets. Fractal 1d represents a rougher surface that would have been detected in the caliper records had such roughness existed. However, no evidence of such roughness was observed in the caliper logs (Figs. 5 and 6). A contrasting depiction of interface roughness, a harmonic sine wave, used in the FHWA method, is shown for comparison in Fig. 23. The results of analyses performed using this roughness profile in a cohesive geomaterial will be described later.

The concept of interface roughness may not be as straightforward to apply in the friable member of the Franconia sandstone as in some other formations because the friable samples recovered from this formation exhibited high porosity and a significant propensity for penetration of liquids, including, presumably, cement paste from the concrete.

Therefore, the real shearing interface may have existed at the extreme limit of cement paste penetration some distance (perhaps 1 to 2 mm) from the actual excavated interface. For this reason, the roughness of the modeled interface may not relate directly to the roughness of the excavated interface.

For this reason, also, the angle of sliding resistance was taken to be very near the angle of internal friction in the rock. It was verbally reported by Minnesota DOT personnel that direct shear tests had been conducted on dense remolded specimens of the friable sandstone, in which a value of 40 degrees was observed for the angle of internal friction. This value was used in the ROCKET simulation, and the angle of sliding friction was assumed to be 38 degrees. Visual inspection of the friable rock cores indicated very little cementitious material within the rock. The fact that it was friable when removed from the sampling barrels is further evidence of a low value of cohesion. A value of 0.05 MPa was therefore assumed for rock cohesion, lacking any numerical data. A value of Poisson's ratio for the rock of 0.25 was assumed arbitrarily. This value is commonly used for the analysis of rock sockets.

The remaining fundamental parameters (Young's modulus of the rock, normal stiffness and initial normal pressure) must be first determined and scaled to the stratigraphic conditions that will exist during construction of the prototype shafts. The effects of different diameters also need to be scaled. This is achieved through adjustment of the normal stiffness in the ROCKET analyses.

Unfortunately, there are no independent data on the Young's modulus of the rock. However, the normal stiffness can be deduced approximately from the results of the lateral split cylindrical socket test, since the initial slope of the lateral pressure applied to the rock versus lateral deflection of the rock is in fact the normal stiffness. The value of normal stiffness, 400 kPa/mm, is obtained from Fig. 24, which shows the results of the lateral socket test in terms of pressure applied to a 4.0 ft. X 5.33 ft projected area versus deflection of one side of the split socket at small values of lateral movement. Socket height of 5.33 ft was used instead of 5.0 ft to account for an assumed inclination of the punching shear plane between the loading plate and the borehole wall. The mode of loading for the lateral split socket test is not identical to the mode of lateral loading due to dilation, which is radially outward. That mode of loading should result in a slightly higher value than the value of the initial slope of the curve shown in Fig 24. However, the axial test socket is at a slightly higher elevation than the lateral test socket, which should result in a slightly lower value, and it is therefore assumed for computational purposes that the value of lateral normal stiffness for axial loading will be identical to the value obtained in the split socket test (400 kPa/mm).

The results of the lateral split socket test can also be used to infer a Young's modulus for the rock at the test depth for the lateral socket. This has been done using the method of Janbu et al. (1966), as documented in Table A-2 in the Appendix. A value of 380 MPa was obtained. However, that value, when used in ROCKET, gave excessive deflections, and a value of 600 MPa was eventually used in the scaling analyses. The

reason that such a higher value was needed is not clear, but the reinforcing of the rock in the immediate vicinity of the interface (where most of the shear strain should have occurred) by migrating cement paste and the differences in the stress paths between the axial and lateral split socket modes of loading may have contributed to the necessity to use a higher value of E (Young's modulus) in the ROCKET analyses than was inferred from the lateral split socket test.

The initial normal pressure at the interface was taken to be equal to the fluid pressure in the concrete immediately after placement of the fluid concrete at the center of the test socket. The test socket had been designed to accommodate 10 feet of concrete; however, during construction it was overpoured to a thickness of 12 feet. Therefore, the appropriate concrete head for estimation of initial normal pressure at the interface is 6 ft (1.8 m). Since the concrete was placed under water, the buoyant unit weight was used, giving a value of 27 kPa. Since some sediment was likely floated on the top of the column of concrete during placement, the value of normal pressure was arbitrarily increased to 30 kPa. It should be noted that this is much lower than the value that would be expected during construction of the prototype sockets provided the construction specifications require the concrete to be poured continuously in the socket and up into the casing/form to the surface of the water or above.

The first step in the ROCKET analysis was to simulate the measured behavior of the axial test socket, in terms of average unit shear resistance over the 12-foot socket vs. movement of the socket. The optimum set of parameters needed to achieve the best match with the load test was: *Fractal 1c* interface roughness model (slightly rough, random roughness pattern); ϕ' (effective angle of internal friction) = 40°; δ' (angle of interface sliding) = 38°; rock cohesion, $c' = 0.05 \text{ MPa}$; normal stiffness = 400 kPa/mm; $E = 600 \text{ MPa}$; and ν (Poisson's ratio) = 0.25. The results of the match between the measured and modeled relations are shown in Fig. 25. The match with the ROCKET analysis is quite good above a simulated socket displacement of about 8 mm. Below that displacement, the predicted movement was somewhat too low, but the overall pattern is considered a satisfactory match.

FHWA Method Analysis. For purposes of comparison, the FHWA method was also used to simulate the axial socket load test. There are several fundamental differences between this method of analysis and the ROCKET method. First, the interface roughness pattern is sinusoidal, as shown in Fig. 23, and the rock is considered to behave as an undrained material with cohesive shear strength, although the interface itself is frictional. This model was developed by calibration against load tests in hard clays, clay shales and limestones. The inputs for this model are shown in Table 2. The most noteworthy difference between the inputs for this model and for the ROCKET model are the values for c' and ϕ' , which were taken as 1 MPa (half of the compressive strength) and 0°, respectively for the FHWA model. The choice of 1 MPa for the cohesion was completely arbitrary. That value is probably not at all representative of the mass of the rock, but was necessary in order to obtain a general match with the measured data. The overall match, however, is much poorer than the match obtained with ROCKET, as can be seen in Fig.

25. In particular, the FHWA model predicts the beginning of plastic failure at a displacement of about 10 mm, which is common in drilled shafts in cohesive geomaterials but which did not occur in the axial load test on this site. It is therefore concluded that the ROCKET model is the more appropriate of the two models for simulating the behavior of drilled shaft sockets in the friable member of the Franconia sandstone at the test site.

Therefore, the values of the parameters given above for the ROCKET analysis of the axial test socket can be considered to be the operational fundamental parameters for axial loading in the friable sandstone, which will next need to be scaled to the conditions in the river.

Scaling to Prototype Conditions Using ROCKET. Before proceeding to scale the values of the ROCKET parameters required to model the test socket behavior to prototype conditions, some of the effects of the choice of values are demonstrated in Fig. 26. First, comparison of the top two curves indicates the effect of the value of concrete head (initial concrete pressure at the interface). The relative results suggest that if the concrete had been poured all the way to the ground surface that approximately a 20 per cent increase in unit shaft resistance would have been achieved.

Comparisons of the three relations using identical conditions except for interface roughness (second through fourth curves in the legend for Fig. 26) suggests that the roughness pattern has a profound effect on the behavior and therefore that the dilation of the socket is having a major effect on the development of unit side resistance. *[This observation makes it imperative that the construction method employed for the prototype sockets produce an interface roughness pattern similar to that achieved in the test socket. In the test socket, final excavation was by means of a rock auger, which should be expected to produce similar effects in the prototype shafts. However, if core barrels, coring casings or similar devices are used to make the final excavation in the prototypes, conditions may be less favorable. It is also critical that drilling slurries that would impede the flow of cement paste into the pores of the sandstone not be used in the construction of the sockets for the prototype shafts.]*

The effect of a reduction in the lateral normal stiffness and in the Young's modulus to one-third of the values that occurred in the test socket (to simulate scaling the behavior to a smaller depth) can be seen by comparing "Fractal 1c (slightly rough) - 1.8 m Concrete Head" with "Fractal 1c - 1.8 m Concrete Head - Modulus and Lateral Stiffness 1/3 of Values Used for Load Test." The effect of these reductions is seen to be significant in that a reduction of these parameters to 1/3 of the values inferred for the test reduces the unit shaft resistance (f) to about 1/3 of the values measured in the test, which were closely simulated by "Fractal 1c (slightly rough) - 1.8 m Concrete Head."

Finally, the effect of reducing the angle of interface shearing is shown by the next-to-last entry in the legend, and the effect of increasing the cohesion to a large value while reducing the angle of interface friction is shown in the last entry in the legend. The latter case would be representative of a cohesive soft rock, it and gives a pattern of f vs.

deflection (w) that is similar to that given by the FHWA model (although the values of f at a given deflection are higher with ROCKET because a larger value of c' has been used).

In order to scale the average $f-w$ relation from the test socket conditions to the prototype conditions using ROCKET, it is necessary to scale E for the geomaterial, normal stiffness and initial concrete pressure. E is scaled according to the square root of the effective overburden pressure. The logic behind this scaling rule is that the socket behavior reproduced by ROCKET clearly emulates the behavior of a granular geomaterial, not a cohesive geomaterial, and that visual observation of the friable sandstone revealed relatively little cementing material. Therefore, the value of E should be a function of the effective confining pressure. No data are available to permit scaling of E for friable sandstone according to effective confining pressure. Therefore, reliance is placed on scaling of E for dense sands. Duncan and Chang (1970) proposed a simple equation for the initial slope, E , of a triaxial compression test on an isotropically consolidated, drained specimen of sand, as follows:

$$E = K p_a \left(\frac{\sigma'_3}{p_a} \right)^n , \quad (1)$$

where K is a constant related to the density of the sand, σ'_3 is the effective confining pressure, p_a is atmospheric pressure in the units used, and n is a scaling exponent that relates E to effective confining pressure. Duncan and Chang suggest values of K of about 2000 for dense sand and n of 0.54 to 0.57 for dense sand and silt. Wong (1985) conducted a study to determine the secant modulus of an unaged, clean silica sand at 90 per cent relative density under a very wide range of confining pressures at 0.5 times the peak principal stress difference and arrived at $K = 750$ and $n = 0.62$. The results of Wong's study are summarized in Fig. A1, in the Appendix. Considering that the friable sandstone does possess a small amount of cohesion, it is reasonable to assume that the operational value of n is slightly less than the average of the values reported above (0.58). A value of $n = 0.50$ was therefore selected for use in scaling E for the test site. The effective confining pressure is modeled as the effective overburden pressure. Consequently, assuming that the material properties of the friable sandstone are identical at the test site and at the location of the prototype shafts in the St. Croix River,

$$\frac{E_{\text{prototype}}}{E_{\text{loadtest}}} = \sqrt{\frac{\sigma'_v(\text{prototype})}{\sigma'_v(\text{test})}} , \quad (2)$$

where σ'_v = vertical effective pressure in the geomaterial.

Since the normal stiffness, k_N , is theoretically a direct function of E of the rock, the scaling rule in Eq. 2 can also be applied to normal stiffness, assuming that the construction method does not produce a different degree of disturbance on the borehole-concrete interface between model and prototype locations. Therefore,

$$\frac{k_N \text{ prototype}}{k_N \text{ loadtest}} = \sqrt{\frac{\sigma'_v(\text{prototype})}{\sigma'_v(\text{test})}} \quad (3)$$

Finally, concerning the scaling of initial normal pressure from the fluid concrete, it is assumed that 30 ft of fluid concrete will exist above the depth within the socket for the prototype shaft at which a value of unit shaft resistance is to be estimated. *This condition can be achieved by placement of concrete continuously in the prototype shaft socket and in the casing/form above the socket so that the slump of the concrete remains at least 6 in. (150 mm) after it is placed at a given elevation for the time required to place 30 ft. of fluid concrete at the same or higher slump above that elevation.*

In order to scale E and k_N , values of vertical effective stress must be estimated at the test shaft location and at the location of the prototype shafts. The most severe scaling occurs on the Minnesota side (e. g., Boring T-43), where the vertical effective stresses in the sandstone are the lowest. Fig. 27 illustrates scaling for unit side resistance, f, at that location. Unfortunately, unit weights are not known for any of the geomaterials, except for the muck, so values had to be assumed. These values are shown on Fig. 27. Values for the muck are average measured values. The others are estimates. At the middle of the axial test socket, the value of σ'_v was estimated as 10 588 psf, assuming that the phreatic surface was at the ground surface. At the location of Boring T-43, the vertical effective stress 2 ft below the top of the sandstone is 1176 psf. [It is recommended that the portion of the socket to which resistance is assigned not extend above about 2 feet below the top of the rock surface to allow adequate room for sealing the casing during construction. The rock into which the casing is sealed will be smoothed, smeared and possibly fractured when the casing is placed and should be discounted for side resistance.] At 30 ft below the sandstone surface, σ'_v is 3069 psf.

The above values of vertical effective stress result in the scaling factors for E of 0.334 2 ft below the top of the sandstone and 0.539 30 ft below the top of the sandstone, as shown on Fig. 27. For purposes of analysis with ROCKET, these values were rounded off to 0.333 and 0.5, respectively. ROCKET was rerun with the parameters deduced from modeling the test socket, with the values of E of 1/3 and 1/2 of those used in the analysis of the axial test socket.

In the ROCKET reruns to replicate the prototype conditions, k_N also had to be scaled. Although k_N scales in direct proportion to E if the diameter of the shaft is invariant, it must be further scaled if the diameter changes. In this study the diameter of the test shaft was nominally 4.0 ft. Caliper logs (e. g., Figs 5 and 6) indicated that the true value of the diameter of the excavated test borehole, d_t , was very near 4.0 ft. It is assumed based on current information that the value of the diameter of the prototype shafts, d_p , will be about 8.0 ft. The lateral strain produced by dilation resulting from a given roughness pattern is approximately inversely proportional to the diameter of the socket. In order to simulate that condition in the CNS (constant normal stiffness) version

of ROCKET, which was used in this analysis, it is necessary to reduce the value of k_N by the ratio d_s/d_p ($4/8 = 0.5$) in addition to the reduction caused by the reduction in E . Therefore, in order to simulate socket behavior at 2 ft below the surface of the sandstone, k_N must be taken as $0.5 (1/3) = 1/6$ of the value for the test socket, or 67 kPa/mm. To simulate socket behavior at 30 ft below the surface of the sandstone, k_N must be taken as $0.5 (1/2) = 1/4$ of the value for the test socket, or 100 kPa/mm.

Considering also the initial normal pressure to be 130 kPa (30 ft of hydrostatic pressure from buoyant concrete), ROCKET analyses were performed again, with the scaled values of E , k_N and initial concrete pressure. The results are shown in Fig. 28. It is noteworthy that the scaled values of f [denoted here f (maximum)] at $w = 25.4$ mm (1.0 in.) are 320 kPa (3.3 tsf) 2 ft below the rock surface and 430 kPa (4.5 tsf) 30 ft below the rock surface. Considering these to be ultimate values, with a factor of safety of 2 on unit shaft resistance (i. e., $f = 1.65$ tsf at 2 ft penetration of the rock to 2.25 tsf at 30 ft penetration of the rock), the deflection at working load predicted by ROCKET would be in the order of 5 to 9 mm. [*Please note that it is beyond the scope of this report to recommend a factor of safety. The value of 2 is used here only as an example.*]

Scaling of End-Bearing Resistance to Axial Loading for Franconia Sandstone

Since the $f-w$ relations are of the displacement-hardening type (i. e., do not reach a peak and drop precipitously thereafter with increased settlement), it is reasonable to use end bearing resistance (q) in the design for compressive loading. Fig. 19 indicates a complex pattern of stress in the reaction socket 2 ft above the base. Two of the strain gages registered significant compression, while two registered tension. This is suggestive of a large bending moment on the bottom of the socket. Considering the average of the strain gage readings, Fig. 20 was developed to show the average normal compressive stress in the socket at the level of 2 ft above the base as a function of settlement of the top of the reaction socket. Fig. 21 provides an explanation of the wide variation in readings in the strain gages in the bottom of the reaction socket (Fig. 19). Apparently, the two gages that registered compression were nearest the location of the tremie, while those that registered tension were situated across the socket from the tremie. It is speculated that some sediment was situated on the bottom of the reaction socket at the time the concrete was placed. This sediment (or some of it) was pushed to the side of the base of the shaft underneath Geokon Gages 9790 and 9791, leaving the side of the base beneath Geokon gages 9789 and 9792 clean and in good contact with the concrete. When the socket was loaded, the reaction developed eccentrically, causing a large bending moment in the bottom of the reaction socket, which produced the gage readings reported in Fig. 19. For this condition the average compressive base resistance that was developed over the entire base area, not just the "clean" area, should be considered as effective.

Returning to Fig. 20, the slope of the average compressive stress vs. settlement curve is slightly higher than the lateral subgrade modulus measured in the lateral split socket test. Considering that the pressure was calculated from the strain gages located 2 ft above the base of the shaft, the comparison is reasonable, which gives credibility to the

interpretation of the compressive stress derived from the average strain gage reading at this level as representative of the actual average stress in the reaction socket near the base. The average unit compressive resistance 2.0 ft (0.6 m) above the base of the reaction socket at a settlement of 5 to 9 mm (say 7 mm) was measured to be about 4.6 MPa. At that point in the load test the average applied compressive stress on the top of the reaction socket was about 10.2 MPa. Assuming uniform shear transfer of load along the reaction socket to the rock, the reduction in compressive stress in the reaction socket was 0.43 MPa per ft of depth, which gives an extrapolated average base resistance of $4.6 - 0.86 = 3.7$ MPa. The rate of development of base resistance with respect to settlement in an elastic medium is inversely proportional to the diameter of the bearing surface and directly proportional to E. Therefore, in an 8-ft-diameter socket at a depth of 30 ft below the top of the sandstone at T-43 E would be about 1/2 of the value deduced at the test site and test socket elevation, leading to the conclusion that an end bearing resistance of 1/2 (due to E) X 1/2 (due to diameter) of that inferred in the reaction socket in the load test would develop at a settlement of 5 - 9 mm. That is, a value of $0.25 \times 3.7 = 0.925$ MPa or 9.7 tsf could be used for the gross working unit end bearing resistance at a deflection compatible with the deflection that will produce a factor of safety of 2.0 in side shear (5 - 9 mm) if the socket penetrates the sandstone 30 ft. For a 20-ft penetration, the corresponding gross unit end bearing resistance should be taken to be about 7.7 tsf for an 8-ft diameter shaft, due to the reduction in E. [For less than 20 feet of penetration, the base failure will transition from a deep failure to a shallow failure, and a severe reduction will need to be made in working end bearing resistance.] *These values should be used with care in a design context, however. It must be demonstrated that the rock within at least 2 socket diameters below the bearing surface is at least as strong and stiff as the rock within the socket, and the quality controls during construction must be such that the base of the socket is clean at the time of concrete placement. That value will also need to be adjusted if the factor of safety for side resistance is other than about 2.*

If higher end-bearing values are desired, post-grouting of the base of the drilled shaft sockets could be considered.

Qualifications for Axial Loading

The values for unit shaft resistance f (maximum) and end-bearing resistance (q) suggested above are scaled to the conditions at Boring T-43, where there is little overburden material except for the low-density muck. Elsewhere, such as at Boring T-48, where considerably more sand exists, the values of q and f (maximum) would be slightly higher. However, considering the uncertainties in the scaling process (assumptions of values and certain aspects of the scaling rules), it is probably an unwarranted sophistication to modify the values for f (maximum) and q for this condition. It should also be specifically noted that the values reported here should be considered gross values, not net values, which means that the weight of the concrete within the shaft should be considered as part of the load on the rock. Again, please note that it is beyond the scope of this report to recommend a factor of safety. The value of 2 is used above only as an example. The factor of safety should be selected after careful study of the uncertainties in

the loads and the variability of the soil and rock properties along the alignment of the structure. It may be prudent to vary the factor of safety where changing site conditions warrant doing so. Decisions regarding the variability of rock properties should be made by Minnesota DOT personnel. In the same context, it is reiterated that the results of the scaling of the test results to prototype conditions in the river is contingent upon the assumption that the rock properties are comparable at both the test and prototype locations. Every attempt should be made during the design and construction processes to verify that assumption and, if not verifiable, to make appropriate changes to the design parameters. It must be specifically assumed that the behavior of socket segments within the glauconitic sandstone, which is interbedded with the friable sandstone in the river, is no worse than that of the friable sandstone.

Values of f were computed at depths of 2 and 30 feet below the top of the rock in the river. It is assumed that a minimum penetration of the rock of two feet will be necessary for seating of casing into the rock, so that skin friction should not be used in the design of the drilled shafts above that depth. However, it may be found during construction that an adequate casing seat cannot be made with two feet of penetration of the rock or that for other reasons the contractor sets the casing deeper. In that case the socket should be considered to begin at the bottom of the casing, regardless of its penetration into the rock, and the length of socket specified in the design should be constructed below that elevation. That is, the final criterion for socket depth should be depth below the bottom of the casing, and not an absolute elevation.

This report does not address design values of unit side resistance for uplift loading. These values will likely be lower than comparable values for compression loading, discussed above, for two reasons. First, the Poisson effect in the concrete in uplift loading is opposite to that in compression loading from the top of the socket (normal loading case) or bottom of the socket (Osterberg Cell loading case). In both of those cases lateral strain in the concrete produces lateral compression in the rock and increases load transfer. With uplift loading, lateral strains are in the opposite direction, which cause a reduction in the load transfer relative to the condition in the load test. Second, with shallow, large-diameter shafts, a surface breakout effect would exist that may produce shearing failure along the surface of an inverted cone with the tip near the bottom of the shaft and not along the socket-rock interface as occurs in compression loading or in deep Osterberg Cell tests of the type conducted here. Judgment is therefore required to reduce the design values of unit side resistance for compression loading to design values appropriate for uplift loading. End bearing resistance should be completely discounted for uplift loading.

LATERAL SPLIT CYLINDER SOCKET TEST RESULTS

The results of the lateral split cylinder test are shown in Fig. 29, in terms of load measured by the Osterberg Cell versus average deflection measured by the two LVDT's placed between the plates. The lateral deflection for one-half of the socket, shown in this figure, is one-half of the deflection measured in the test. The deflections of the two LVDT's were generally consistent; however, the deflection measured in the lower LVDT

was larger than the deflection of the upper LVDT. More details can be observed by referring to the report from Loadtest, Inc. (1995).

The 2-ft overpour of concrete in the lateral shaft socket provides some difficulty in interpreting the results of this test. In reducing the data, it is assumed that this concrete did not carry any of the load generated in the socket by the Osterberg Cell, as it likely would have split in tension at a relatively small load (100 - 200 tons) and that the Cell load was transmitted to the wall of the socket along a vertical surface 5.33 ft high, or 0.33 ft taller than the vertical dimension of the steel loading plates by 4.00 ft in diameter. It is also assumed that no shearing resistance developed at the bottom of the socket, since that surface was greased prior to placement of the Cell and the concrete.

Each of the two unloading loops consisted of three complete one-way cycles. (The final unloading was not accompanied by any cyclic reloading.) There is no evidence of any major cyclic degradation having occurred during the three cycles of either of these unloading loops. It appears, therefore, that the p-y curves that are derived from this test, described below, are appropriate for a small number of significant one-way lateral load cycles on the socket.

Development and Scaling of p-y Curves for Franconia Sandstone

It is assumed here that the behavior of drilled shafts in the St. Croix River will be analyzed by the Minnesota DOT or its consultants using a numerical method based on nonlinear, Winkler-type subgrade reaction (the soil or rock) acting against a linear or nonlinear beam-column (the drilled shaft). Common software for such analysis is "COM624P" (FHWA program) or "LPILE" (private sector program). [Identification of this software does not constitute an endorsement thereof by the authors.] In order to conduct such an analysis, it is necessary to define the nonlinear, Winkler reaction-displacement functions, commonly known as "p-y" curves. For the muck, it is recommended that the built-in criterion known as "Matlock's soft clay criterion" be used to generate the p-y curves for the muck, using the parameter $\epsilon_{s0} = 0.03$ to 0.05 . This value can be estimated more accurately by determining typical values of the axial strain (expressed as a ratio) at one-half of the principal stress difference at failure in UU triaxial compression tests that were conducted on the muck. Such values may exist in Minnesota DOT files; however, they are not shown on the boring logs. For the sand and gravel, it is recommended that the "Reese" sand criterion be used. It is recommended that the built-in criteria for rock in the above software not be used. The remainder of this section addresses the criteria for p-y curves in the Franconia sandstone.

The measured Osterberg Cell load vs. one-half of the average displacement between the two loading plates (one-way displacement) is shown for the lateral split cylinder test in Fig. 29. These data have already been converted to lateral pressure on the rock vs. one-way displacement in Fig. 24. The partial recovery of displacement upon unloading at three points in the loading test suggest that there is a significant elastic component to the rock resistance. One can use these results directly to formulate p-y

curves for analyzing lateral behavior of drilled shafts in the sandstone. However, since the prototype sockets will be constructed at considerably less penetration and with a greater diameter than the test socket, scaling of the p-y relations is also necessary for analysis of the lateral mode of loading.

It is assumed that the sandstone is a frictional material; that is, that the cementing agent is present in insufficient amount to make the properties of the rock independent of confining pressure. This assumption is based upon the observation that the sandstone was very friable when being removed from core barrels. Three factors need to be considered in the scaling of the results of the lateral split cylinder socket test to p-y curves for the design of individual laterally loaded drilled shafts in the St. Croix River. These factors do not include scaling for group action, which is beyond the scope of this report but which will need to be considered by the designers if drilled shafts are installed in closely spaced groups. The factors are:

- Mode of loading of a drilled shaft relative to mode of loading of the split cylinder.
- Depth of the drilled shafts in the river relative to depth of the test socket on shore.
- Diameter of the drilled shafts in the river relative to the diameter of the test socket.

These factors are considered in sequence below.

Mode of loading. Fig. 30 illustrates in general the effects on the sandstone of a split cylinder test, which was the mode of testing for this study, relative to those produced by lateral loading of a drilled shaft socket. In the former, the rock is fractured laterally parallel to the loading plates in addition to the rock in front of the cylinder being loaded in a complex manner, which keeps most of the rock volume in compression. In the latter, a gap is formed behind the socket as the shaft debonds from the rock, making the stress conditions in the rock unsymmetric from front to back of the shaft. Intuitively, the differences should not be large; however, a series of simple finite element analyses were conducted to observe the effects of the different stress fields in these two modes of loading. The software used for the analyses was "STARDYNE®," a Windows-based package that runs on a PC platform, produced by Research Engineers, Inc., of Yorba Linda, CA. All of the analyses were linear elastic analyses that were performed with the objective of scaling of the modulus of subgrade reaction. In all analyses plane strain conditions were assumed, and a socket diameter of 48 inches (1.22 m) was used.

In the first analysis, the mode of loading used in the test was modeled. The mesh for this case is shown in Fig. 31, and the input parameters are given in Table 3. The boundary plane between the two halves of the sandstone mass was modeled using elastic constraints of very small magnitude at the outer boundaries and no constraints elsewhere along the boundary plane to simulate tensile splitting along that plane. That is, the tensile strength of the sandstone was assumed to be virtually zero on that plane. The Young's modulus of the rock mass was varied until the computed load per unit of depth divided by one-way lateral deflection was equal to the average initial slope, expressed in terms of resistance per unit length of the socket divided by lateral deflection, E_s , observed in the

loading test.. This step was necessary because no independent data existed on the modulus of elasticity of the sandstone. The modulus inferred from the axial load test was inappropriate for reasons discussed earlier and because the range of lateral deflections for lateral loading is greater than is necessary for modeling axial loading, necessitating fitting a wider range of deflections. The modulus so obtained in this first analysis was then used in the second analysis, which is illustrated in Fig. 32, in which the gap was modeled, but radial fractures were not modeled explicitly. During this analysis tension was observed in elements in the general area of the tensile fracture zone in the first analysis. In this case, the Young's modulus of those elements was reduced to 1/100 of the value input and the analysis repeated. The load on the socket per unit of depth per unit of deflection was then computed from the results of the final run. The ratio of this value to the value obtained in the first analysis (assumed equivalent to the value obtained from the load test) is taken as the multiplicative factor ψ required to scale lateral stiffness, E_s , from the value obtained in the load test to lateral stiffness for a laterally translating drilled shaft socket of the same diameter and at the same depth as that at which the split cylinder that was tested.

The results of the two finite element analyses are shown on Fig. 33. The test mode scaling factor ψ is the ratio of the p value from the dashed line to that for the thin solid line at common values of y in Fig. 33, or 1.146.

It is assumed that the mode of loading had no effect on the ultimate value of lateral resistance of the rock per unit length of the socket (p_u). This assumption may not be strictly valid, but since an objective of the design of the bridge piers in the St. Croix River is to keep lateral deflections (y values) small, the consequences of this assumption should not be significant. p_u is scaled, however, for both depth and socket diameter, discussed next.

Depth and Diameter of Socket. Scaling of depth and diameter are necessary because of the frictional nature of the sandstone. Because the overburden pressure, which controls the ultimate strength of a frictional geomaterial, is much lower in the St. Croix River than at the onshore test site, both E_s and p_u must be reduced below the values obtained from the test and scaled for mode of loading.

There are no standard scaling rules for drilled shaft sockets in sandstone. It is assumed that the scaling of $p-y$ curves for sandstone can be treated as per scaling of $p-y$ curves for dense sand, for which criteria exist, with appropriate modifications. The current expression for $p-y$ curves in sand recommended by the American Petroleum Institute is based on a report by Murchison and O'Neill(1983), which gives the following $p-y$ relationship for circular piles in sand:

$$p = A p_u \tanh \left[\frac{(kz)}{Ap_u} y \right], \quad (3)$$

where p is the local lateral resistance of the geomaterial per unit of depth (e. g., lb/in.), y is lateral deflection of the pile (e. g., in.), p_u is the ultimate value of p (same units as p), k is the subgrade modulus (e. g., lb/in.³), z is the depth at which the p - y curve is being determined (e. g., in.), and A is a dimensionless factor that depends on whether the loading is static or cyclic.

The use of Eq. 3 for scaling p - y relations is not entirely useful for the tests under consideration. First, Eq. 3 presumes that $E_s = kz$; that is, E_s increases linearly with depth. Since E_s can be assumed to vary according to E in a dense sand or, in this case, sandstone, it is more appropriate to replace kz with E_s and to scale E_s according to the square root rule established earlier. In addition, the parameter A is used to account for surface effects in the ultimate resistance p_u . Since the surface of the sandstone is not a free surface, it will be assumed that $A = 1$, except when cyclic loading is being considered, in which case $A = 0.9$, according to Murchison and O'Neill.

Equation 3 is thus modified to

$$p = Ap_u \tanh\left[\frac{E_s}{Ap_u} y\right] . \quad (4)$$

In order to use Eq. 4 in the design of drilled shaft sockets in the St. Croix River, both p_u and E_s need to be scaled from the values obtained in the load test, which was conducted at a much greater overburden pressure than will be available for the shafts in the St. Croix River and upon a socket that had a diameter that will likely be smaller than the diameters of the pier shafts (about 8 ft).

Scaling of p_u . It is assumed for analysis purposes that the center of the socket in the lateral split cylinder test was at approximately El. 525 ft. From the assumptions in Fig. 27, the vertical effective stress at that depth at the test site was approximately 11,775 psf = 81.8 psi. From Fig. 24, it is estimated conservatively that $p_u = 10,000 \text{ kPa} \times 1.22 \text{ m (diameter)} \text{ kN/m} = 69,600 \text{ lb/in.}$

According to the procedure outlined in Murchison and O'Neill (1983), at large depths, where failure is in a flow-around or plane strain configuration,

$$p_u = C_3 D \sigma'_v , \quad (5)$$

where C_3 is a function of ϕ , the angle of internal friction of the geomaterial, D is the pile or socket diameter, and σ'_v is the vertical effective stress at the depth at which calculations for the p - y curve are to be made.

At shallower depths, where failure is in a surface wedge configuration and where the presence of the surface influences the value of p_u , the expression is

$$p_u = (C_1 z + C_2 D) \sigma'_v , \quad (6)$$

where all parameters are as defined above except for C_1 and C_2 , which are also geomaterial factors that are functions of angle of internal friction, and z , which is depth below the free surface.

Because ϕ is not known for the sandstone, C_3 must be estimated using Eq. 5, $p_u = 69,600$ lb/in., $D = 48$ in., and $\sigma'_v = 81.8$ psi = 11,780 psf (estimated at the middle of the lateral test socket). [Some question arises about whether to use the actual vertical effective stress of 81.8 psi at the depth of the test or a value corresponding to a lesser value of z (lesser depth). In fact, the frictional strength of the rock is probably not proportional to z or to σ'_v below the depth at which lateral failure begins to occur in the flow-around configuration. However, since the relation between rock strength and vertical effective stress is not known, in the calculations for p_u , the actual value of vertical effective stress is used, because doing so should result in a conservative scaling factor.] Therefore,

$$C_3 = \frac{69,600}{48 \times 81.8} = 17.7 .$$

The theoretical relationship between C_1 , C_2 , C_3 and ϕ is shown in Fig. 34. From that figure, for a value of $C_3 = 17.7$, a mobilized value of $\phi = 26^\circ$ is inferred, from which $C_1 = 1.40$ and $C_2 = 2.20$. Therefore, for the test site, according to Eq. 6,

$$p_u (\text{lb/in.}) = (1.4z(\text{in.}) + 2.2D(\text{in.}))\sigma'_v (\text{psi}) \leq 17.7D(\text{in.})\sigma'_v (\text{psi}) . \quad (7)$$

In the St. Croix River, distance z can conservatively be taken to be the distance from the top of the rock down to the elevation at which the p-y curve is to be generated. σ'_v should be computed as the actual value of vertical effective stress, including the effects of the rock, muck and sand/gravel, at the location and depth where the p-y curve is being determined. Note that since a conservative procedure was used to evaluate C_3 , p_u near the top of the rock may actually be lower than p_u at the bottom of the overlying sand.

Scaling of E_s . The lateral stiffness from the lateral split cylinder socket test is denoted E_s and is defined as $(p/y)_s$, where $(p/y)_s$ is the slope of the first quarter-inch (6 mm) of the p-y curve at depth z . E_s in the load test on the split socket is equal to the initial slope for lateral loading, shown on Fig. 24, times the test socket diameter = 1.22 m. Note that the average slope over the first quarter-inch (6 mm) of displacement (267 kPa/mm) is different from the average slope over the first 1 mm of displacement (400 kPa/mm). Since axial loading involves very small lateral deflections due to the dilation of the rock and to the Poisson effect, an initial tangent value was used for the ROCKET analyses. However, lateral loading involves larger lateral deflections. Therefore, the average value of lateral applied pressure divided by deflection over 6 mm was used in

developing the p-y relation. For this reason, $E'_s = 267 \times 1.22 = 326 \text{ kN/m/mm} = 47,230 \text{ lb/in./in.}$ (pounds per inch along the socket per inch of lateral deflection). This value is appropriate for lateral deflections, y , of up to 6 mm. For values of y in excess of about 6 mm (0.25 in.), Fig. 24 indicates that the rock appeared to stiffen, possibly due to closing of small fractures that may have opened during excavation of the deep test socket, so that the lateral resistance-deflection curve exhibited reverse curvature at this point, which is not accounted for in Eq. 4. Use of Eq. 4 along with a value of E_s ascertained from the load test will therefore result in conservative resistance (p) values beyond a lateral displacement of about 0.25 in.

E_s is needed for the analysis of a drilled shaft socket. Considering the scaling factor for mode of loading, $\psi = 1.146$, $E_s = \psi E'_s = 54,130 \text{ lb/in.}^2$. E_s is not dependent on the shaft diameter, so no explicit scaling for diameter is required.

E_s is now scaled for depth in exactly the same manner as k_N for modeling axial behavior using ROCKET, using the square root of vertical effective stress rule. At depth z below the surface of the sandstone, $E_s = E_{sz}$, which can be computed from

$$E_{sz} = E_{s \text{ test}} \sqrt{\frac{\sigma'_{v \text{ test}}}{\sigma'_{vz}}} = 54,130 \sqrt{\frac{\sigma'_{vz} (\text{psf})}{11780}} \text{ (lb / in./in.)}. \quad (8)$$

The p-y relation for the sandstone can then be computed from Eq. 4, using Eqs. 7 and 8 to compute p_u and E_s , respectively, based on values scaled from the onshore load test.

A simple aid for hand calculations from Murchison and O'Neill is given in Fig. 35. The expression "kz" in that figure should be replaced with the value determined for E_s . For example, at the location of Boring T-43, for an 8-ft-diameter socket at a depth of 2 ft below the rock surface, $\sigma'_{vz} = 1176 \text{ psf}$, so that $E_{s,2\text{ft}} = 54,130 (1176/11,780)^{0.5} = 17,100 \text{ lb/in./in.}$ Then, $p_u = [1.4(24) + 2.2(96)](1176/144) = 1999 \text{ lb/in.}$ (which is less than $17.7(96)(1176/144) = 13,877 \text{ lb./in.}$, which comes from Eq. 5). If Eq. 4 or Fig. 35 are used, these are all of the parameters that are required to develop the p-y curve for a that depth. A similar procedure can be followed to develop the p-y curve for any other depth.

Qualifications for Lateral Loading

An important assumption that is made in scaling the results of the lateral split socket test to prototype conditions in the river is that the properties of the sandstone are equivalent at the test site and prototype site locations. If this equivalence does not exist, the scaling methodology is not valid.

It is also assumed that the construction procedure does not significantly damage the rock. Since it will very likely be necessary to set permanent casing into the surface of the sandstone to construct the drilled shafts, it is recommended that lateral resistance not be allowed in the sandstone above the bottom of the permanent casing, since fractures may be formed in the rock by installation of the casing, and a gap (void) may be produced outside of the permanent casing. Alternatively, the fractures or annular gap outside of the permanent casing can be grouted with a material that has a shear strength equivalent to or higher than that of the sandstone, and the lateral resistance for the rock can then be allowed to the surface of the grout or the sandstone, whichever is at the lowest elevation. This should not be assumed to apply to axial resistance, however.

PILE LOAD TEST IN ST. CROIX RIVER

It is anticipated that some of the piers for the bridge may be supported on driven piles. It is reported that the designers anticipate that pile foundations will be required to resist uplift loads and will therefore need to penetrate sufficiently into the founding geomaterial to generate uplift resistance in skin friction. Subsurface conditions on the Wisconsin side are generally conducive to penetration of the geomaterials with piles by driving, as a substantial thickness of muck and sand/gravel exist there above the sandstone. See Fig. 4. If driven piles are used, however, there is concern about the buckling resistance of the piles because much of the lateral resistance needed to inhibit buckling must be generated within the muck. A test pile was therefore driven in the St. Croix River and tested in compression to 400 tons axial load to evaluate the buckling load, following which it was tested in uplift to failure.

The contractor for the pile installation and the load test was also Case Foundation Company, Inc. The location of the pile test is shown in Fig. 3. The load tests, both in compression and uplift, were conventional top-loading tests that were accomplished with a hydraulic ram jacking against a reaction system that was constructed in the river. Loads were measured using a pressure gage which reportedly was calibrated with the loading ram against load. Pile head settlement, rotation of the pile head in two perpendicular planes and pile-head lateral displacement in two perpendicular directions were measured by GME, Inc., and Minnesota DOT personnel. Rotations were measured using a slope inclinometer, and deflections were read using mechanical dial gages.

Load Test Results

The idealized subsurface conditions used in analyzing the compression load test are shown in Table 4. This information was taken from Boring T-48, whose location is shown relative to the test pile in Fig. 3 and which is logged in detail in the Appendix. The SPT driving resistance varied from 47 to 68 blows per 0.3 m in the sand and gravel, which was the founding stratum for the test pile. The undrained shear strength profile within the muck layer from UU triaxial compression tests for Borings T-48 and T-43 is shown in Fig. 36. A conservative idealized profile, shown on that figure by the dashed line, was used in the analyses to evaluate buckling. The muck appears to be a normally consolidated

organic clay of recent origin. The idealized profile was therefore developed assuming a normally consolidated clay with $\phi' = 16^\circ$ with 14 psf of cohesion to represent the effects of slight aging. It was also assumed, since no data were given, that the axial strain at 50% of failure stress in the UU triaxial compression tests (ε_{50}) was 0.03 (3%). This parameter is a necessary input to the analytical model.

The values of effective unit weight in Table 4 are average measured values for the muck, which was sampled with sampling tubes and returned to the laboratory for testing. The buoyant unit weight γ' and effective angle of internal friction ϕ' for the sand and gravel are assumed based on judgment and the SPT blow counts, which suggest that the sand is medium dense to dense.

The pile itself was a 24-in.-diameter steel pipe pile with a conical driving shoe. Its final length after driving and cutoff was 119.5 ft. The pile is shown schematically within the soil profile in Table 4. Note that the pile does not penetrate to the surface of the sandstone, so that it was completely embedded in soil. The depths are shown from the head of the as-driven pile. The pile was filled completely with concrete seven days before it was tested. Concrete filling will theoretically increase the resistance of the pile to buckling. Other relevant data for the test pile are given in Table 5.

The pile was driven with a hammer and cushion for which documentation was not given. However, the pile was monitored with a pile driving analyzer during driving, and the resulting data were subjected to a "CAPWAP" analysis. The results, given in a separate report by Goble Rausche Likins and Associates (Nov. 1995), indicate that the compressive capacity of the pile at the time of driving was 749.6 k, or 375 tons. The pile was later restruck, but instrumentation necessary for acquisition of data by the pile driving analyzer failed, so it was not possible to determine the pile capacity upon redriving by that method. Anecdotally, the field superintendent for the contractor indicated that the pile drove harder for the last foot of penetration during restrike than it drove initially, indicating that the expected compression capacity should be in excess of 375 tons, probably in excess of the 400-ton maximum load prescribed for the compression load test.

The results of the compression test on the pile are shown in Figs. 37 and 38. These data are taken from a report on the load test provided by GME, Inc. (Nov., 1995), and by the Minnesota DOT.

In Fig. 37 are shown the load-settlement curve superimposed on relations between axial compressive load and horizontal translations of the pile head in two orthogonal directions. The loads were measured by means of a calibrated pressure gage on the hydraulic ram that applied the load, and the settlements and horizontal translations were measured by means of dial gages suspended from a reference frame constructed around the test pile and supported by three smaller driven piles founded in the soil at the bottom of the river. The jacking reaction consisted of water-filled tanks supported on a frame founded on piles in the soil at the bottom of the river that was constructed outside the reference frame piles.

In Fig. 38 are shown the measured load-settlement relation superimposed on relations between the axial compressive load and the rotation of the pile head in two orthogonal planes.

Analysis of the data in Figs. 37 and 38 to evaluate the buckling load in the pile was based on the following: If the pile had buckled during the compression load test, both the pile-head translation (in at least one direction) and the pile-head rotation (in at least one plane) would have experienced sudden increases as the axial load was increased, and these increases in translation or rotation would have continued at an increasing rate as further axial compression load was applied. While some changes can be seen in Figs. 37 and 38 in lateral deformations at the pile head at small loads, they did not increase at an increasing rate as more axial load was applied, suggesting that the observed lateral rotations and translations were the result of normal bending in the pile during loading, due to imperfect plumbness or lack of perfectly axial loading, and/or were the result of the tendency of the reaction system, which was not completely rigid, to translate laterally as it was loaded.

The fixity condition of the pile head is very important in evaluating buckling load. In the compression load test a swivel head was placed above the hydraulic ram to minimize moments at the pile head. If the pile head were fixed against any lateral translation, the head condition for buckling analysis would have been a "pinned-restrained" head condition (head free to rotate but not free to translate, which makes the pile very resistant to elastic buckling). The test data in Figs. 37 and 38 suggest that this condition did not exist. That is, the reaction system was flexible enough to permit lateral translation of the pile head when the pile was loaded axially. A second possible head fixity condition is the "pinned-free" head condition, sometimes referred to as the "flagpole" condition. In this case, the head is free of any moment and is also completely free to translate. Since the flexible reaction system undoubtedly provided some resistance to lateral translation of the pile head, this condition is unlikely. In fact, the head condition probably fell between the pinned-free and pinned-restrained conditions. Therefore, both conditions will be analyzed with the objective of bracketing the expected buckling load for the pile.

The results for the uplift test are shown in Fig. 39. The uplift resistance at 1.0 inches of movement was approximately 175 tons. No attempt was made to further analyze the uplift test results. If further analysis is to be performed by Minnesota DOT personnel, it should be remembered that the reported loads include the dead (mostly buoyant) weight of the pile and the concrete filler.

Analysis for Buckling

The axial compression load test was analyzed further using a numerical computer model known as *LPILEPLUS for Windows* (Ensoft, Inc., 1995). This model treats the pile as a two-dimensional elastic beam-column. The nonlinear resistance to lateral movement of the pile provided by both the muck and the sand/gravel was modeled with

standard p-y criteria available with the software. The Matlock static (non-cyclic) soft clay criterion with $\epsilon_{50} = 0.03$, and with other properties given in Table 5, was used to represent the muck. The sand was represented by the "Reese" static (non-cyclic) sand criterion, using the values for the inputs given in Table 5. Table 5 also gives the data for the pile itself that was used in the LPILEPLUS analysis. (The API p-y criterion for sand used to scale the p-y curves for the drilled shaft socket tests is also available in LPILEPLUS, but the algorithm for using that criterion computationally has not been extensively checked and, for that reason, was not used in the LPILEPLUS analysis for buckling of the pile.) Static, not cyclic, p-y criteria were used because the buckling process is viewed as a one-time extreme event loading phenomenon. Degradation of the soil due to prior cyclic loading to the same lateral deflection as will occur at buckling, which is modeled in the cyclic p-y criteria, will not have occurred and will therefore not affect the lateral resistance in the soil at buckling.

LPILEPLUS was utilized with both of the head constraints described in the previous section. The results for the pinned-free head case are shown in Fig. 40. A very small head shear was applied in addition to increasing axial load in order to produce the initial lateral deflection necessary to initiate buckling. A sudden increase in lateral deflection occurred at about 300 tons axial load. Above about 320 tons axial load, the mathematical solution did not converge. Only after the axial load was increased above 370 tons did the solution once again converge; however, the lateral deflection was negative. With further increases in axial load the value of the negative head translation decreased. This behavior is indicative of buckling. It is therefore concluded that the buckling load for the pinned-free head condition is approximately 325 tons. This is the lower theoretical limit for elastic buckling load for a pile of the type tested here, considering the constraining effects of the muck and the sand/gravel with the pile having the length and driven to the position relative to the soil layers indicated in Table 4.

Fig. 41 shows the lateral displacement pattern along the pile determined from the LPILEPLUS analysis described above for the pinned-free head condition at an axial load of 300 tons. Most of the lateral deflection decays between the top and bottom of the muck layer, which indicates that the muck provides substantial lateral resistance and aids materially in the inhibition of buckling. The soil reactions that result from the deflection pattern in Fig. 41 are shown in Fig. 42. The maximum soil reaction, at a depth of about 560 inches is 36 lb per inch along the pile, or 1.5 psi (for a 24-in.-diameter pile). This is less than the ultimate lateral resistance that is predicted by Matlock's criterion at that elevation, where the undrained cohesion, c , of the muck is 0.64 psi. Matlock's criterion gives an ultimate lateral resistance of about 2.0 psi at that elevation. Above that elevation, the soil is approximately in a failure state, since c varies linearly with depth. Below that elevation, the soil is not in a failure state.

The LPILEPLUS solution for the same problem, but for the case of a pinned and laterally restrained pile head, is shown in Fig. 43. In this case, the elastic buckling load increases enormously to 3490 tons, which is well beyond the structural "squash load" of the pile. Reviewing Figs. 40 and 43, the buckling load should have been between 325 and

3490 tons. The test revealed that it was at least 400 tons, which is reasonable according to the LPILEPLUS simulations.

It is assumed that design personnel will check driven piles for buckling stability assuming the piles to be equivalent cantilevers. The results of the LPILEPLUS simulations can be used to estimate the locations of the apparent depth of fixity below the pile head for the test pile. The buckling loads obtained from the LPILEPLUS analyses, termed P_{cr} , were applied to simple elastic buckling formulae for cantilevered beam-columns to compute the depth to fixity, L_f , as summarized in Table 6. The results depend somewhat on the way in which the fixity of the pile head is modeled. If the maximum load applied in the test, 800,000 lb, is used as P_{cr} for the pinned-free condition, L_f becomes 62.8 ft, and depth to fixity below the top of the muck becomes 33.3 ft. For the pinned-restrained condition, L_f becomes 54.9 ft, or 25.4 ft below the top of the muck, for $P_{cr} = 800,000$ lb. It is suggested that fixity could be considered conservatively to be at 33.3 feet below the top of the muck for the pile tested at this test site. Note that changing the pile diameter, pile penetration, pile material properties, moment of inertia and/or soil properties will change the apparent fixity depth.

Some question exists regarding whether the depth to fixity should be adjusted for group action if piles are to be driven in clusters or groups. It is possible that two or more adjacent piles in the group could buckle simultaneously in the same direction, thereby mutually reducing the lateral resistance in the soil around each pile and effectively increasing the depth of the apparent point of fixity. Simultaneous buckling of piles is most likely when adjacent piles are loaded almost identically. This effect should be considered in the design of the piles.

SUMMARY

The following salient points are summarized.

1. All data used in the analyses reported here were obtained from others. The assumption was made that all such data were true and correct; however, the authors make no representation that any data are valid. Where no data existed, assumptions were made about values of parameters necessary to perform the analyses. The authors also make no representation that such assumptions are correct.
- 2.. Any application of the test results, scaled or unscaled, to design conditions for drilled shafts sockets depends upon the properties (density, permeability, internal friction and cohesion) of the friable sandstone being equivalent at the site of the prototype drilled shaft socket and at the test site. The authors make no representation that such is the case anywhere on the bridge site.
3. Furthermore, since no load tests were conducted in other than friable sandstone in the Franconia formation, no representation is made that any application of the test results, scaled or unscaled, to design of drilled shaft sockets in non-friable sandstone (e. g.,

glauconitic sandstone, which commonly interbeds with the friable sandstone in the St. Croix River) is valid.

4. Several details of construction appeared to influence the behavior of the test foundations, or to have the potential to influence their behavior. These should be considered when developing construction specifications for the prototype foundations.

a. Drilling slurries that can clog the pores of the rock should not be used in the rock sockets in the sandstone. If drilling takes place under water, the head of the water in the borehole should be kept continuously at or above the phreatic surface in the formation.

b. Placement of concrete under water is acceptable, provided the concrete has a slump in the range of 8 - 9 inches. Concrete used in drilled shafts should have a slump of at least 4 inches for a period of four hours after batching. No more than seven days should be permitted between opening of a socket and concreting of the socket if the socket remains under water.

c. The slump of the concrete in place at any elevation within a socket should remain at least 6 inches until at least 30 feet of concrete has been placed above such elevation.

d. Prior to placing concrete, the base of the socket should be thoroughly cleaned of loose debris and sediment. No more than one-half inch of sediment should be permitted on the bottom of the socket at the time of concrete placement.

Comment: The contractor who constructed the test sockets could not meet this criterion. However, the test sockets were placed in approximately 135 feet of open borehole (below about 47 feet of surface casing), with only water as a drilling fluid to maintain hole stability. The boreholes were also open for 15 to 17 days before the sockets were concreted. These conditions appeared to contribute to sloughing in the boreholes for the test shafts. Much less distance should exist between the bottom of the casing and the bottom of the borehole in the prototype shafts and presumably the time required to drill and concrete each socket should be less.

e. Casing should neither be screwed, vibrated nor otherwise placed into the rock or soil, nor unscrewed, vibrated or otherwise removed from the rock or soil more than 4 hours or less than 24 hours after concrete has been placed in the shaft being constructed or in any other shaft within three shaft diameters clear spacing of the shaft that is being constructed.

Comment: This requirement is to protect very green concrete from damage due to movement of the ground produced by installing or extracting casing.

e. The roughness of the prototype rock sockets should be equivalent to or better than that of the test socket. In order to achieve this condition, it is recommended that either the final socket excavation be performed with an auger that will not produce a smooth borehole (i. e., a standard rock auger of the type used by the contractor on the test

sockets) or that an artificial roughening tool be used to scarify the walls of the borehole (e.g., if a core barrel or coring casing is used to advance the excavation).

f. The specific gravity of the drilling water in the socket, if any, should be no greater than 1.02; the Marsh funnel viscosity should be no greater than 27.5 seconds/quart; and the sand content should be equal to or less than 0.25%.

Comment: These values are based on measurements in the test sockets two days after completion of drilling.

g. Consideration should be given to performing structural integrity tests on completed drilled shafts. A nondestructive evaluation method not involving longitudinal low-strain stress-wave measurement, such as the cross-hole ultrasonic method (which measures concrete modulus) or the gamma-gamma logging method (which measures concrete density), is recommended. In such tests, tubes are cast into the shaft at the time of construction and instruments lowered down the tubes after concreting.

h. Driven piles should be appropriately monitored for driving resistance during installation to verify the design axial resistance.

5. The following values of maximum unit side shear resistance (no factor of safety applied) appear to be appropriate for 8-ft-diameter drilled shaft sockets in compression in the St. Croix River based on the on-shore load test:

- a. 2 feet below top of sandstone: 3.3 tsf
- b. 30 feet below top of sandstone: 4.5 tsf

Linear interpolation can be used between these depths for design purposes. If the penetration is required to be deeper than 30 ft, a value of 4.5 tsf should be used below 30 ft of penetration unless further analyses are conducted.

Comment: These values correspond to movements in the order of 1.0 in. Reduction of these values by a factor of safety will reduce the corresponding settlement about the same ratio as the reduction in resistance, since the axial unit load transfer vs. movement relations were nearly linear. These values apply to one-way cyclic loading as well as to static loading. They may be applied to sockets with nominal diameters smaller than 8 feet, but not to sockets with larger diameters without further analysis.

Comment: The above values and commentary do not consider the effects of group action. Group action should be checked to assure that block failure does not occur. Settlements of an axially loaded socket within a group of drilled shaft sockets may be larger for a given load than indicated here.

6. For purposes of computing side shear resistance in a rock socket, the top of the socket should be considered to begin 2 ft below the top surface of the sandstone. If either a permanent or a temporary casing penetrates more than 2 feet below the top of the sandstone during construction, then the top of the socket should be considered to begin at the depth of the bottom of the deepest casing.

7. The information on end bearing from the axial test socket was meager. It appears that trapped sediment existed under the reaction socket for the test; however, it also appears that a value of gross end-bearing pressure of 9.7 tsf (8 to 10 tsf) would be appropriate at a depth of 30 feet into the sandstone or 7.7 tsf 20 feet into the sandstone under working load conditions (0.25 - 0.50 in. settlement) for the production shafts, provided the base of the shaft is clean according to the standards given above and there does not exist weaker rock below the base of the socket than exists at the base of the socket.

8. Because of the need for scaling of the test results to conditions in the St. Croix River, the meager data on end bearing, and the unusual, extremely ductile behavior of the axial test socket, the Minnesota DOT should consider verifying the capacities of the prototype test shafts by placing bottom-hole load cells, such as the Osterberg Cells used in the test sockets, at the bases of a representative number of the production sockets for the bridge piers, and loading such sockets to at least 1.5 times their design loads prior to placing any drilled shaft caps or superstructure elements. Corresponding measurements of socket movement should be made, and minimal instrumentation should be installed to delineate resistance in the rock socket from resistance developed in the sand/gravel and the muck. Following any such tests, the load cells and any annular space around such cells should be grouted with high-strength grout.

9. Lateral load behavior for both driven piles and drilled shafts can be analyzed using COM624P, LPILE, or similar software. Conventional p-y curves can be used to represent the muck (Matlock's soft clay criterion) and the sand/gravel (Reese's sand criterion). Cyclic versions of these criteria should be used if the critical lateral loading is cyclic.

The p-y relation developed in this report for the sandstone is as follows. This relation can be used for static loading or for several major one-way cycles of loading.

$$p = Ap_u \tanh \sqrt{\frac{E_s}{Ap_u}} y , \quad (4)$$

where

$$p_u (\text{lb/in.}) = (1.4z(\text{in.}) + 2.2D(\text{in.}))\sigma'_v (\text{psi}) \leq 17.7D(\text{in.})\sigma'_v (\text{psi}) , \quad (7)$$

and

$$E_s = E_{s \text{ test}} \sqrt{\frac{\sigma'_v \text{ test}}{\sigma'_v z}} = 54,130 \sqrt{\frac{\sigma'_v z (\text{psf})}{11780}} (\text{lb/in./in.}) . \quad (8)$$

The reader is referred to the main text for the definition of terms.

Lateral resistance in the sandstone should be assumed to exist only below the bottom of the permanent casing unless grout is placed outside the casing, as indicated in the main text. Whether lateral resistance can be used in the sand and gravel and the muck depends on whether the method of construction will produce an integral contact between the soil and the permanent casing. If the casing is driven or vibrated into place, and the soil removed from inside the casing after installation, conditions will be favorable for using lateral resistance in the soil. If the casing is set by first drilling an oversized borehole in the soil and then setting the casing in the borehole, lateral resistance should not be used in the soil.

Comment: The above relations do not consider the effects of group action. Appropriate references are available for reducing p and y values for laterally loaded piles in close proximity to one another depending on spacing and relative position of piles. One such reference is Brown and Shie (1991).

10. The muck provided substantial lateral resistance against buckling of the driven test pile. The test suggests that 24-inch diameter steel piles, with 3/4 inch walls and backfilled with concrete with f'_c equal to or greater than 3500 psi may be analyzed for buckling assuming they are cantilevered beam-columns with fixed ends 33.3 feet below the top of the muck. Appropriate consideration should be made of group action during buckling and of the type of fixity that will exist between the production piles and the substructure (e. g., pile cap).

REFERENCES

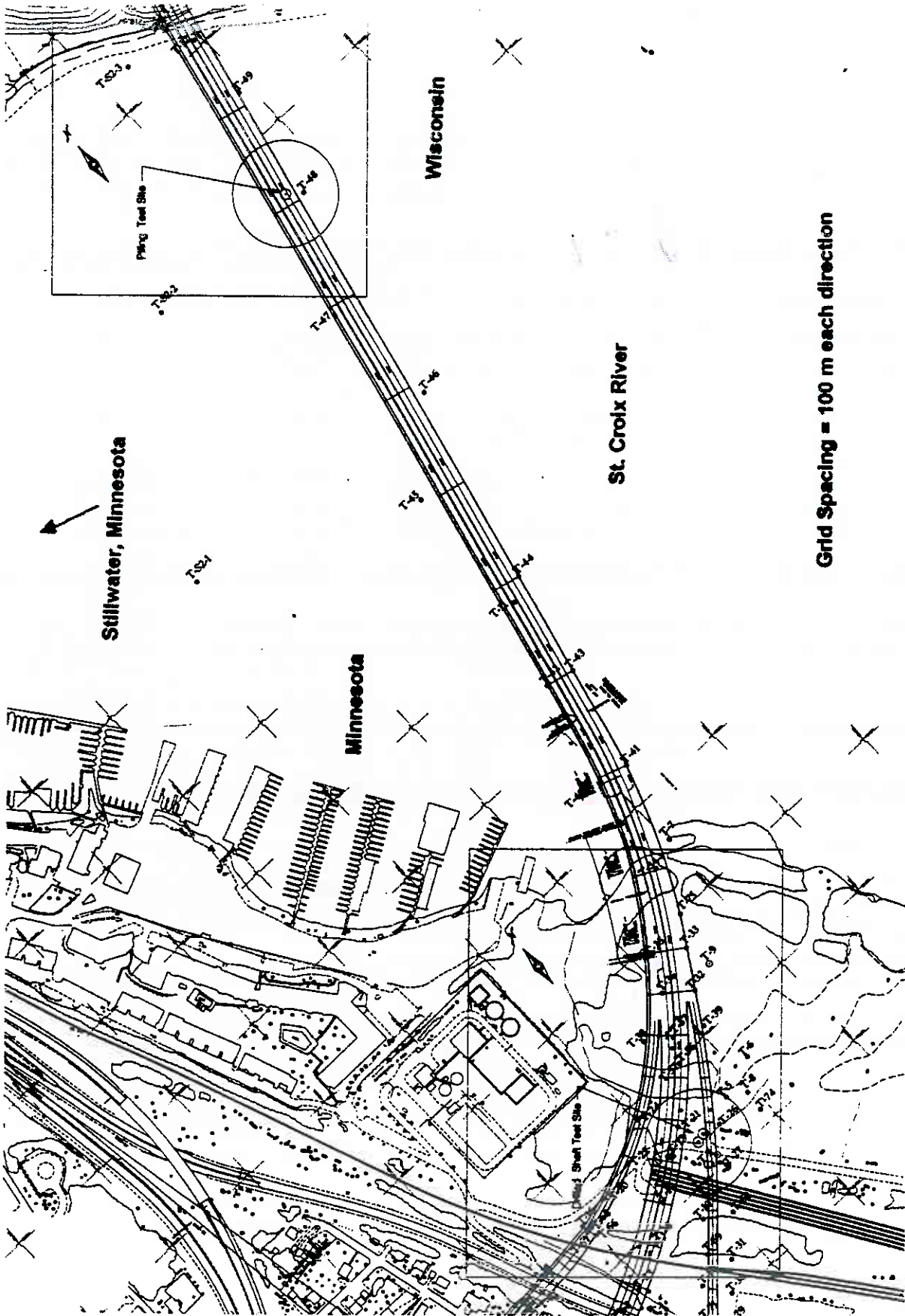
- Brown, D. A., and Shie, C-F, "Modification of p-y Curves to Account for Group Effects on Laterally Loaded Piles," *Proceedings, Geotechnical Engineering Congress, ASCE Geotechnical Special Publication No. 27*, ASCE, Vol. I, 1991, pp. 479 - 490.
- Duncan, J. M., and Chang, C-Y, "Nonlinear Analysis of Stress and Strain in Soils," *Journal of the Soil Mechanics and Foundations Division, ASCE*, September, 1970, pp. 1629 - 1653.
- Ensoft, Inc., *LPILE^{PLUS} for Windows*, Version 2.0, Austin, TX, 1995.
- GME, Inc., Report on Pile Load Test in St. Croix River (informal), Minnesota DOT, November, 1995.
- Goble Rausche Likins and Associates, Inc., Report on CAPWAP Analysis of Pile in St. Croix River (informal), Minnesota DOT, November, 1995.
- Janbu, N., Bjerrum, L., and Kjaernsli, B., *Publication No. 16*, Norwegian Geotechnical Institute, Oslo, 1966, pp. 30 - 32.
- Loadtest, Inc., Report on Osterberg Cell Load Tests at St. Croix River Site (informal), Minnesota DOT, November, 1995.

Murchison, J. M., and O'Neill, M. W., "An Evaluation of p-y Relationships in Sands," A Report to the American Petroleum Institute (PRAC 82-41-1), *Report No. GT-DF02-83*, Department of Civil Engineering, University of Houston, May, 1983, 174 pp.

O'Neill, M. W., Townsend, F. C., Hassan, K. M., Buller, A., and Chan, P. S., "Load Transfer for Drilled Shafts in Intermediate Geomaterials," *Report No. FHWA-RD-95-172*, Federal Highway Administration, Washington, DC, December, 1995, 184 pp.

Seidel, J. P., *Program ROCKET*, Department of Civil Engineering, Monash University, Melbourne, Australia, 1994.

Wong, D. O., "Design and Analysis of an Apparatus to Simulate Density and Stresses in Deep Deposits of Granular Soils," Unpublished Master's Thesis, Department of Civil Engineering, University of Houston, August, 1985, 133 pp.



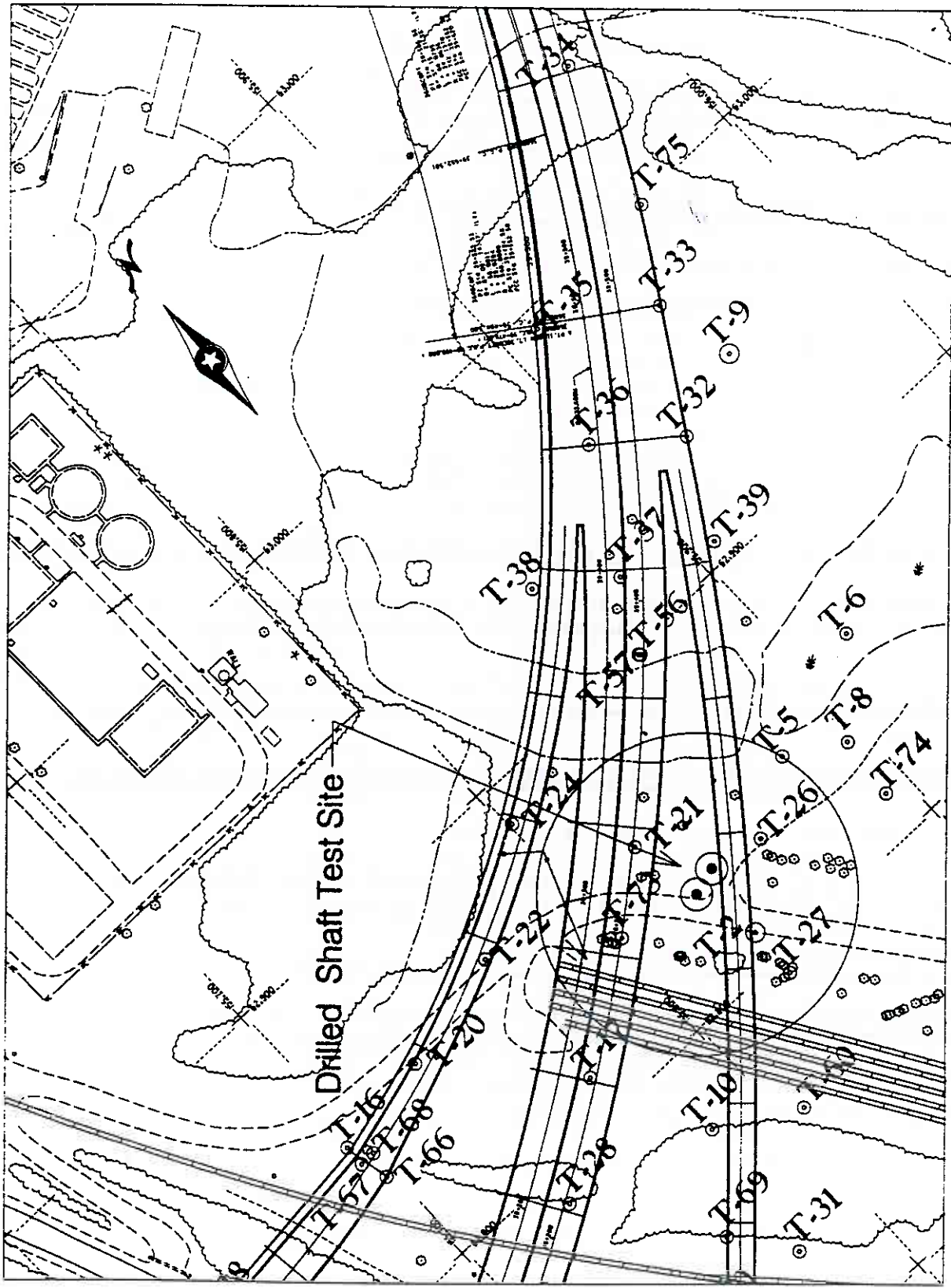
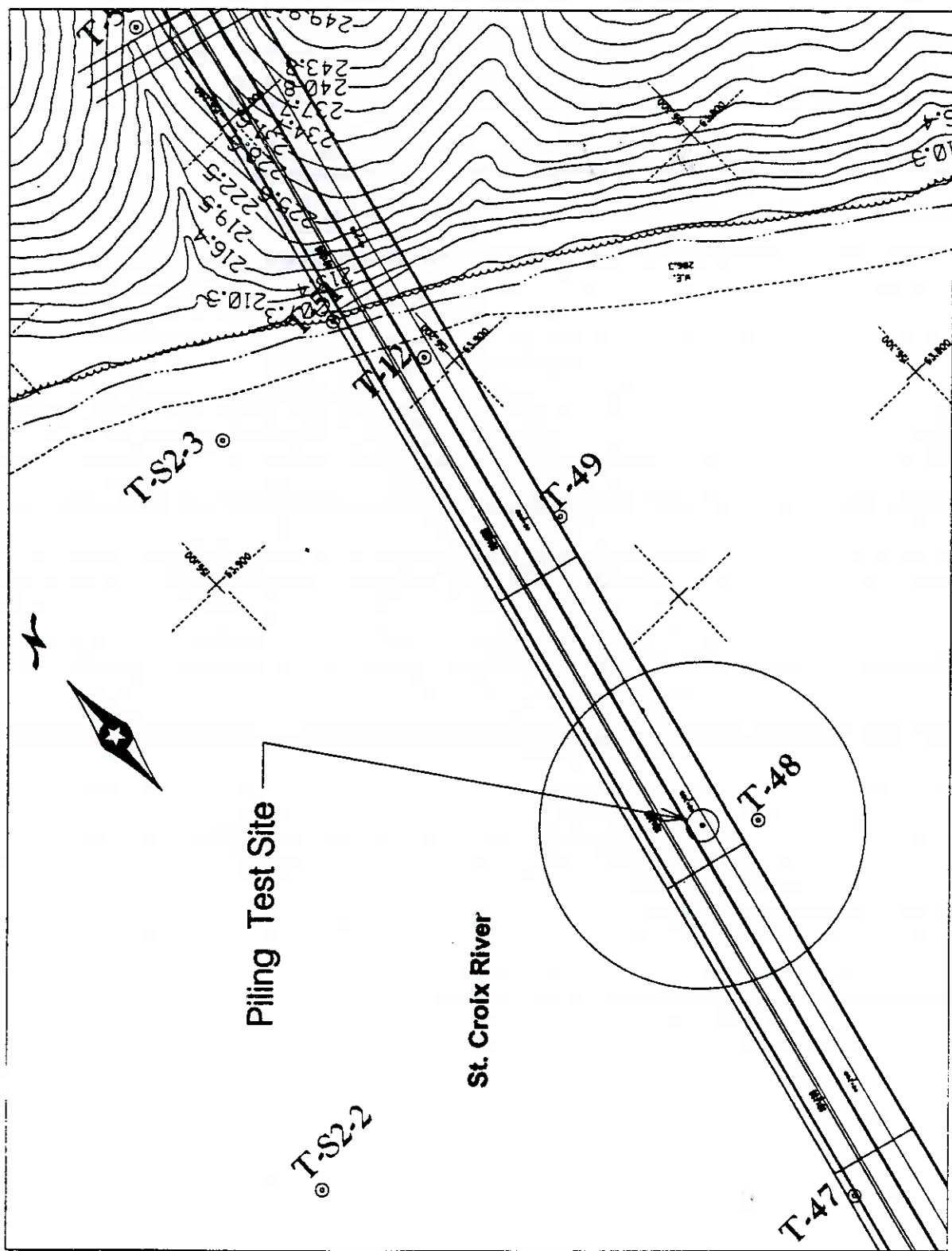


Fig. 2. Small-Scale Plan of Drilled Shaft Test Site

Fig. 3. Small-Scale Plan of Piling Test Site



PROFILES OF TEST AND PROTOTYPE CONDITIONS

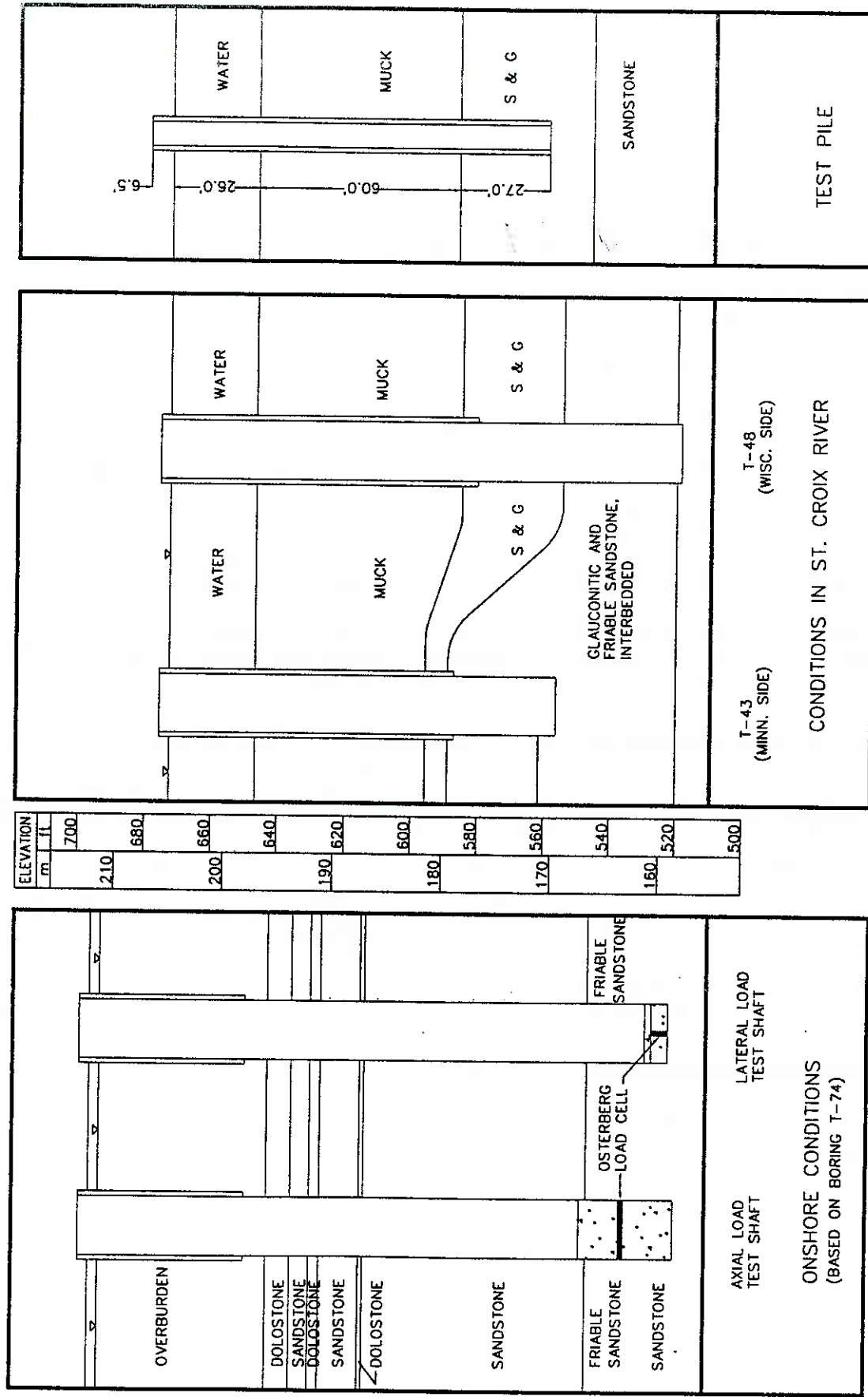


Fig. 4. General Profile of Test Elements and Possible Bridge Pier Foundations

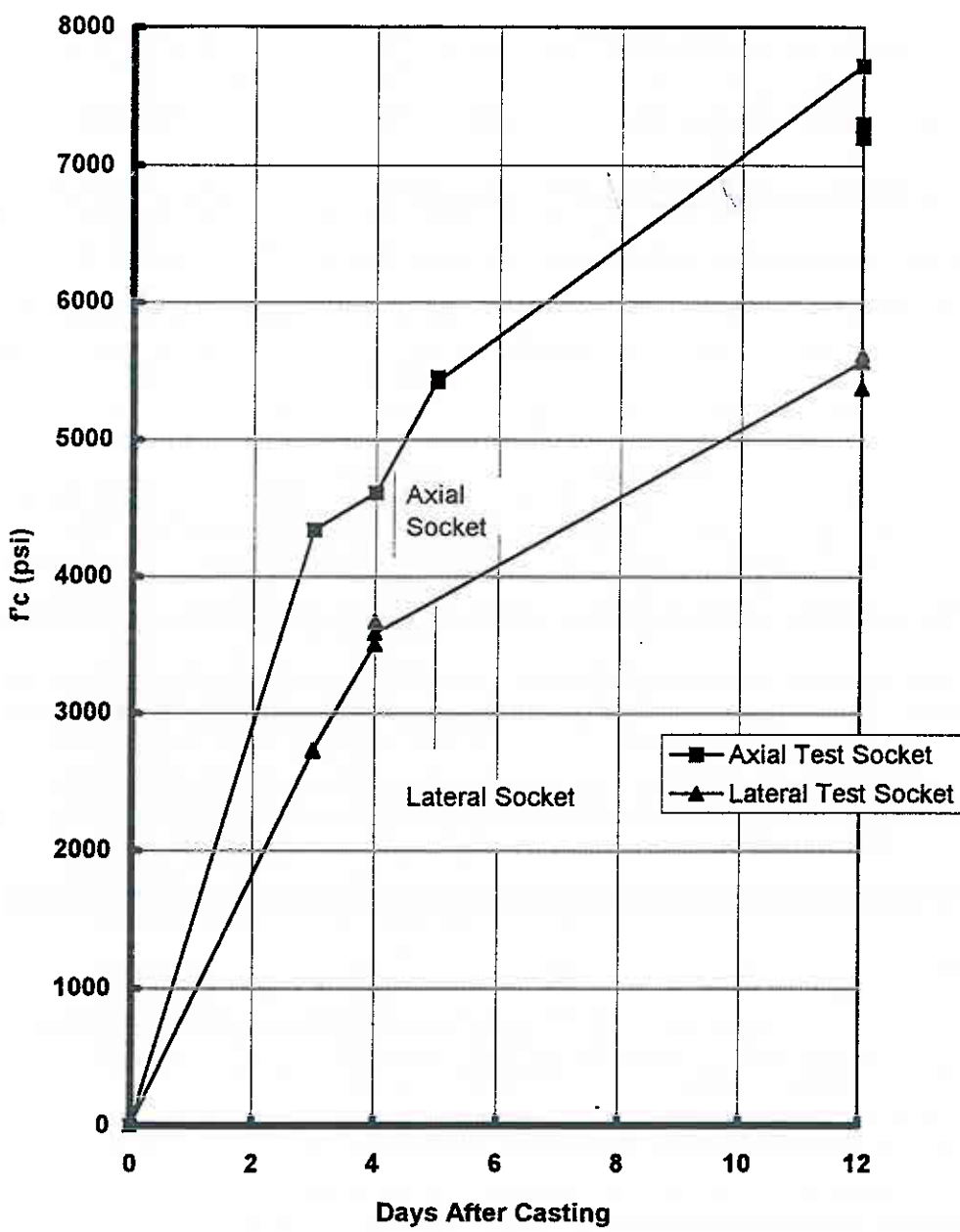
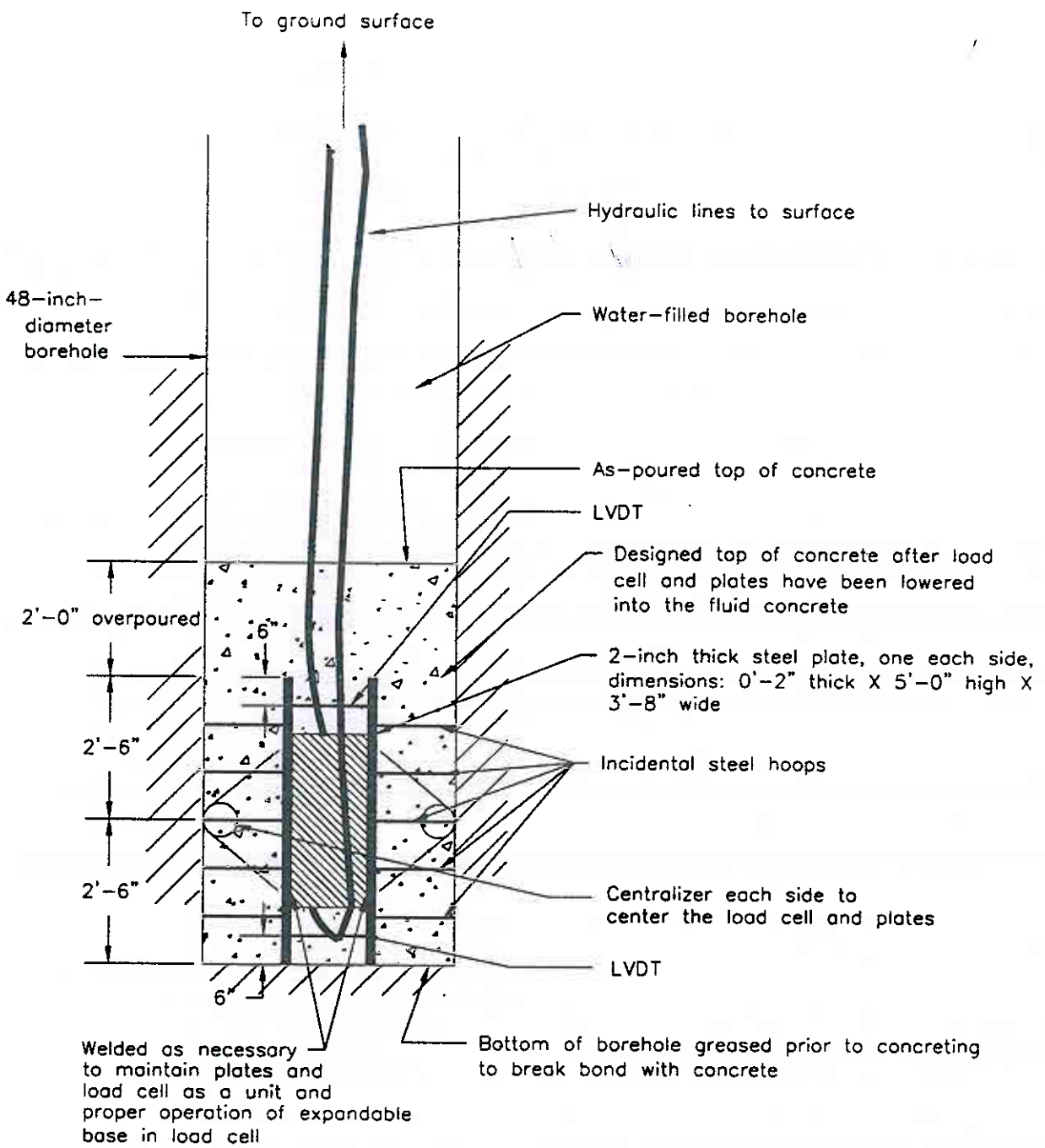


Fig. 9. Concrete Cylinder Strength Vs. Days After Sampling



NOT TO SCALE

Fig. 12. Schematic Side Elevation View of Lateral Test Socket

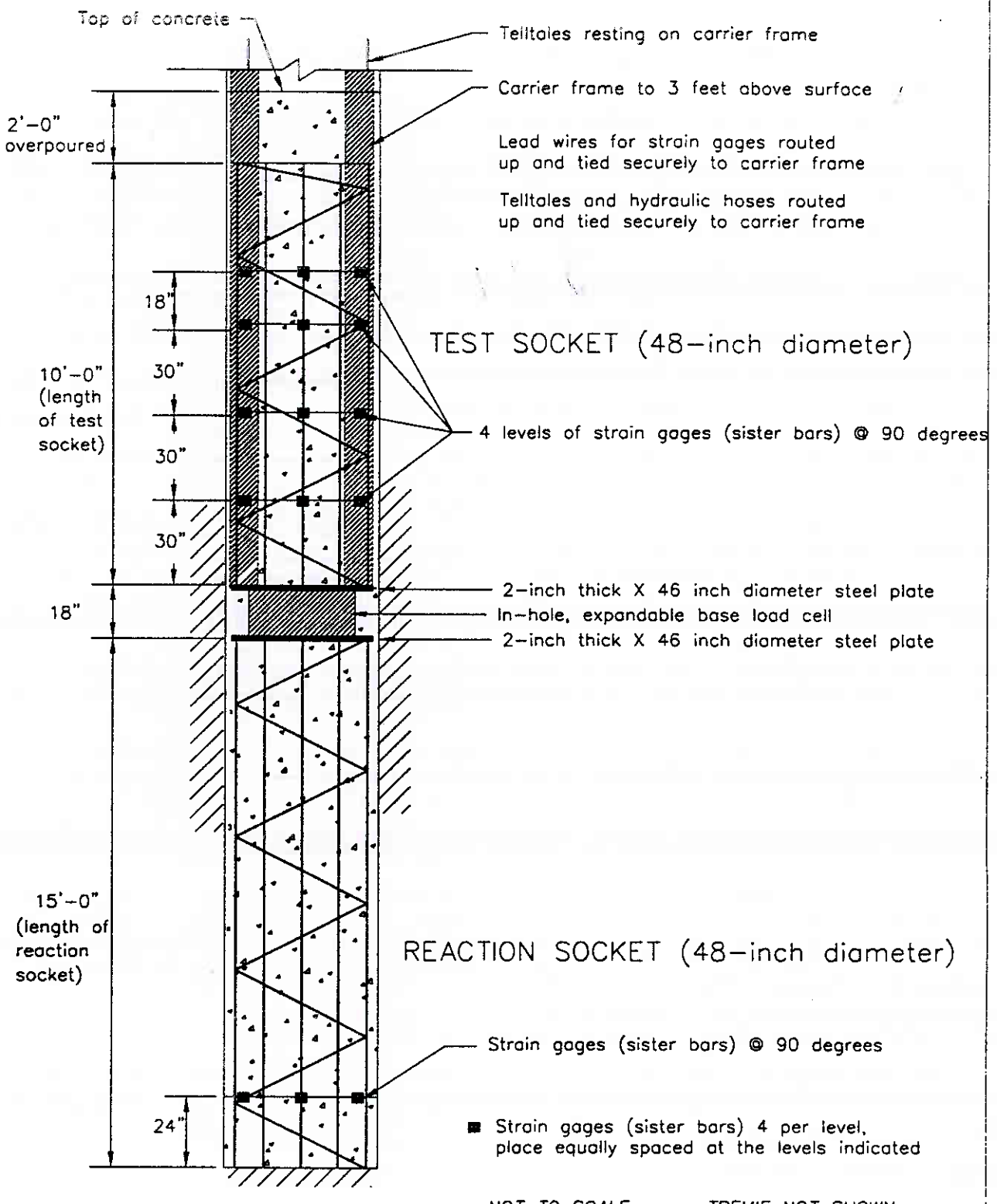
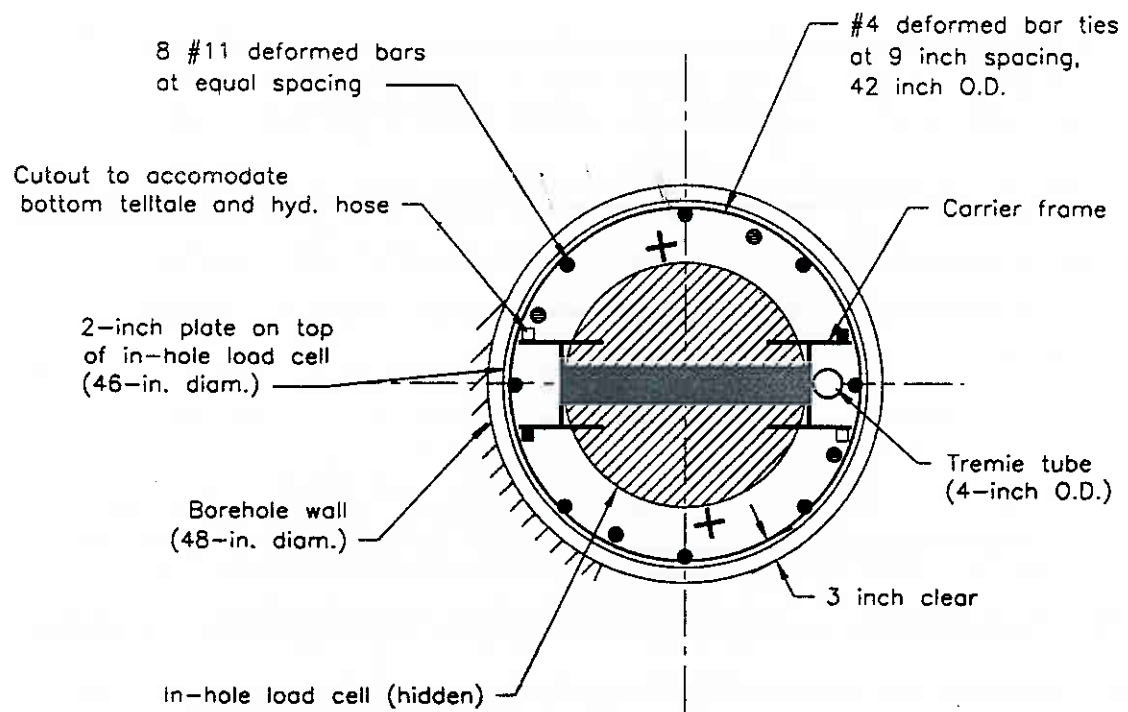


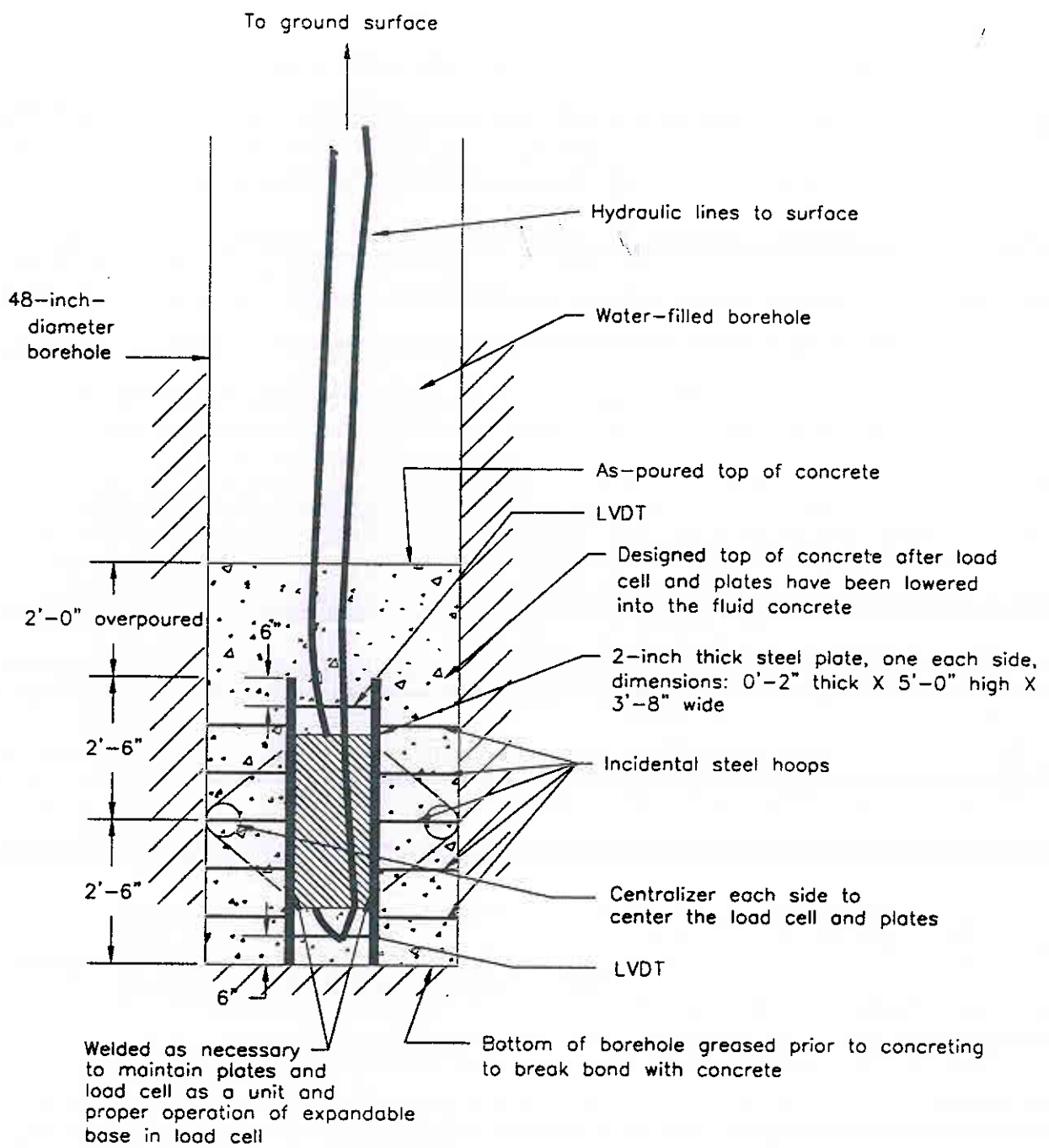
Fig. 10. Schematic Elevation of Instrument Location on Axial Test and Reaction Sockets.



- Strain Gages (sister bars)
- Telltales for upper plate
- + Telltales for socket compression
- Telltales for cell expansion

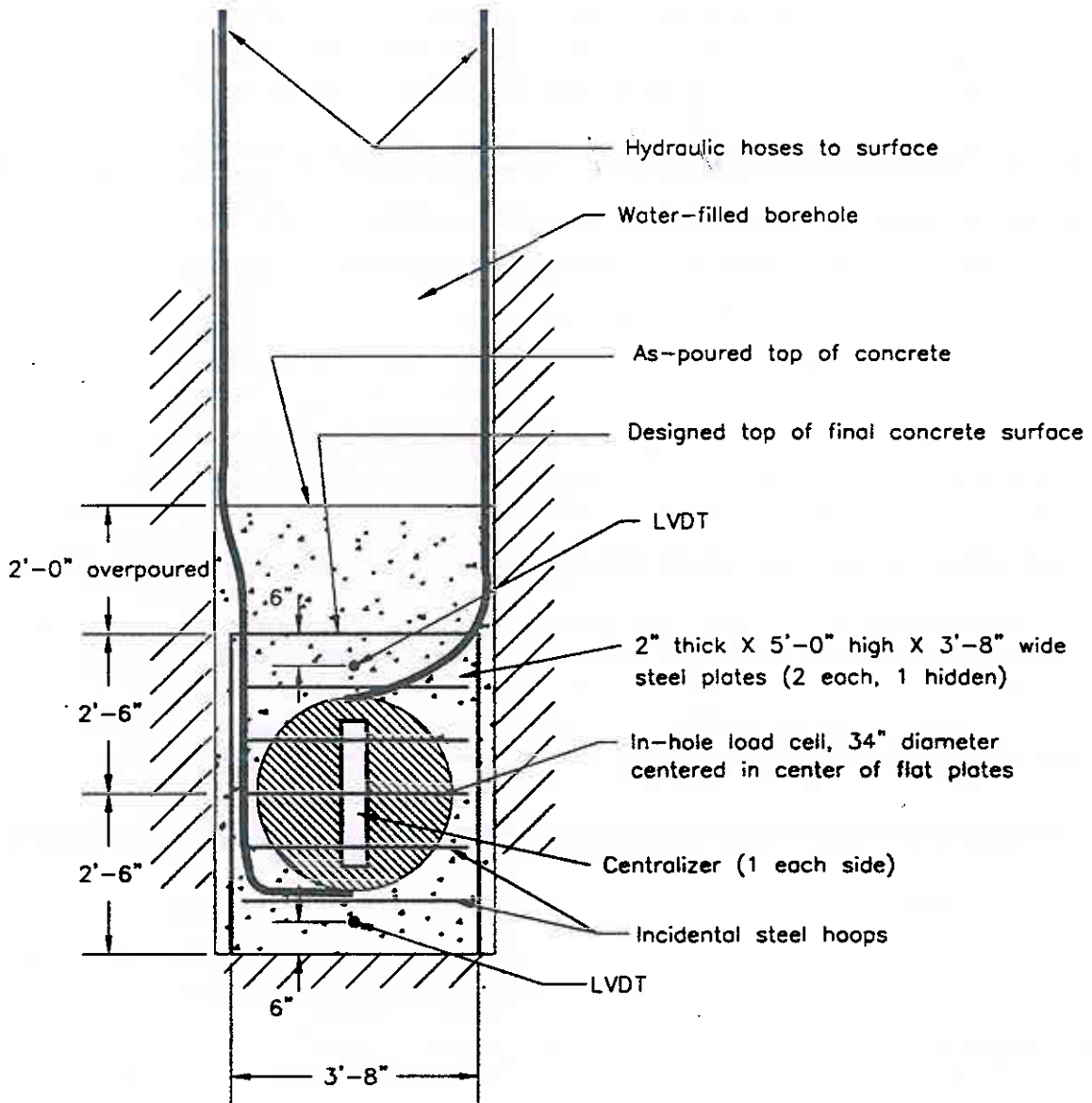
NOT TO SCALE

Fig. 11 Schematic Plan View of Test Socket Instrumentation Cage and Load Cell For Axial Test Socket



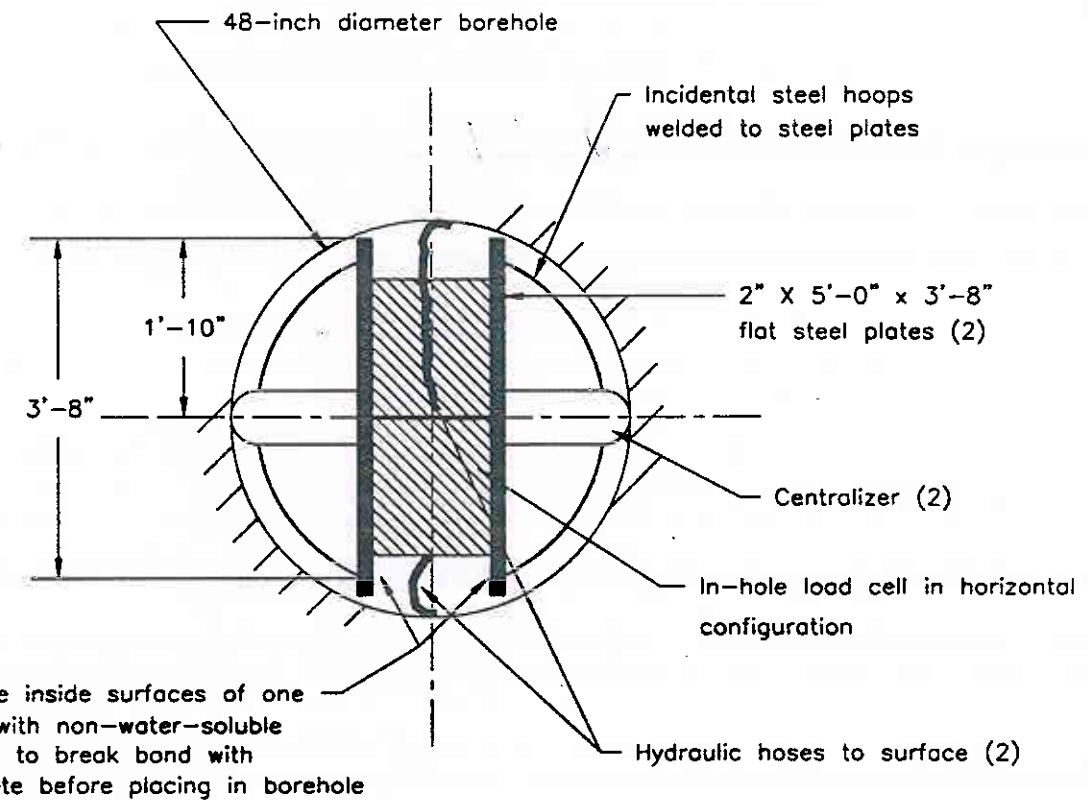
NOT TO SCALE

Fig. 12. Schematic Side Elevation View of Lateral Test Socket



NOT TO SCALE

Fig. 13. Schematic Front Elevation View of Lateral Test Socket (Rotated 90 degrees from Figure 12)



NOT TO SCALE

Fig. 14. Schematic Plan View of Lateral Test Socket

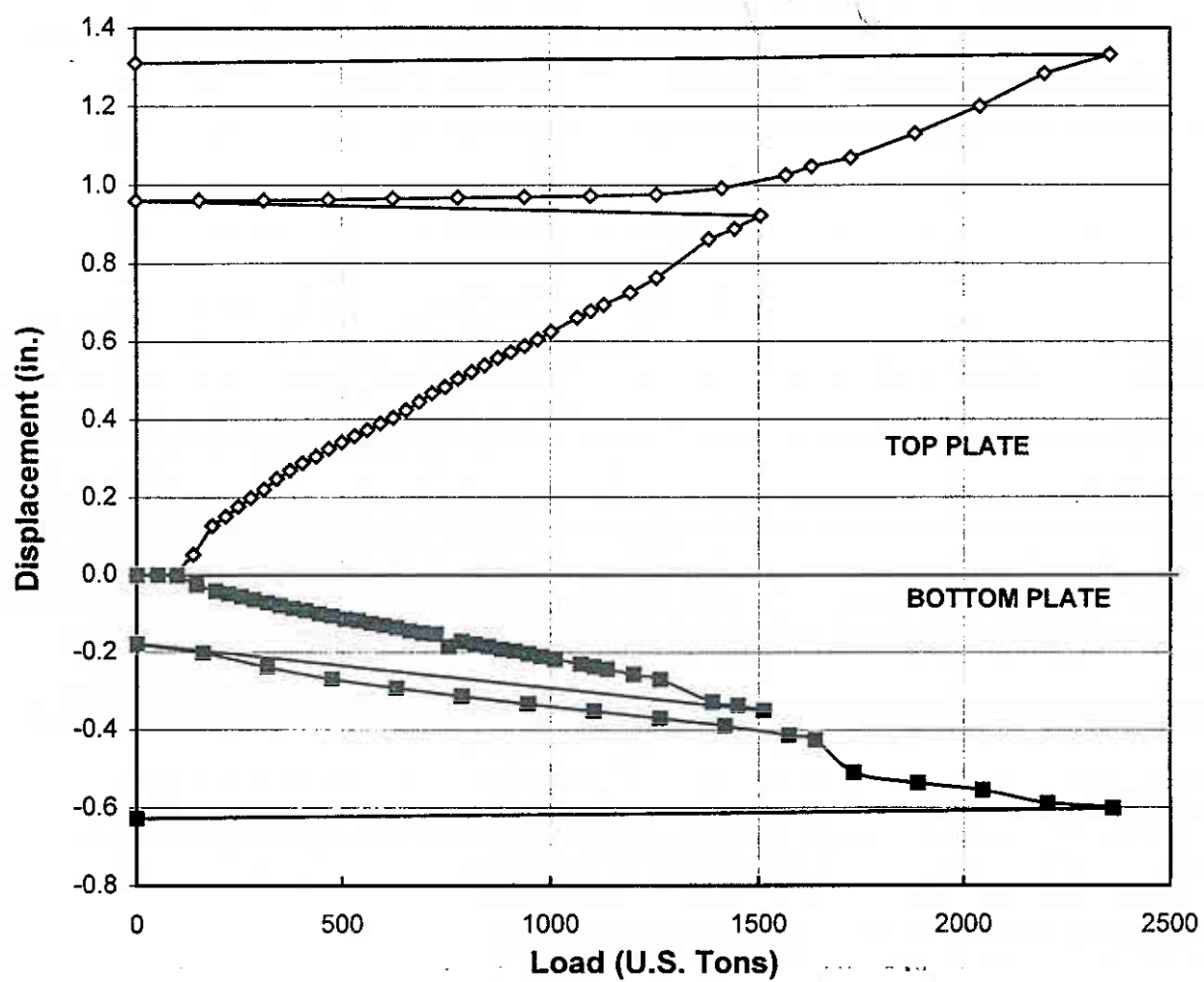


Fig. 15. Measured Load-Movement Relationship for Test Socket (Top Plate) and Reaction Socket (Bottom Plate) for Axial Socket Test.

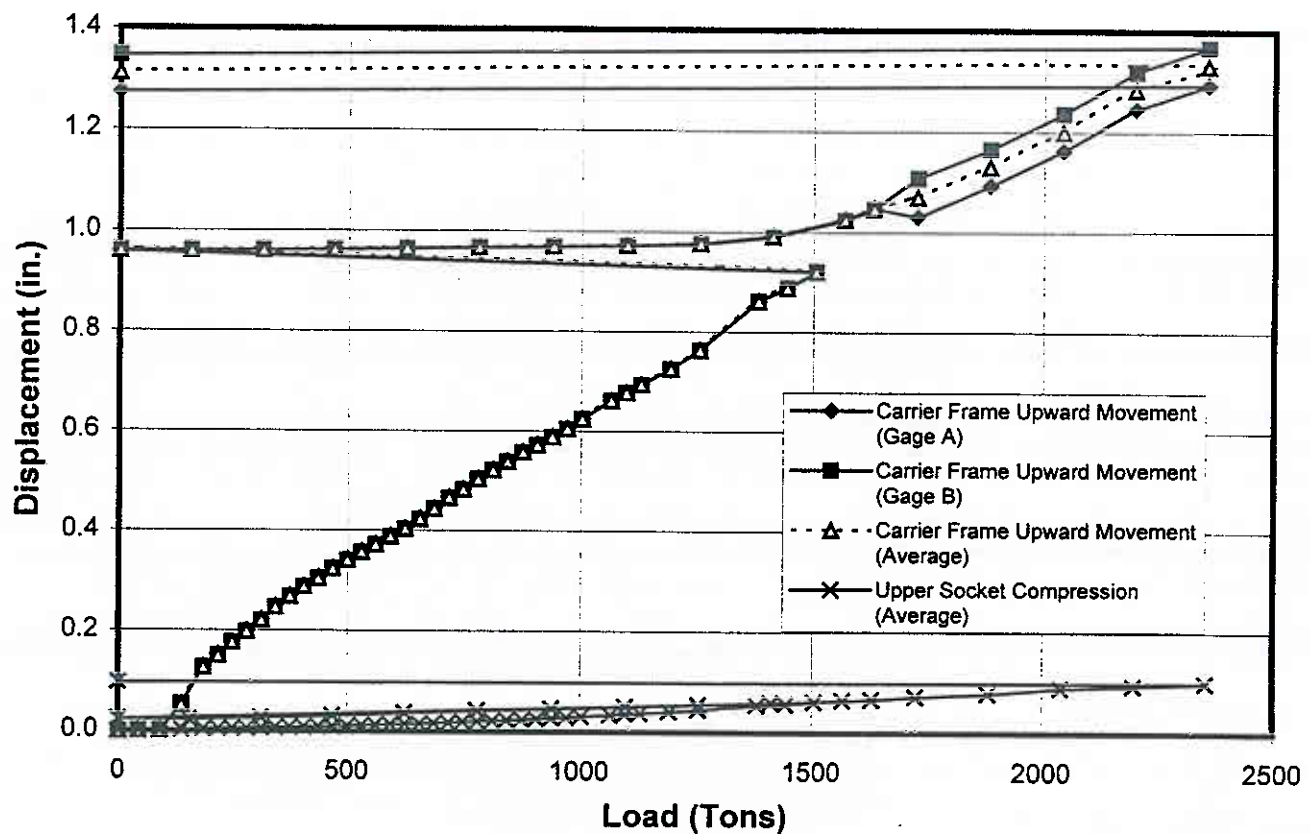


Fig. 16. Measured Load (Net Load Registered by Osterberg Cell) Vs. Movement of Top Plate and Compression of Test Socket

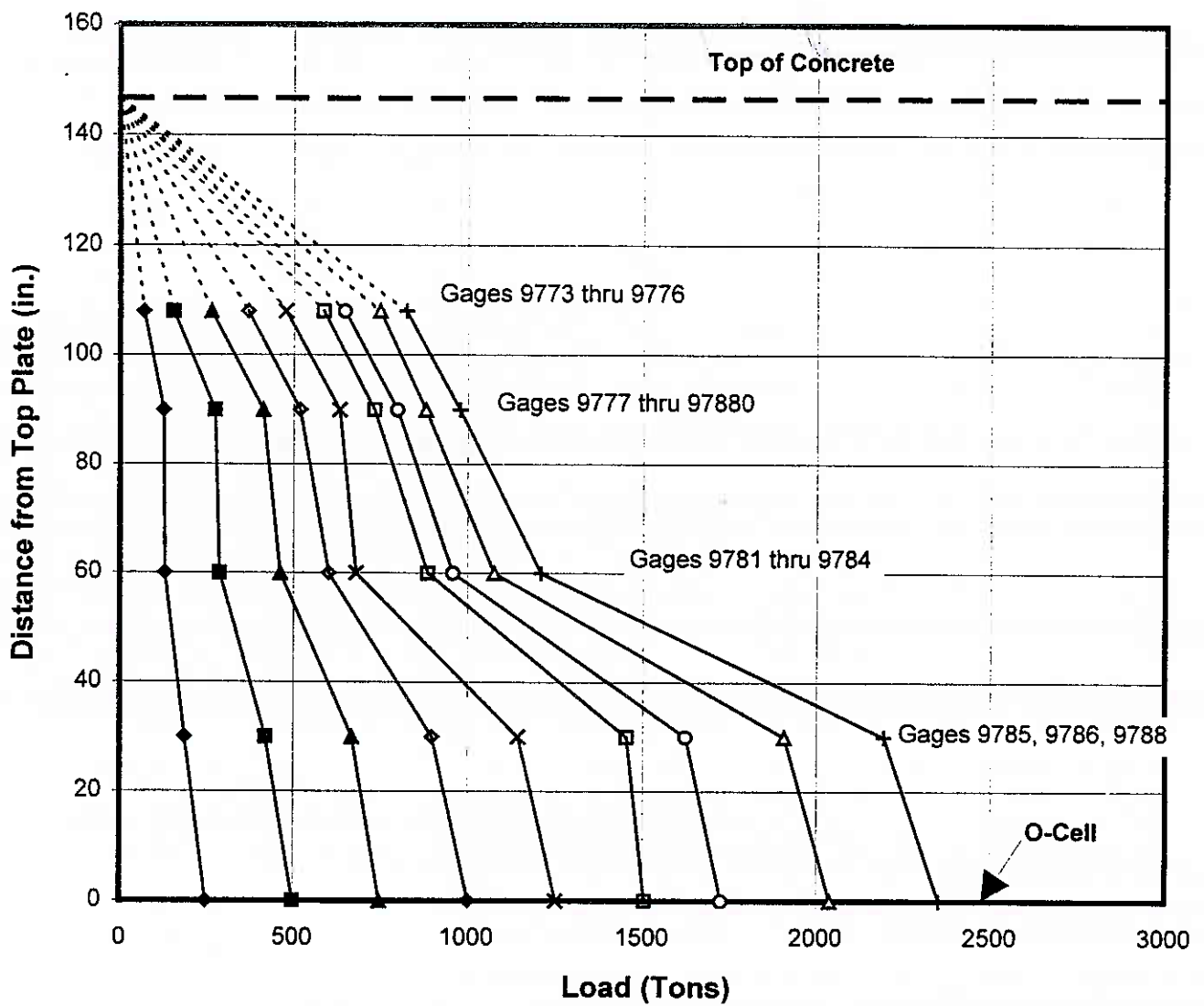
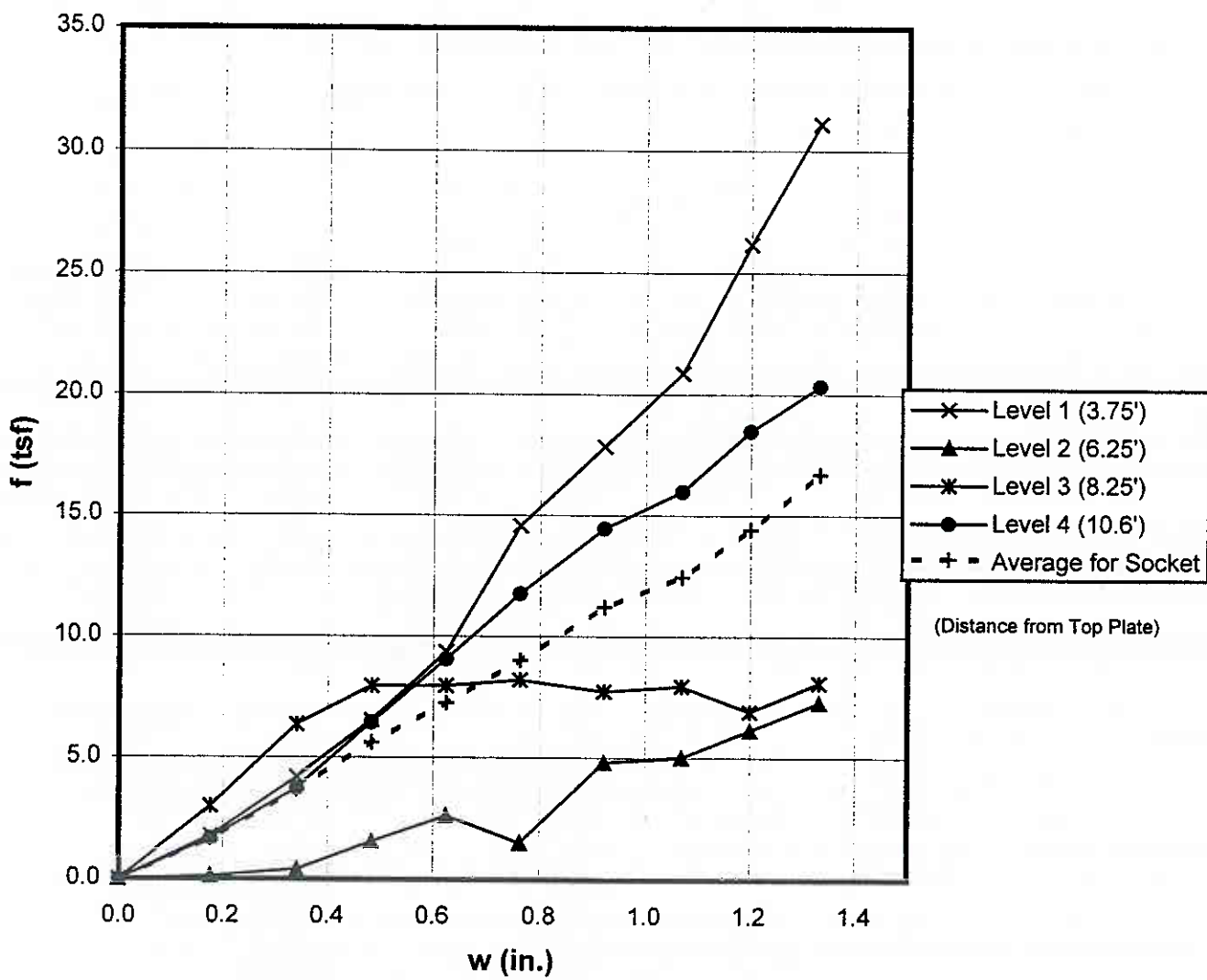


Fig. 17. Measured Load (Net Load Registered by Osterberg Cell) Vs. Depth in Axial Test Socket Derived from Test Data



**Fig. 18. f-w Relations for the Four Intervals in Axial Test Socket
Derived from Test Data**

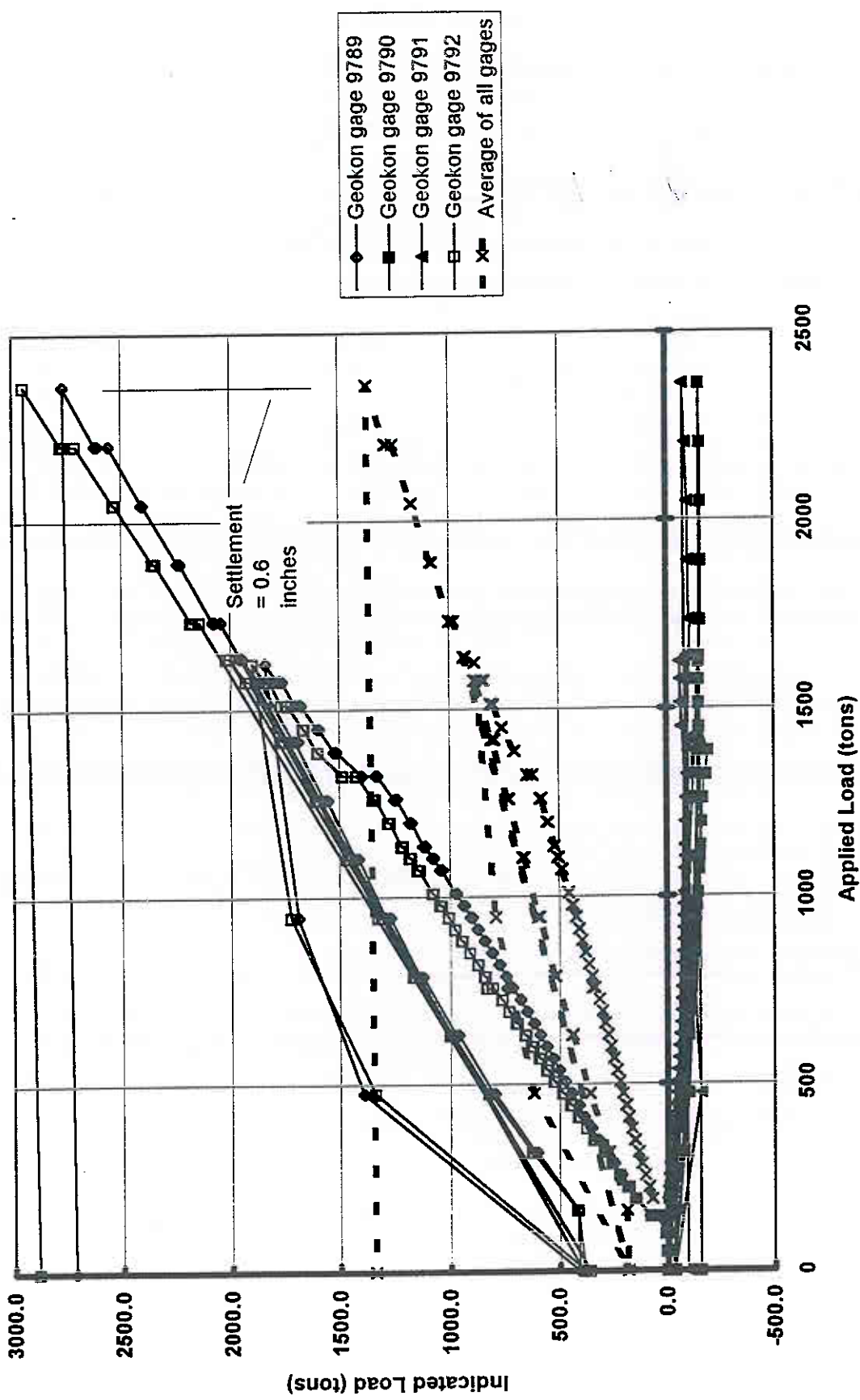


Fig. 19. Registered Osterberg Cell (Applied) Load vs. Load Indicated by Geokon Gages 0.6 m above Base of Reaction Socket

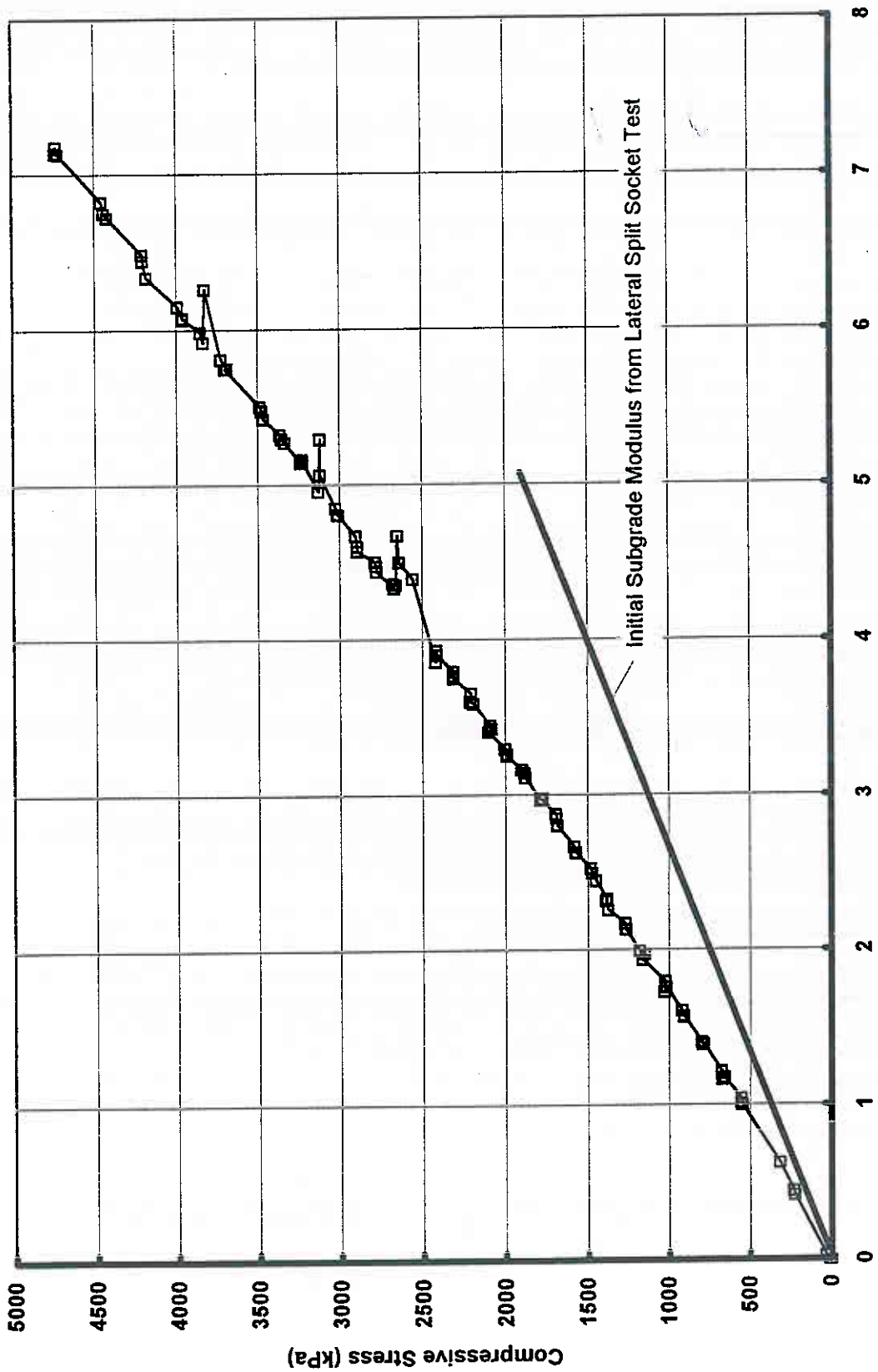


Fig. 20. Average Compressive Stress in Socket vs. Settlement 0.6 m above Base of Reaction Socket (Initial Portion of Test)

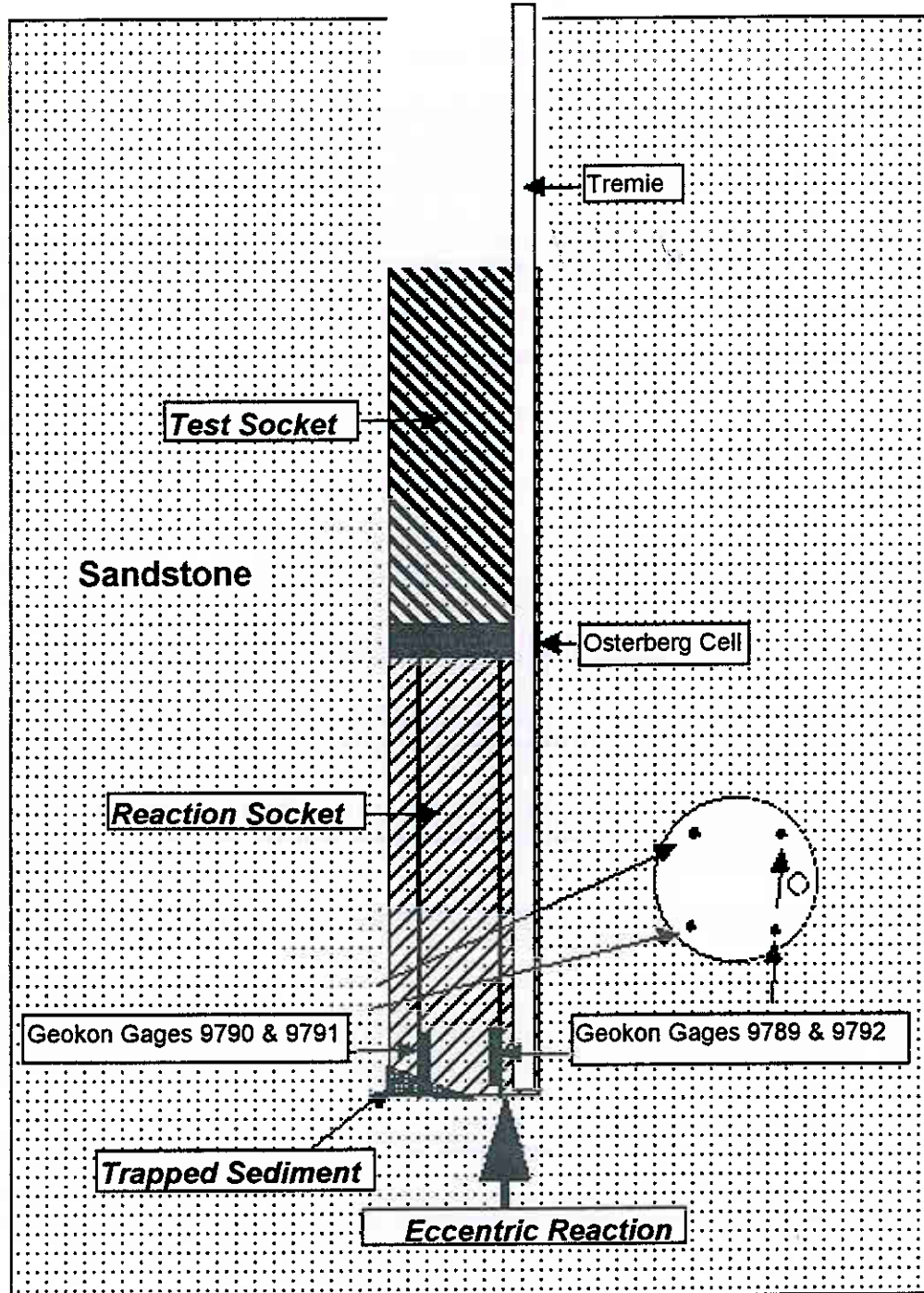


Fig. 21. Possible Explanation for Divergent Strain Gage Readings above Base of Reaction Socket

Table 2. Parameters for simulation of axial test socket behavior using two numerical methods

Method	Parameter	Value
ROCKET (Seidel, 1994)	Interface roughness	Random triangular joints using standard fractally generated roughness patterns denoted Fractal 1b, 1c and 1d. See accompanying graph. Segment length of each linear segment was chosen to be 32 mm based on comparison with measured behavior of test socket.
	Young's modulus of rock	380 MPa was estimated from lateral split socket test. See addendum. However, 600 MPa produced closer comparisons with axial socket test. 600 MPa was used in all analyses of the load test. This value was adjusted for simulating prototype sockets in the St. Croix River by assuming E varied according to the square root of effective overburden pressure.
	Normal stiffness	400 kPa/mm was used for condition of the load test. This value was determined from the lateral split socket test. See the accompanying figure. Normal stiffness was assumed to be inversely proportional to shaft diameter and also to vary according to the square root of effective overburden pressure for simulating behavior of prototype sockets in the St. Croix River.
	Angle of internal shearing resistance	40 degrees based on verbal reports by MnDOT of direct shear tests on remolded specimens of friable sandstone.
	Angle of interface sliding resistance	38 degrees. Assumed. This value is assumed to be near the angle of internal shearing resistance because the sandstone is open-pored, which allows for penetration of cement paste, forcing shearing to occur in the rock and not on a disturbed interface.
	Rock cohesion	0.050 MPa. Assumed, lacking any data on rock cohesion.
	Rock Poisson's ratio	0.25. Assumed, lacking any data on rock Poisson's ratio.
	Initial normal interface stress	30 kPa, which is the fluid pressure of approximately 2 m of buoyant concrete, which was the head at the center of the test socket.
	Simulation state	CNS (constant normal stress) plane surface.
FHWA method for "Intermediate Geomaterials" (O'Neill et al., 1995)	Interface roughness	Sinusoidal with 0.305 m wave length and 12.7 mm single amplitude. See accompanying graph for comparison with roughness patterns assumed in ROCKET analysis.
	Young's modulus of rock	Same as for ROCKET.

Table 2 (Cont'd). Parameters for simulation of axial test socket behavior using two numerical methods

Method	Parameter	Value
FHWA (Cont'd)	Normal stiffness	Not required (considered implicitly using input modulus)
	Angle of internal shearing resistance	0 (rock assumed cohesive and to shear undrained)
	Angle of interface sliding resistance	30 degrees (standard value).
	Rock compression strength	2 MPa. Assumed.
	Rock Poisson's ratio	0.25 (standard value).
	Initial normal interface stress	30 kPa, as per ROCKET.
	Simulation state	1.22-m-diameter socket

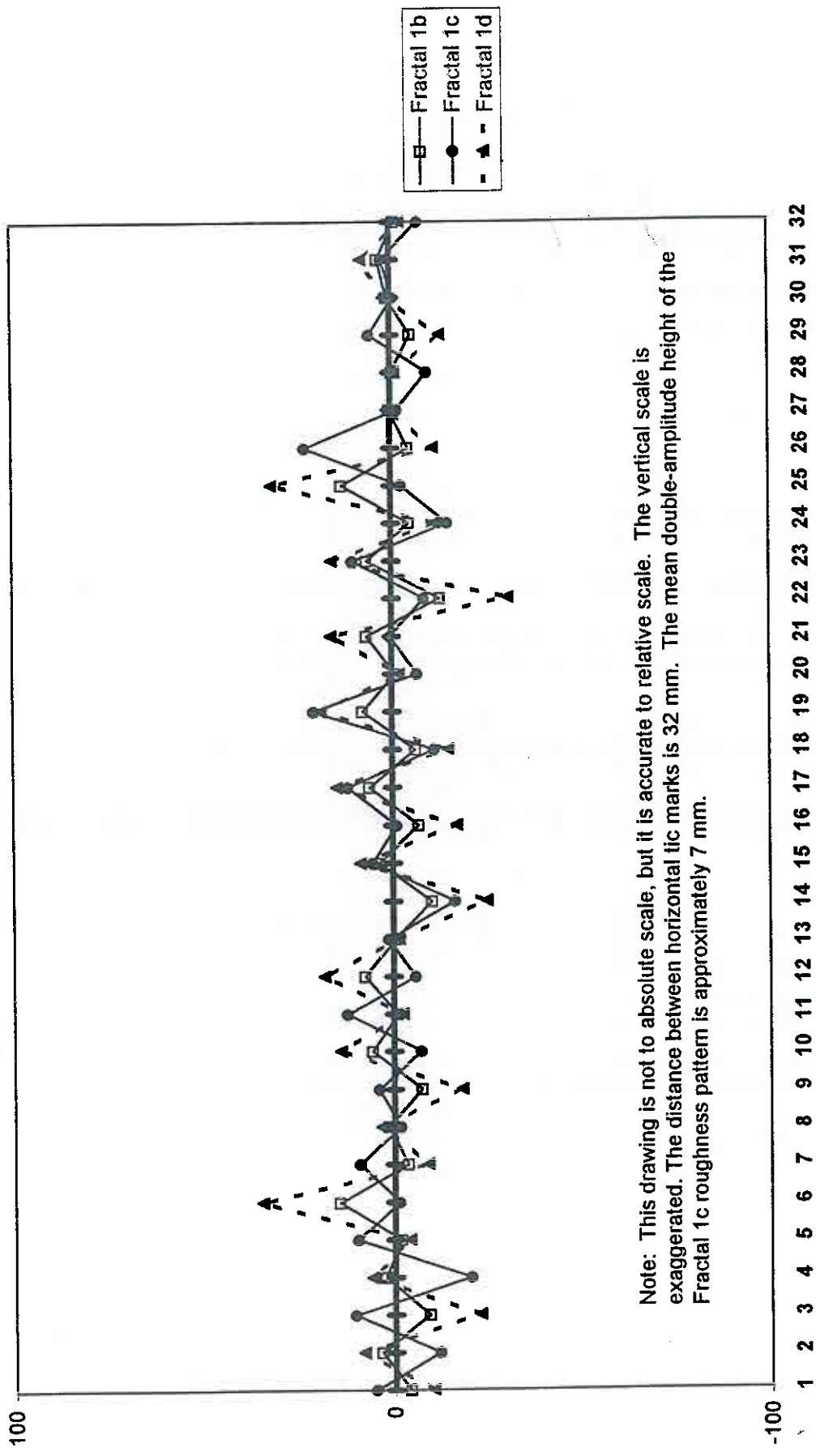


Fig. 22. Relative Fractal Patterns used in "ROCKET" Analysis

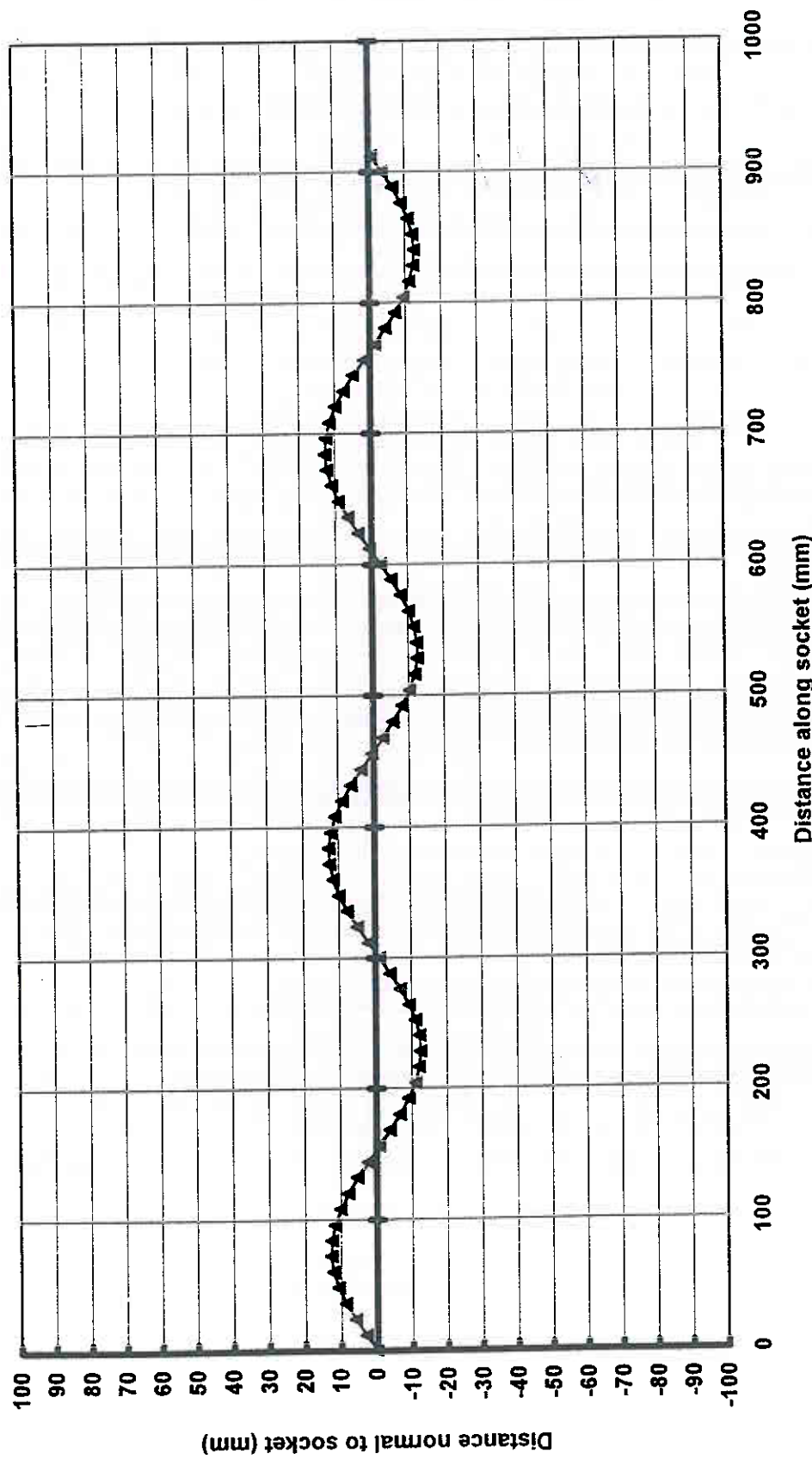


Fig. 23. Roughness Pattern Assumed in FHWA Method

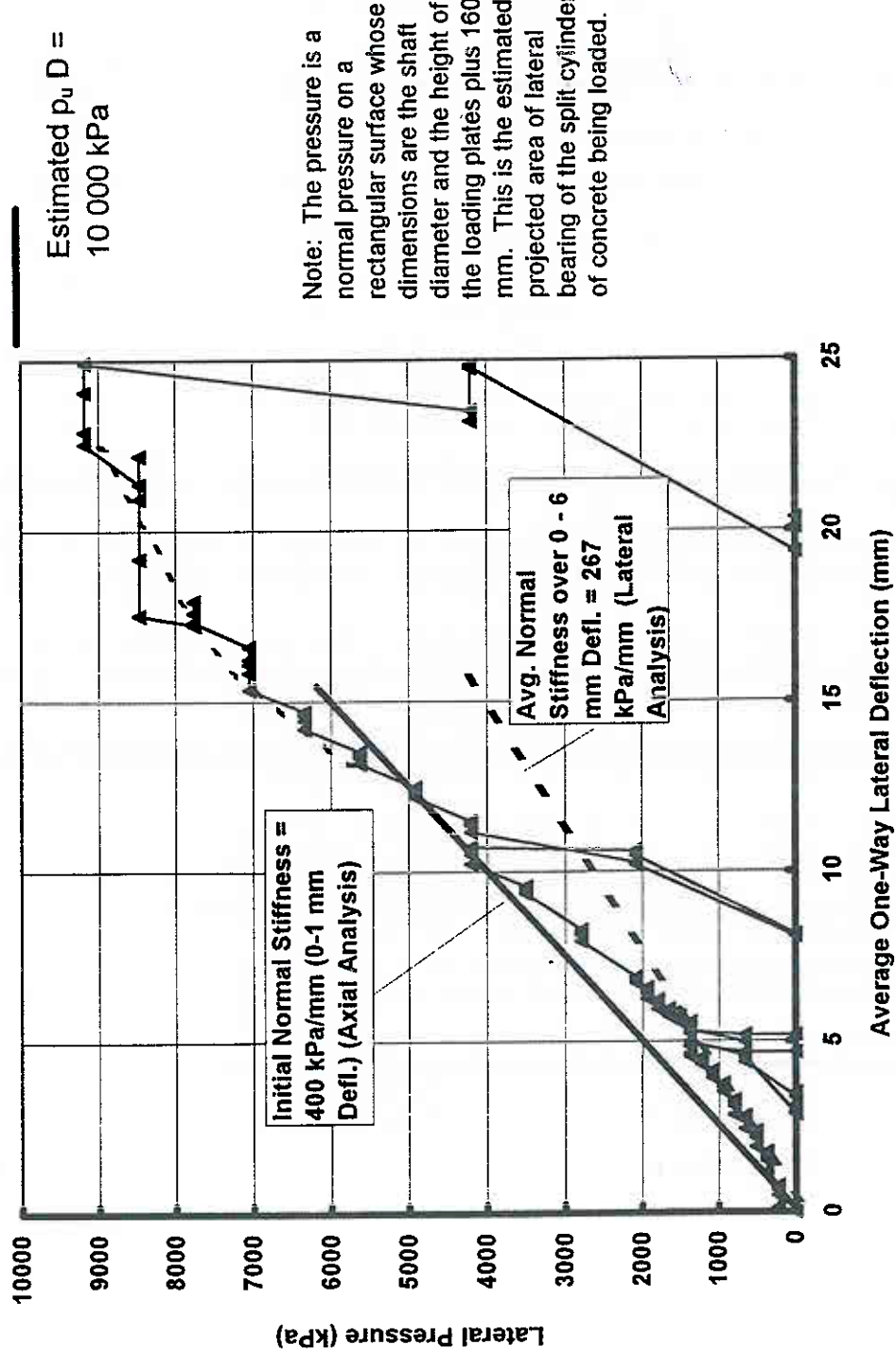


Fig. 24. Lateral Pressure on 1.22 X 1.63 m Surface vs. Lateral Deflection from Lateral Split-Cylinder Socket Test

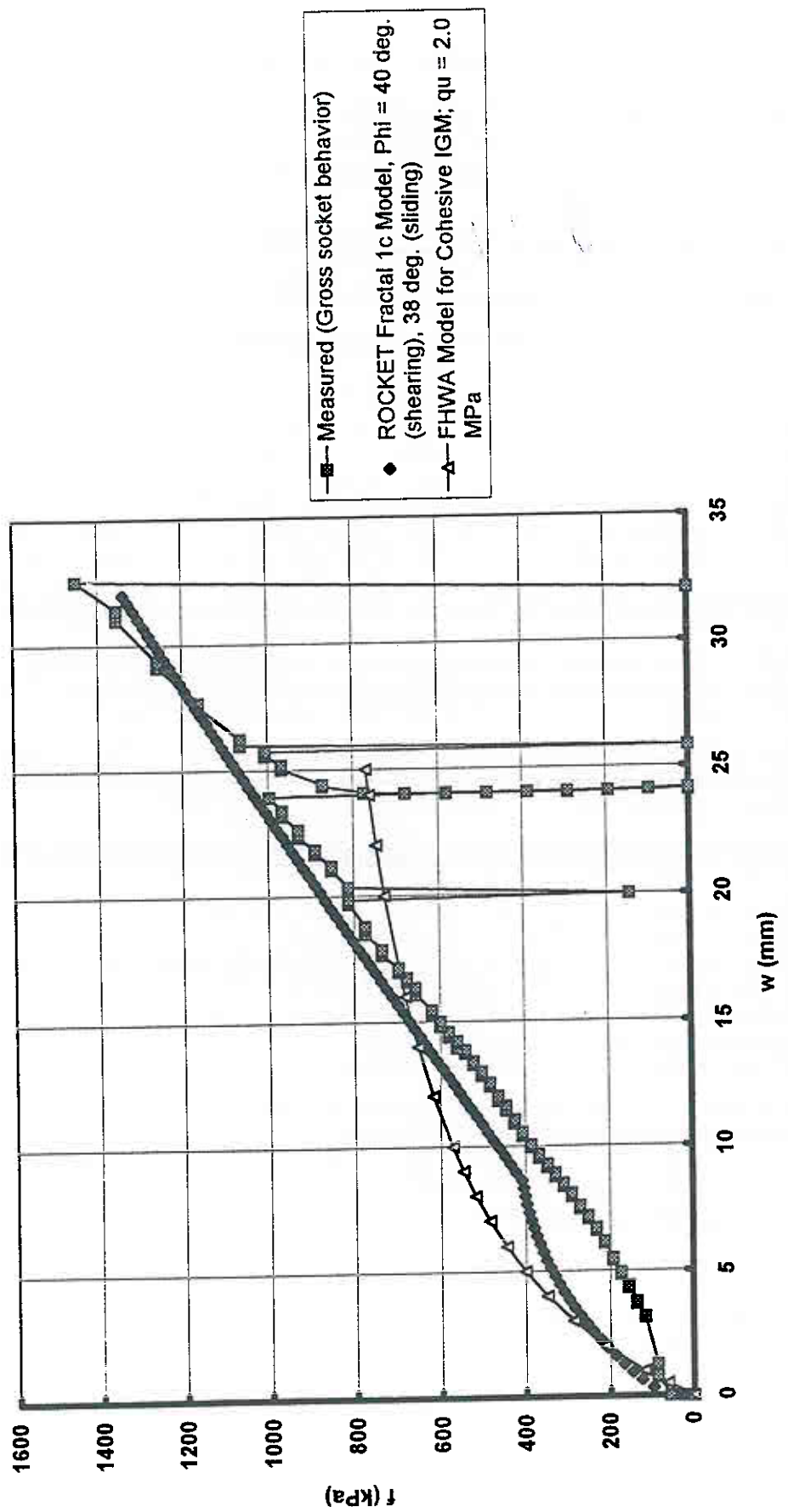


Fig. 25. Gross Measured Socket Shear Stress vs. Movement and Comparison with Two Numerical Models

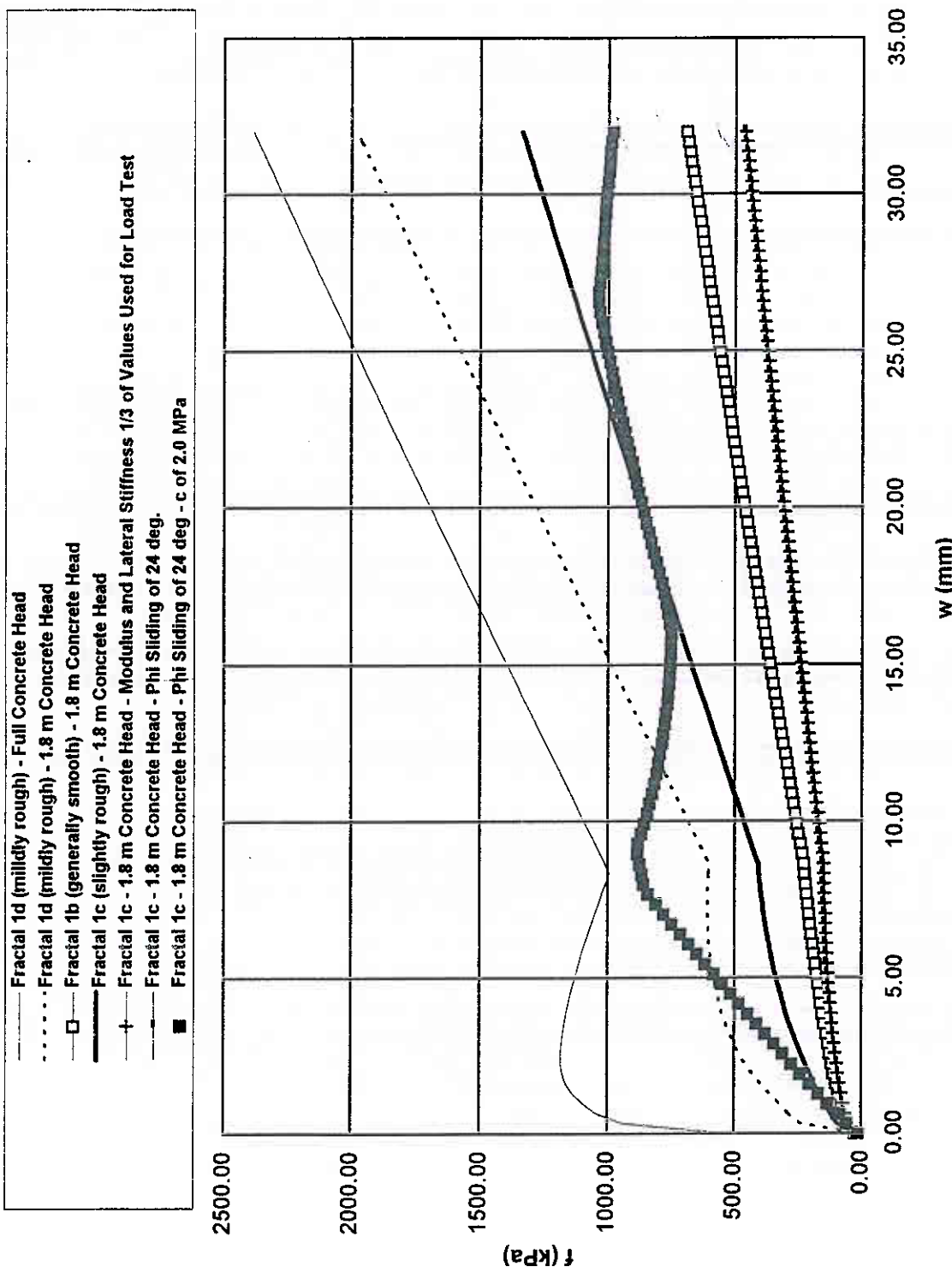


Fig. 26. Analysis of Interface Behavior for CNS Conditions Using ROCKET

All unit weights are assumed based on typical values for geomaterials of the type described.

Phreatic surface at ground surface

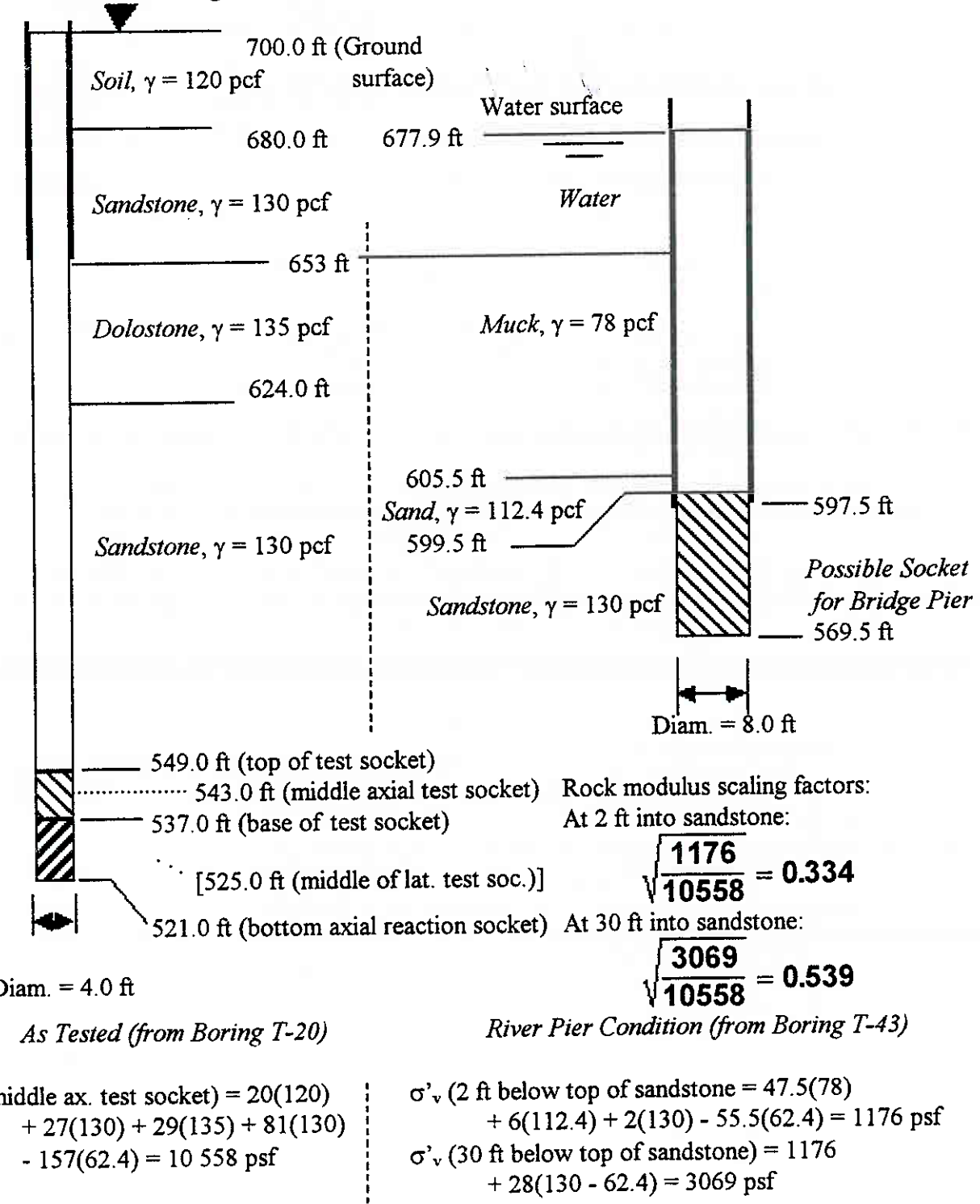


Fig. 27. Idealized Vertical Effective Stresses Used in Scaling Axial Test

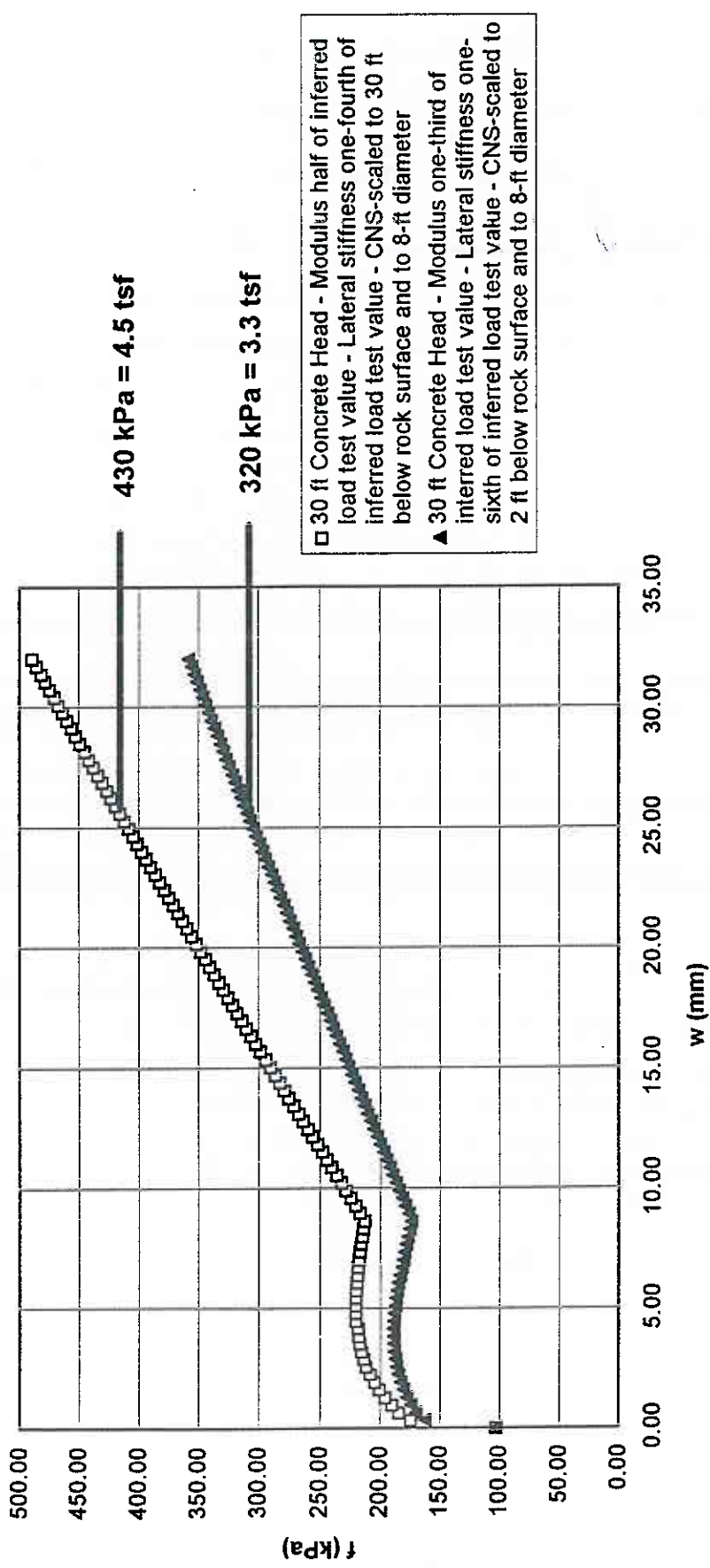


Fig. 28. Scaling of Interface Behavior from Axial Socket Test for CNS Conditions to Shallow Penetration of Rock and 8-foot Shaft Diameter Using ROCKET

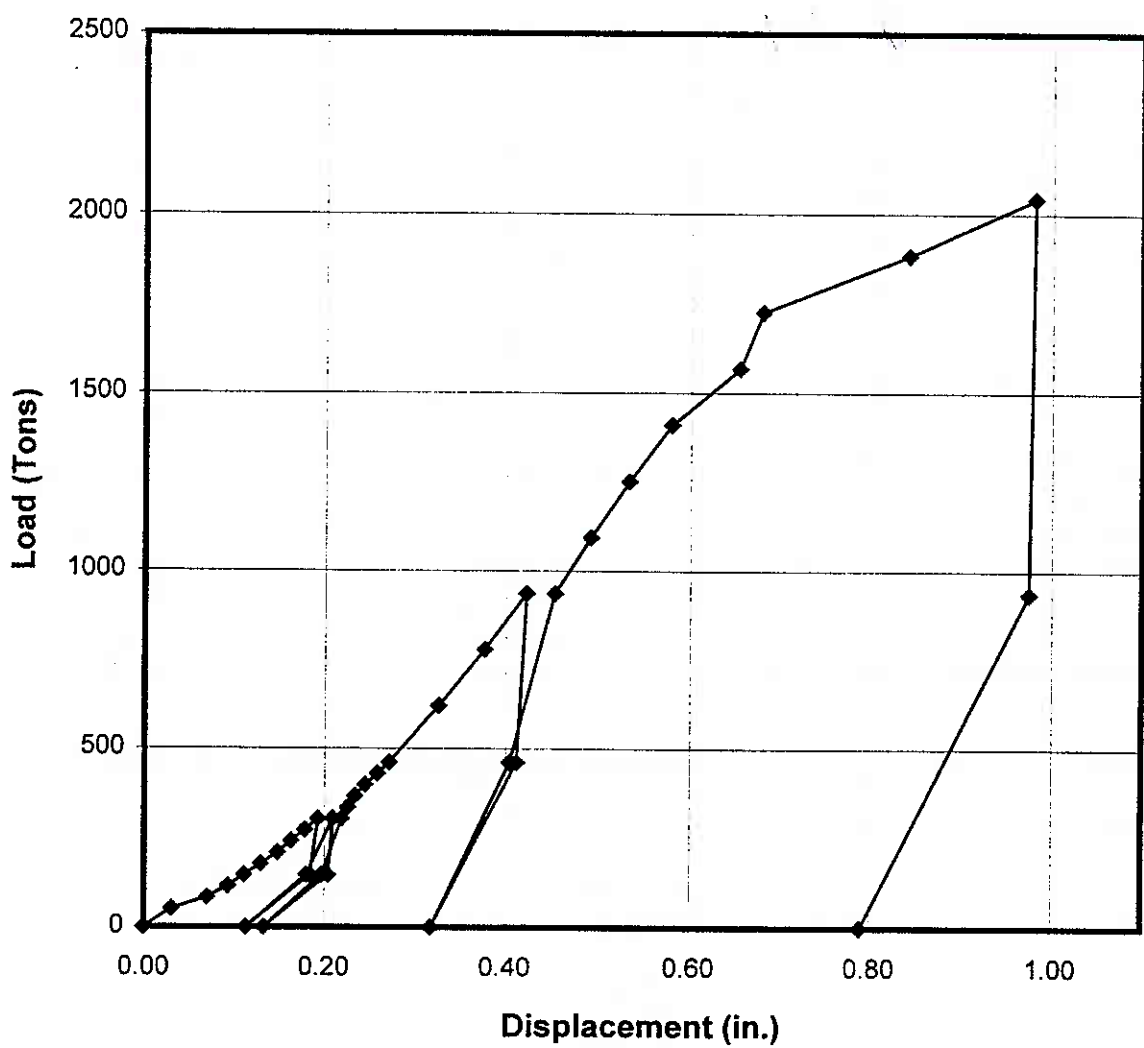


Fig. 29. Osterberg Cell Load Vs. Half Average Displacement Between Steel Plates for Lateral Split Cylinder Socket Test

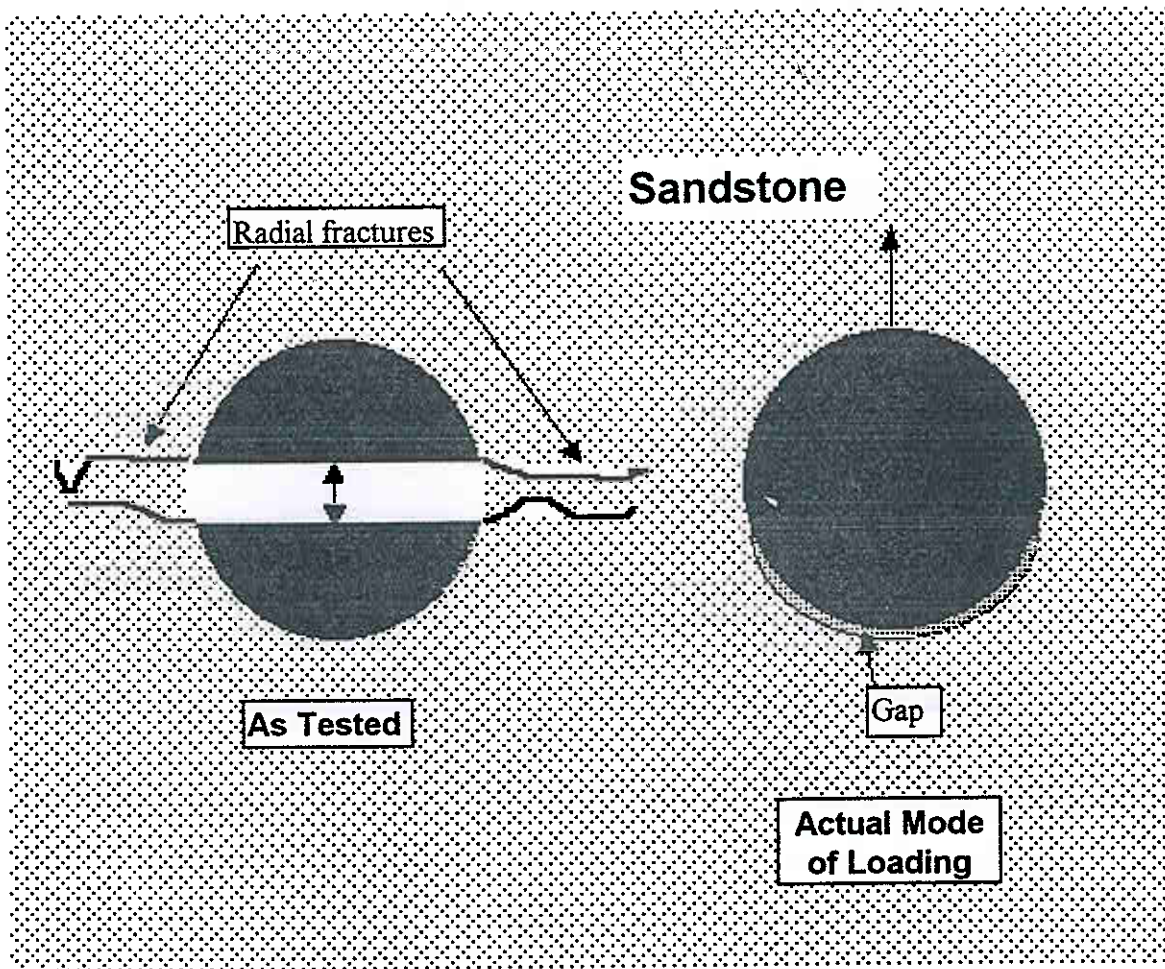


Fig. 30. Illustration of Differences in Mode of Loading Between Lateral Split Cylinder Test (As Tested) and Lateral Translation of Prototype Drilled Shaft (Actual Mode of Loading of Bridge Pier Foundations)

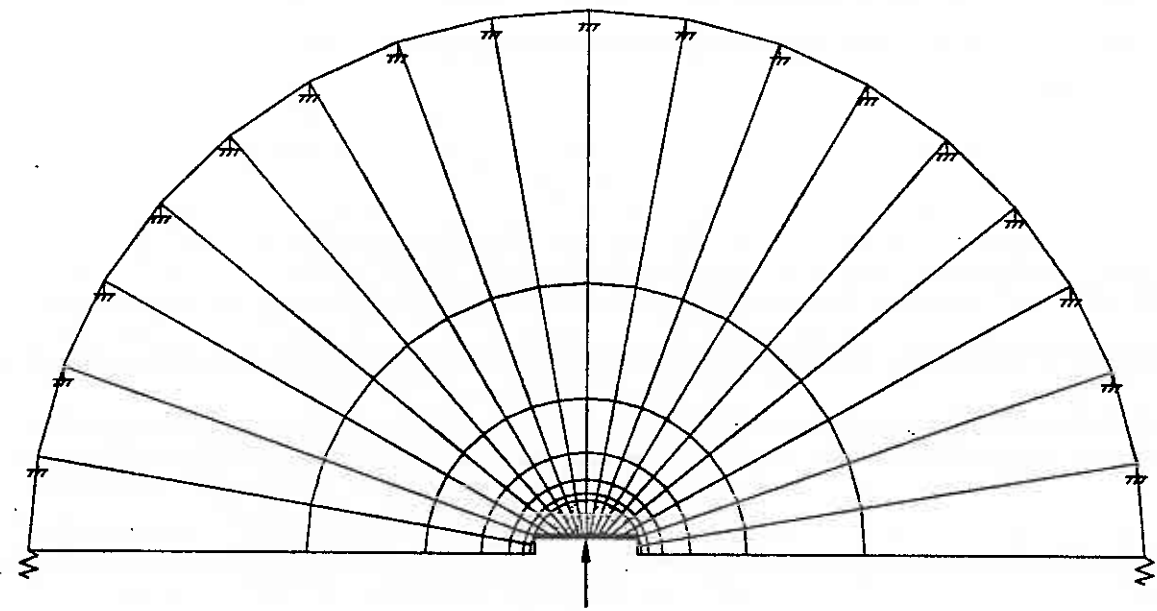


Fig. 31. FEM Mesh for Analysis of Initial Load-Movement Behavior of Half Split Cylinder

TABLE 3 Input for FEM Analysis

Material	E (psi)	μ
Steel	2.92E+07	0.30
Concrete	3.00E+06	0.25
Rock	4.65E+04	0.25

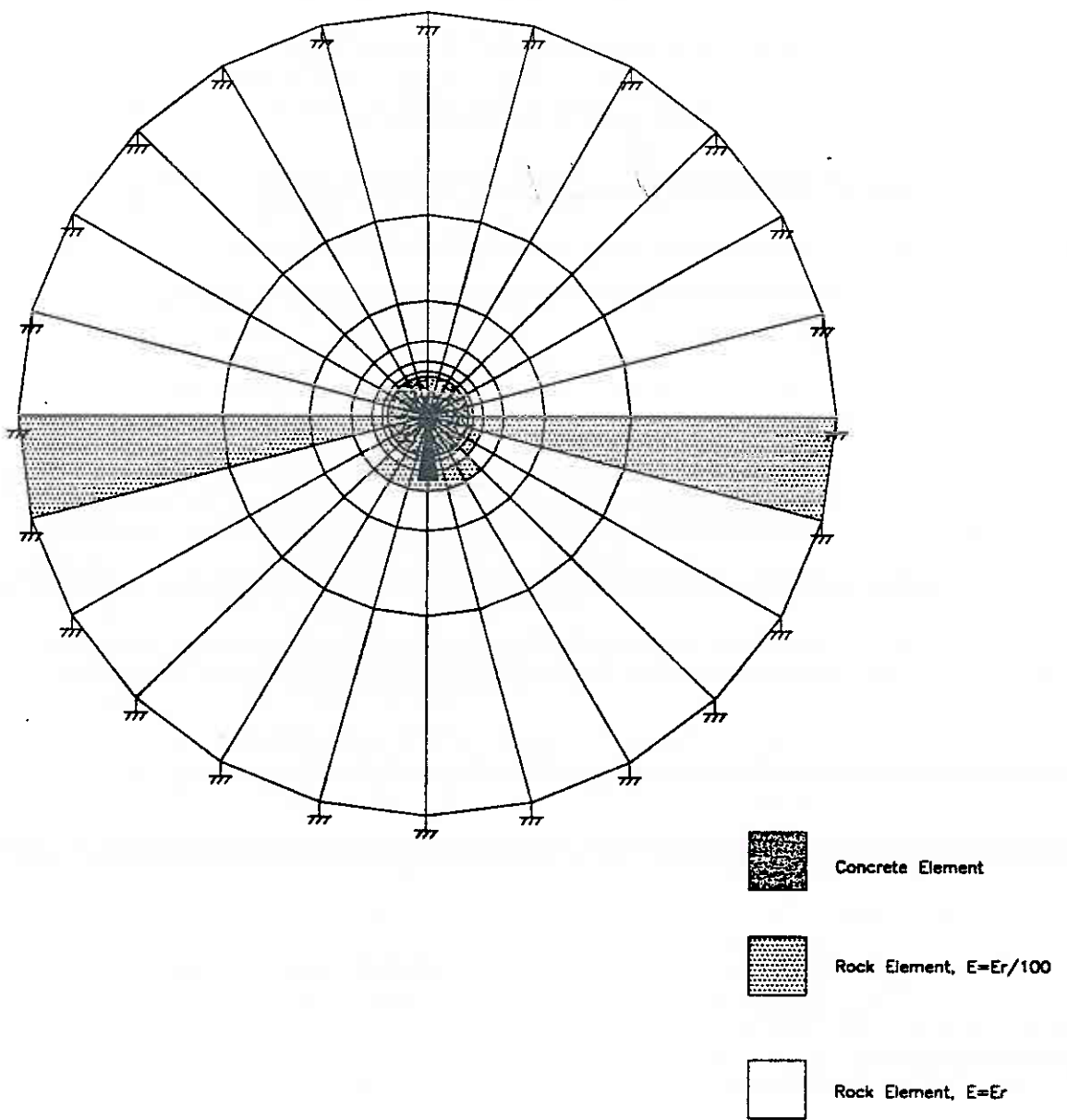


Fig. 32. FEM Mesh for Analysis of Initial Load-Movement Behavior of Full Shaft

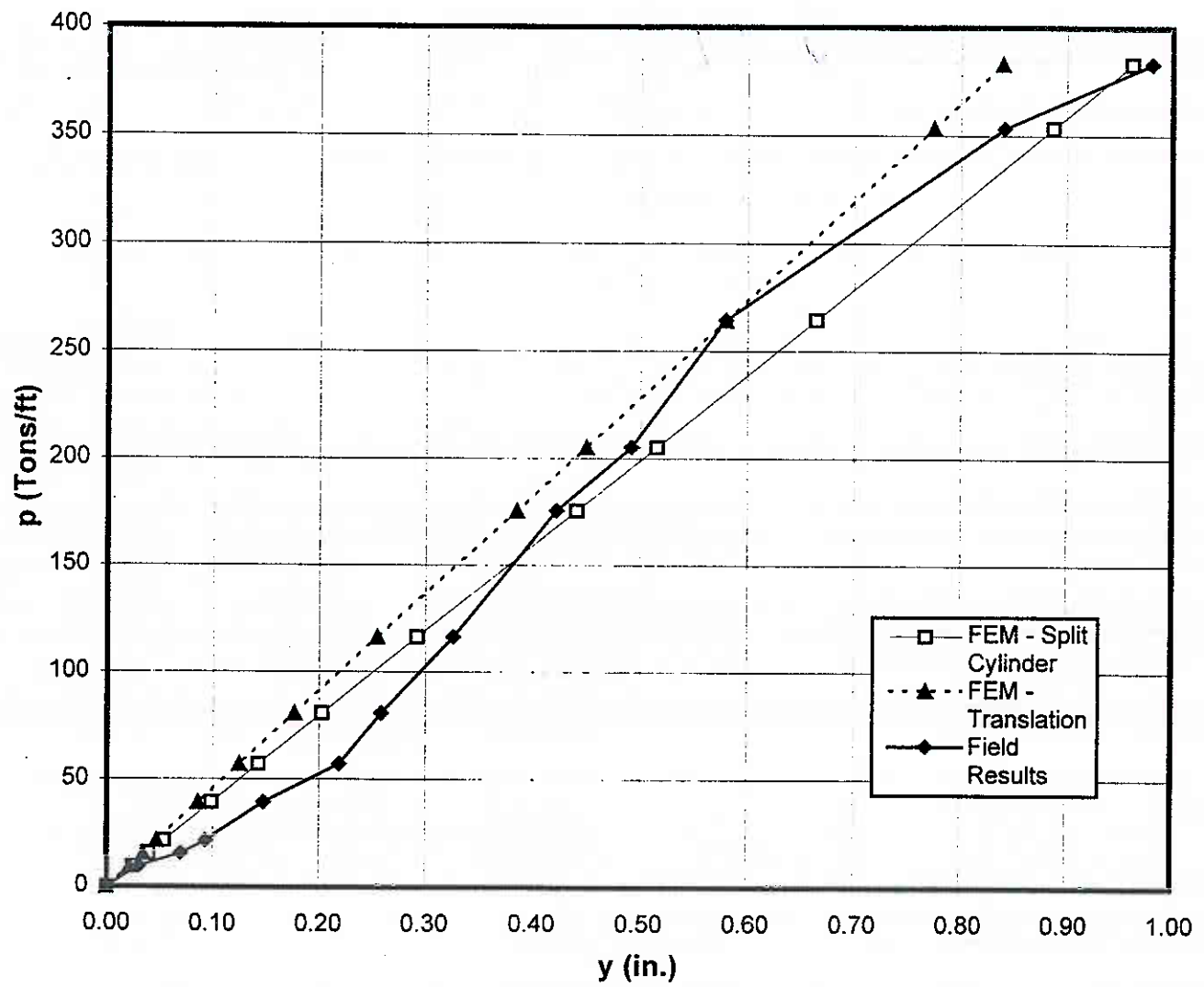


Fig. 33. Summary Results of FEM Analysis and Scaling Factor Ψ

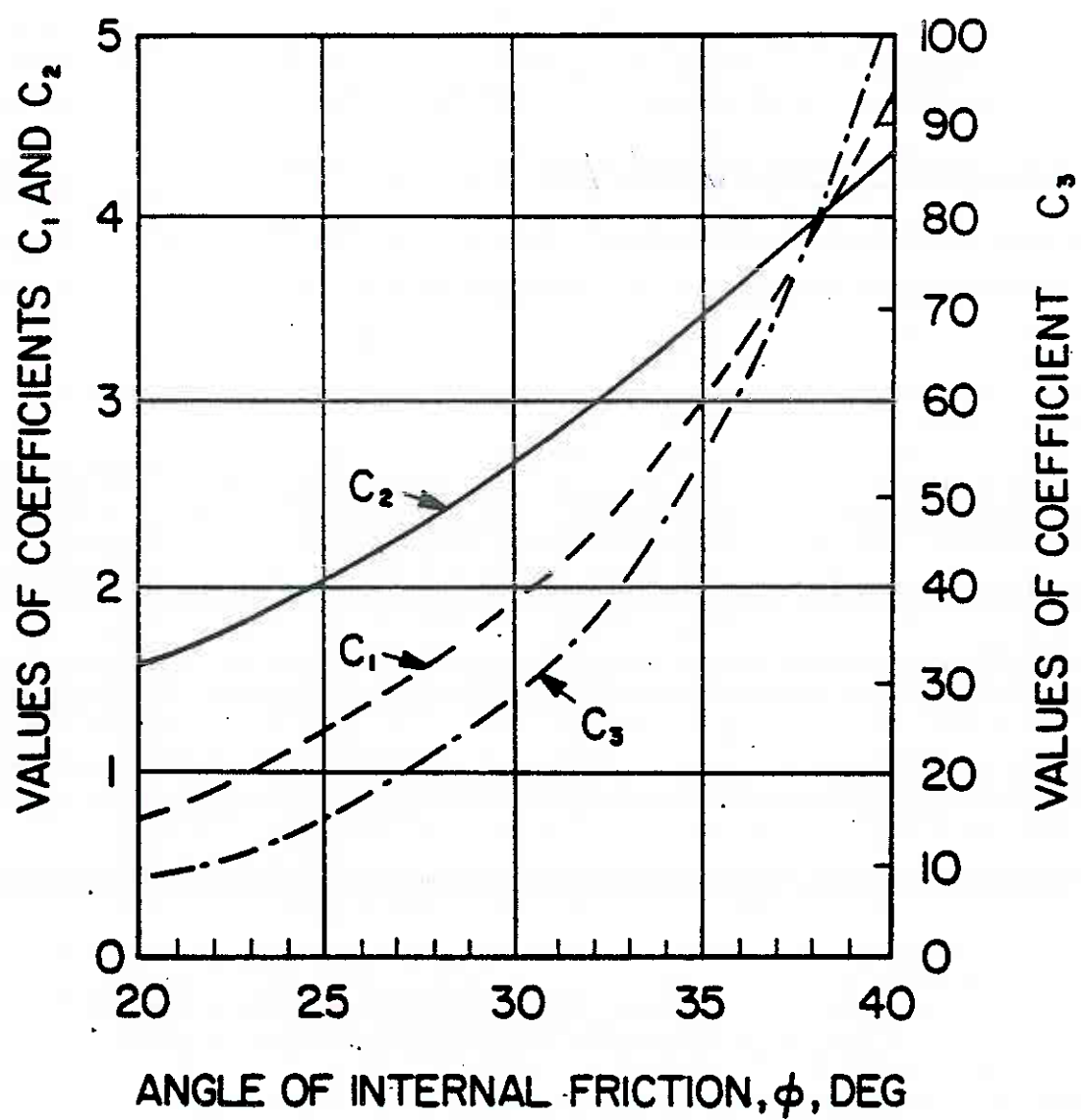


Fig. 34. Values of C Parameters vs. Angle of Internal Friction of Soil, ϕ

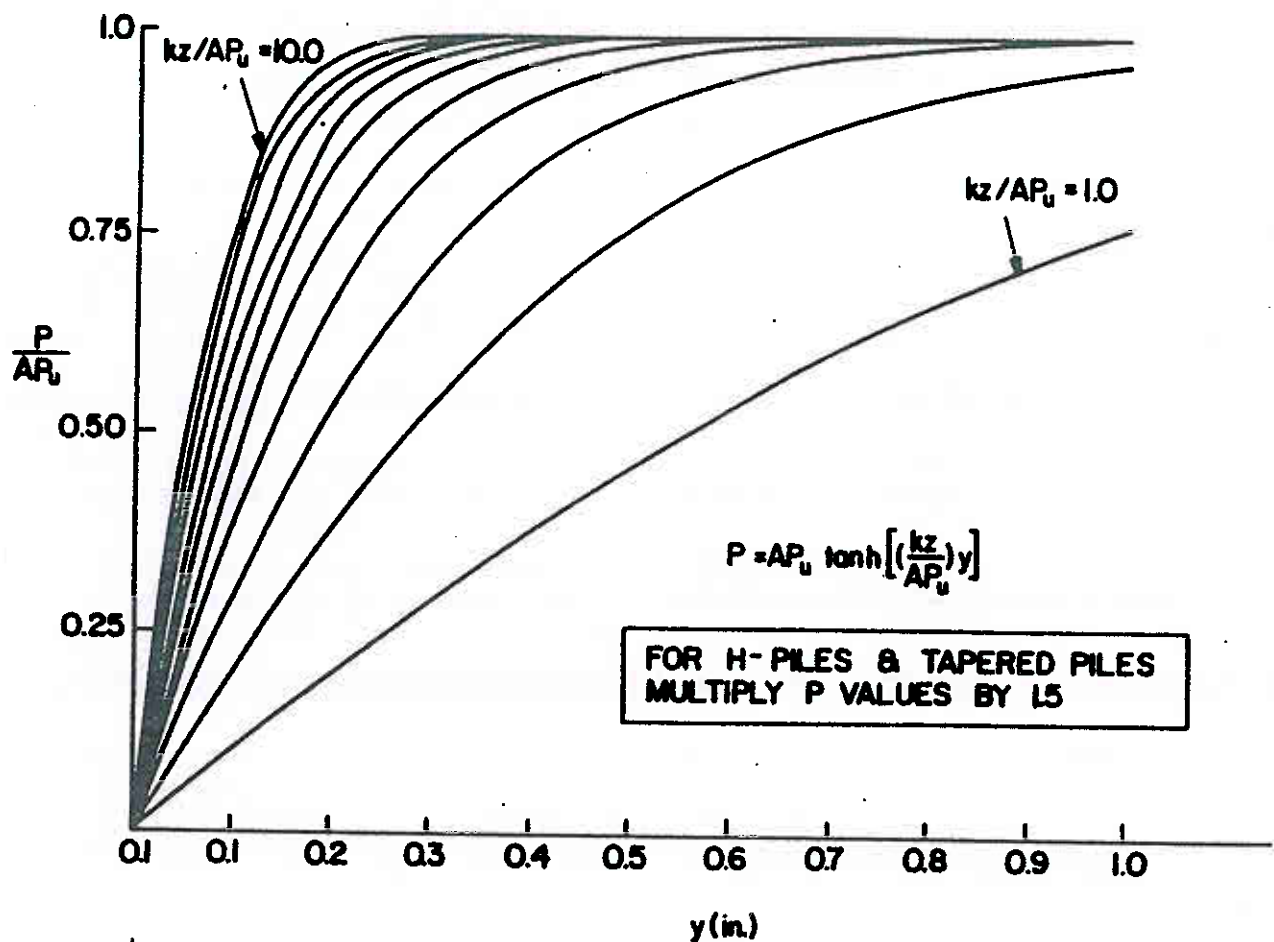


Fig. 35. Aid for Hand Calculation of p-y Curves According to Murchison and O'Neill (1983)

Table 4. Idealization of conditions at location of 24-in. test pile for LPILEPLUS analysis

	<u>Depth in feet</u>		c (psf)	ϕ' (deg.)	γ' (pcf)
Inferred from Boring T-48		Inferred from Driving Record			
Air	5.3	6.5			
Water			0	0	0
	29.5	32.5	14	0	15.6
Muck		(w = 160%)		Linearly varying	
	86.9	92.5	290	0	15.6
Sand and Gravel		(N = 47 - 68 B/0.3 m)	0	35	57.6
	119.5	119.5			
Sandstone					

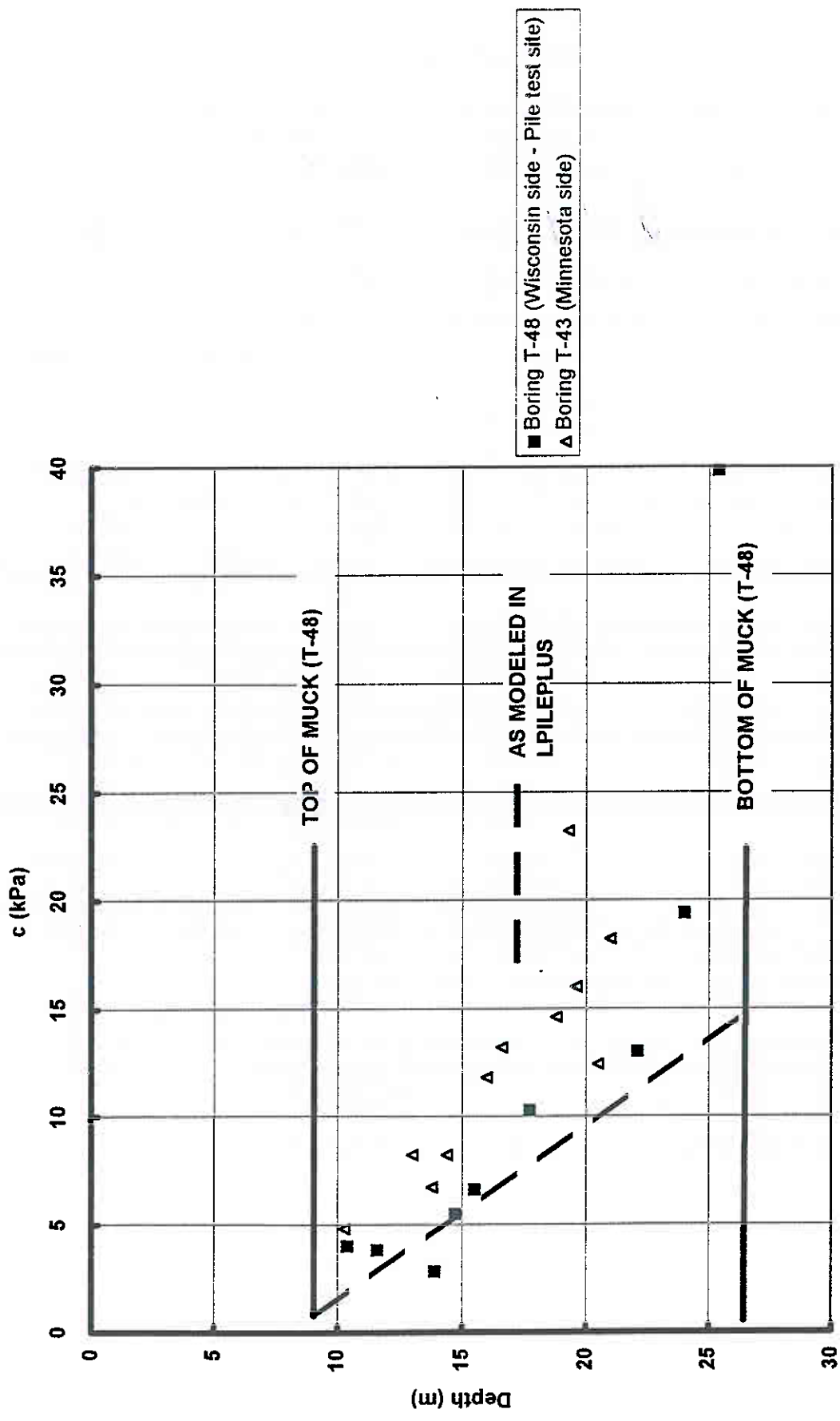


Fig. 36. Variation in Undrained Shear Strength (c) in Muck from UU Triaxial Compression Tests

Table 5. Pile and Soil Parameters for Buckling Analysis of 24-in. Pile Using LPILEPLUS

Parameter	Value or Criterion	Comments
Pile length	119.5 ft	
Pile O. D.	24.00 in.	
Pile Wall Thickness	0.75 in.	
Pile Material	Steel	Modulus = 29×10^6 psi
Filler Material	Concrete	
Date Driven:	18 October 1995	
Capacity Estimated from "CAPWAP"*	749.6 k [544.7 k on toe - 204.9 k in side shear]	Compression, based on initial drive. Pile was later restruck with no PDA data.
Date concreted	2 November 1995	Pile driven with a conical shoe -- no soil removal required.
Date tested	9 November 1995	Axial compression (buckling) test
Concrete strength	3460 psi	
Concrete modulus	3.35×10^6 psi	Computed per ACI formula
Composite EI of pile	14.97×10^{10} lb-in ²	
p-y criterion for muck	Matlock's static soft clay criterion	c = 0.1 psi at top, 2.02 psi at bottom with linear variation. Unit weight = 0.010 pci. $\epsilon_{50} = 0.03$.
p-y criterion for sand-gravel	Reese's static sand criterion	$\phi = 35$ (uniform). Unit weight = 0.0330 pci.
Head constraints	a. Free-head / pinned	No constraint of lateral head movement
	b. Restrained-head / pinned	Lateral head movement constrained to be zero
Section conditions	Elastic	EI independent of axial load

* Per report supplied by Goble Rausche Likins and Associates, Inc. (Nov. 1995)

Note: Shear strength parameters for p-y criteria were estimated, not measured. For the muck, c was estimated assuming the muck was a normally consolidated clay with slight aging to give effective cohesion, c', of 0.1 psi. The clay was assumed to have had a value of $\phi' = 16$ degrees. The shear strength values from this estimation are generally confirmed by the results of UU triaxial tests noted on the boring log for Boring T-48 (Fig. 36). For the sand, ϕ' was based on the minimum N value in the sand in Boring T-48 (N = 47) using Murchison and O'Neill (1983), which is the current API recommended practice.

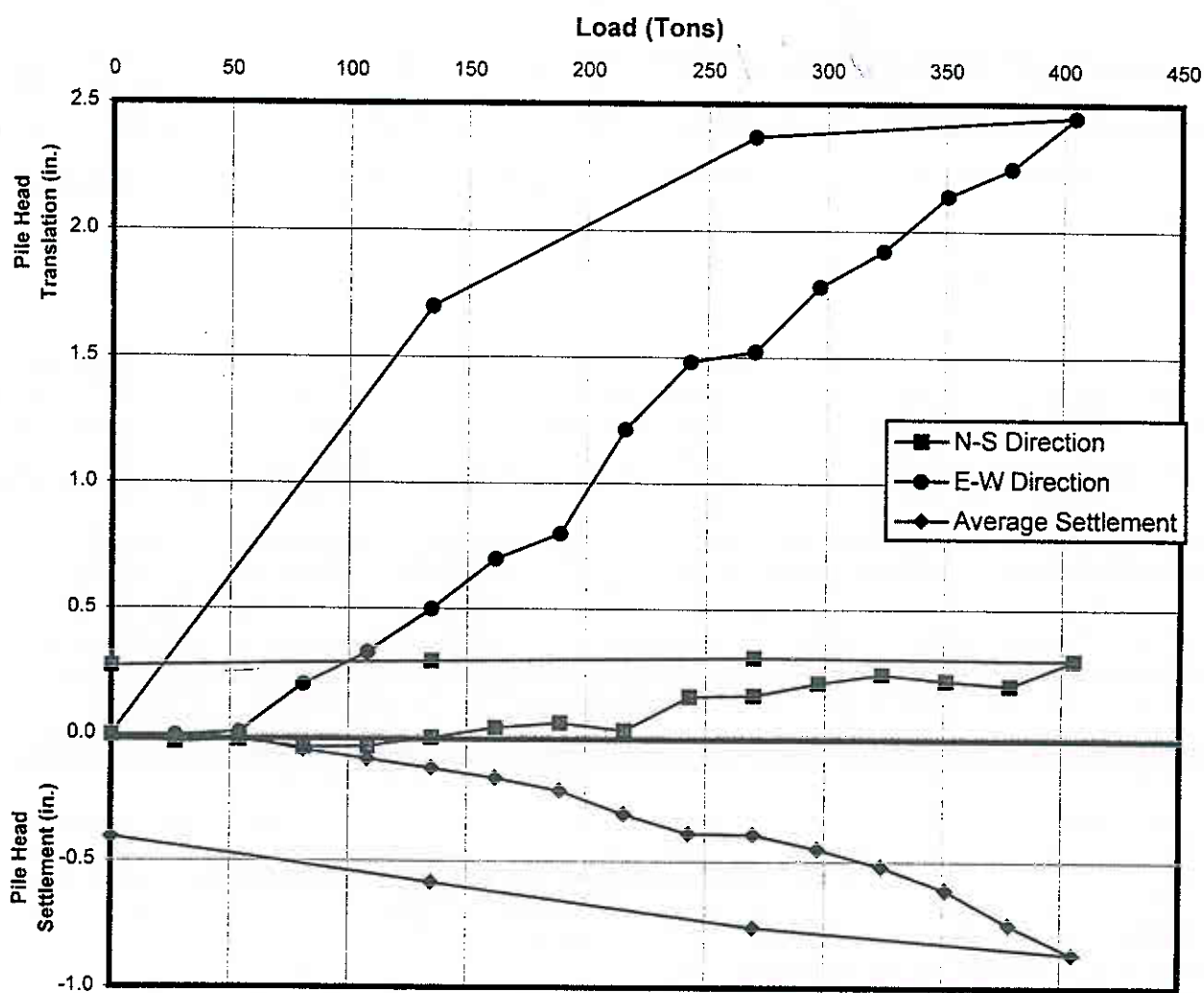


Fig. 37. Axial Load vs. Settlement vs. Lateral Translation of Head of Test Pile -- Compression Test

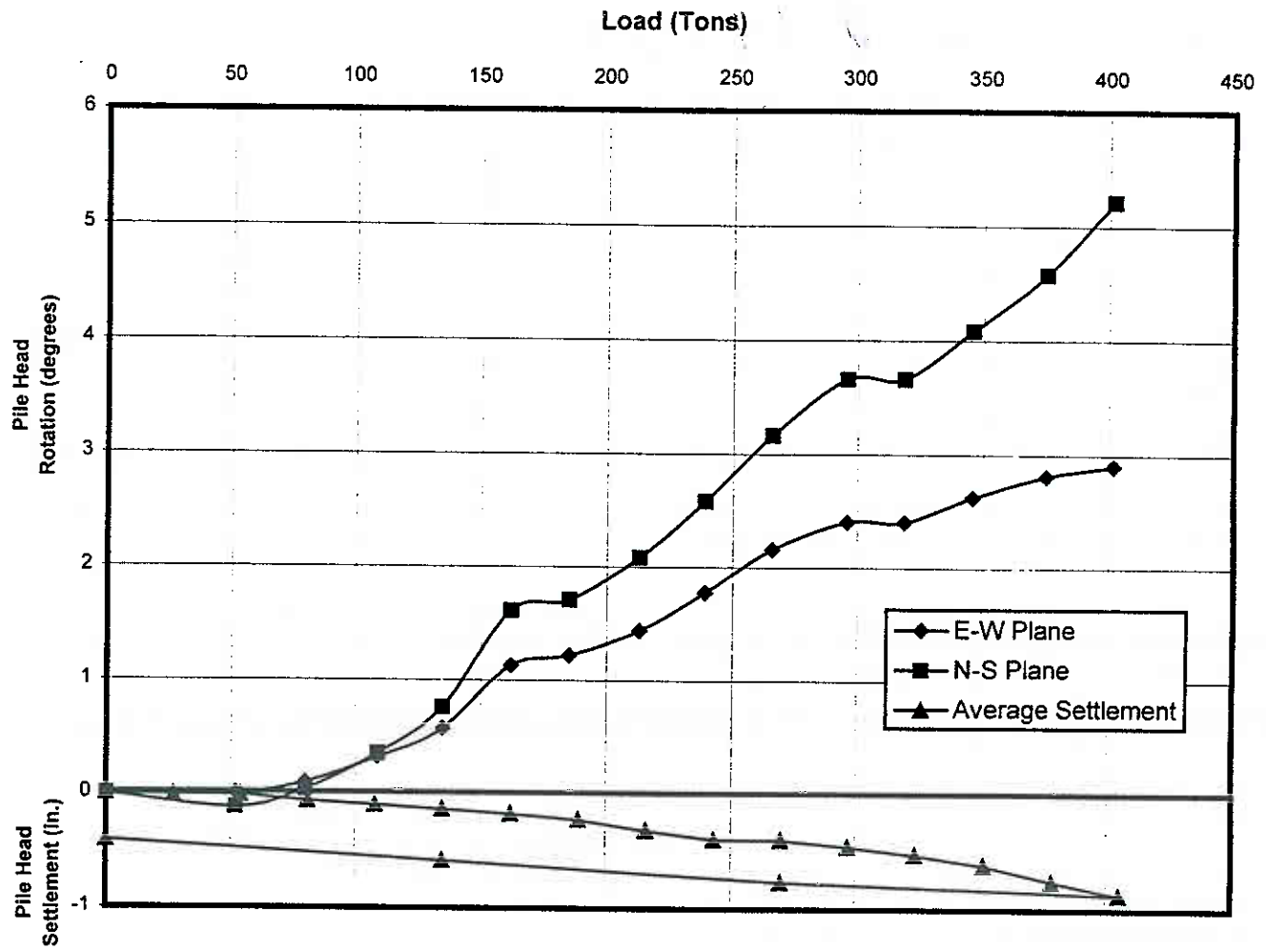


Fig. 38. Axial Load vs. Settlemet vs. Rotation of Head of Test Pile -- Compression Test

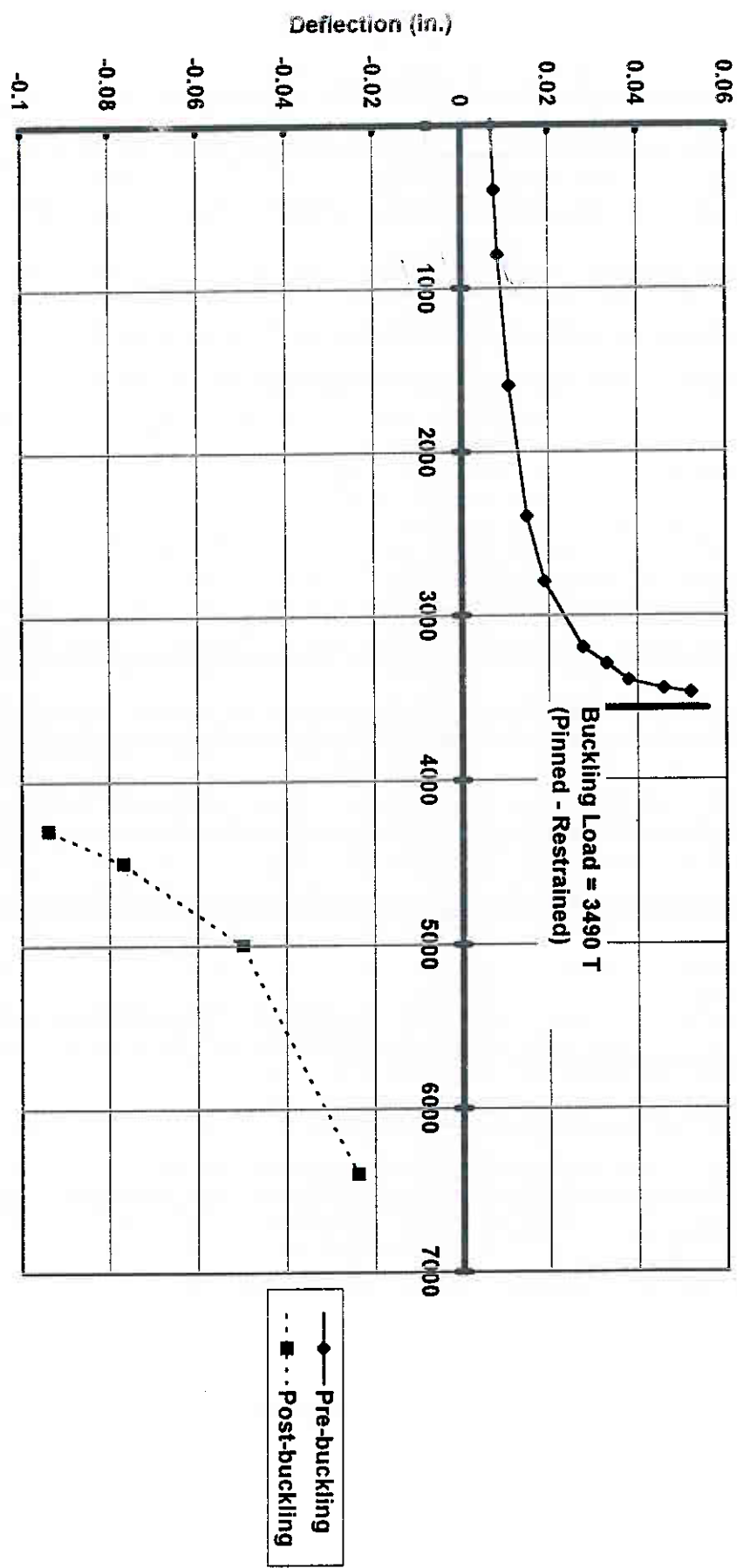


Fig. 43. Axial Load vs. Maximum Lateral Deflection Along Pile for 24-in. Pile - Pinned-Restrained Head (PILEPLUS)

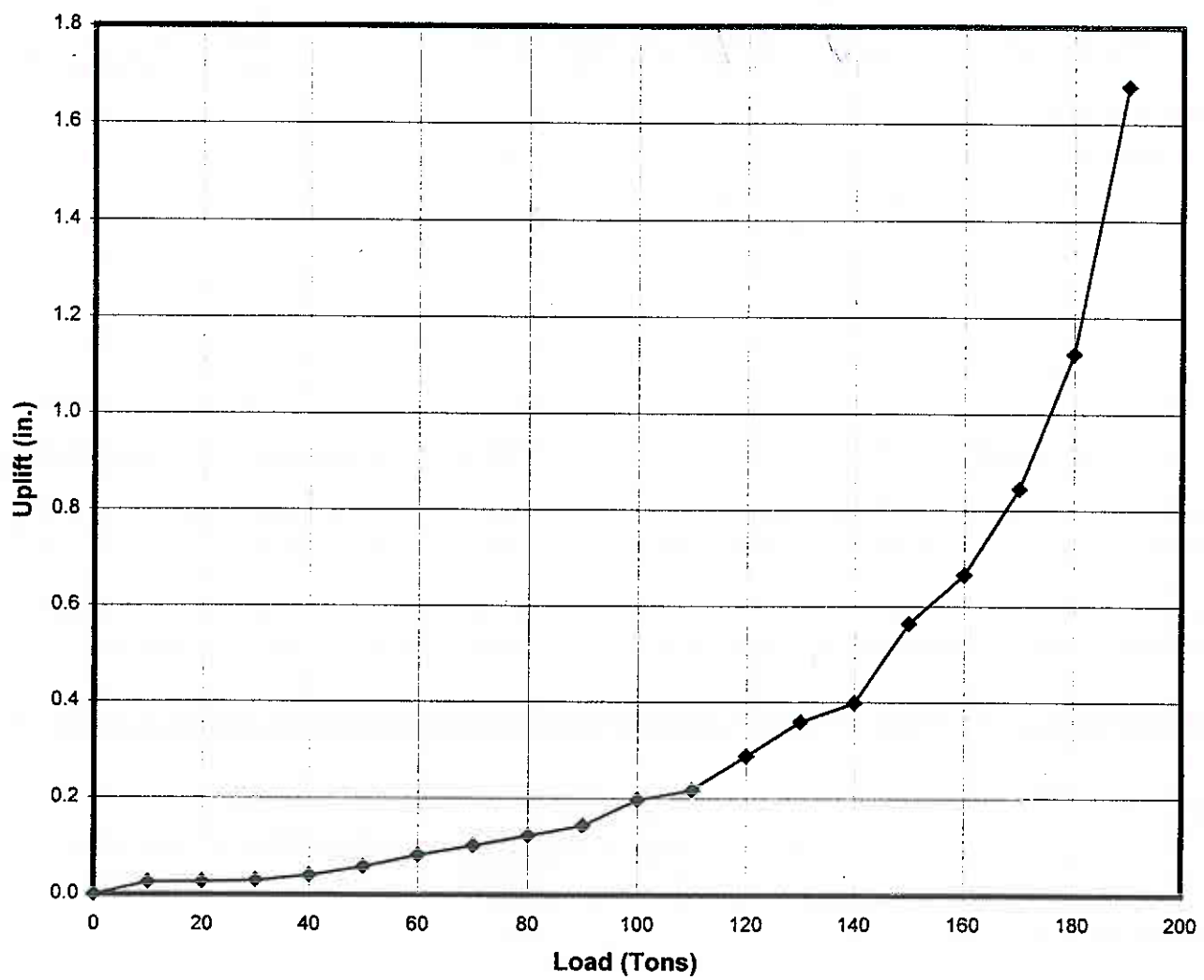


Fig. 39. Axial Load vs. Uplift of Head of Test Pile -- Uplift Test

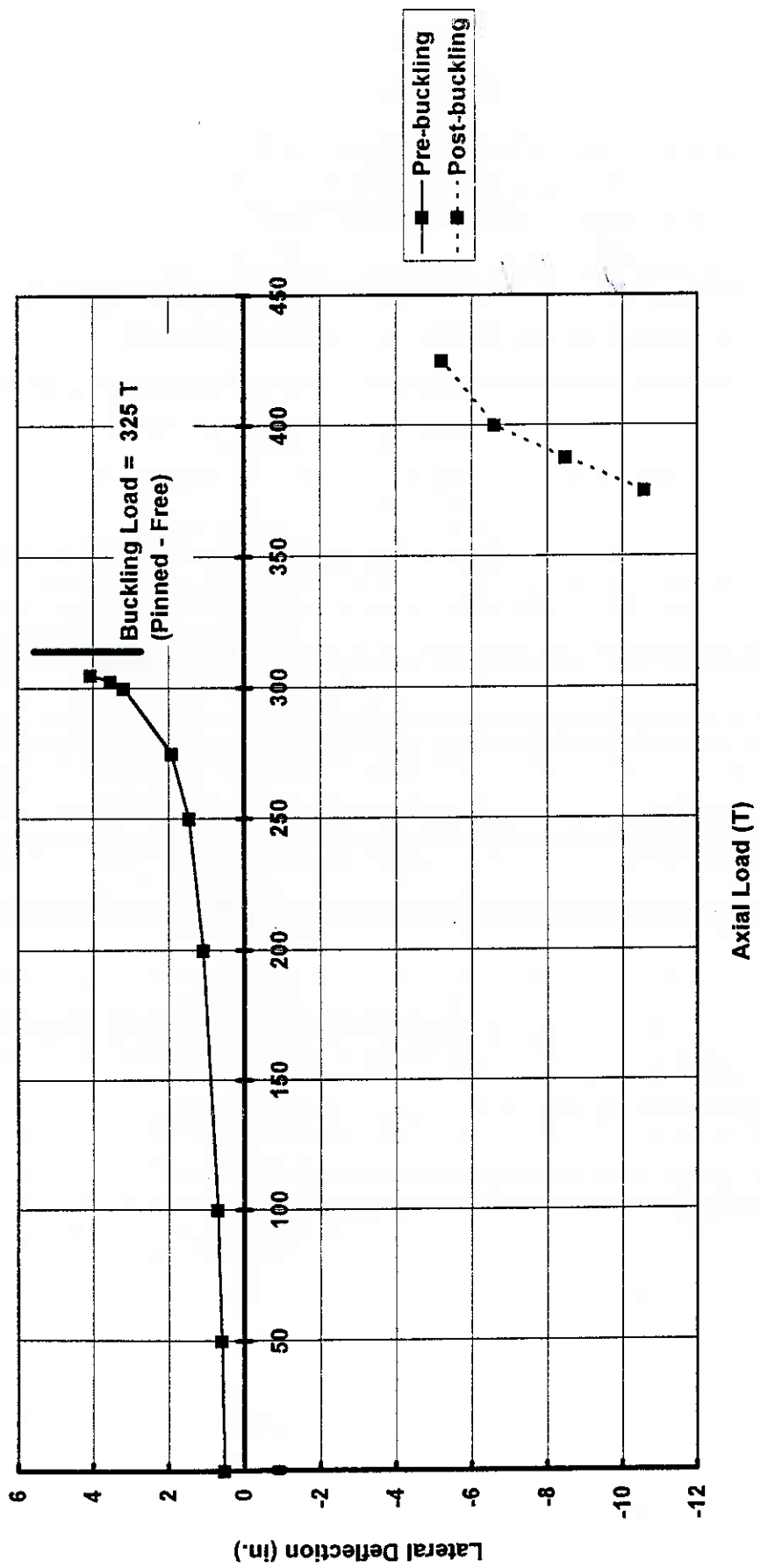


Fig. 40. Axial Load vs. Lateral Pile-Head Deflection for 24-in. Pile - Pinned-Free Head
(PILEPLUS)

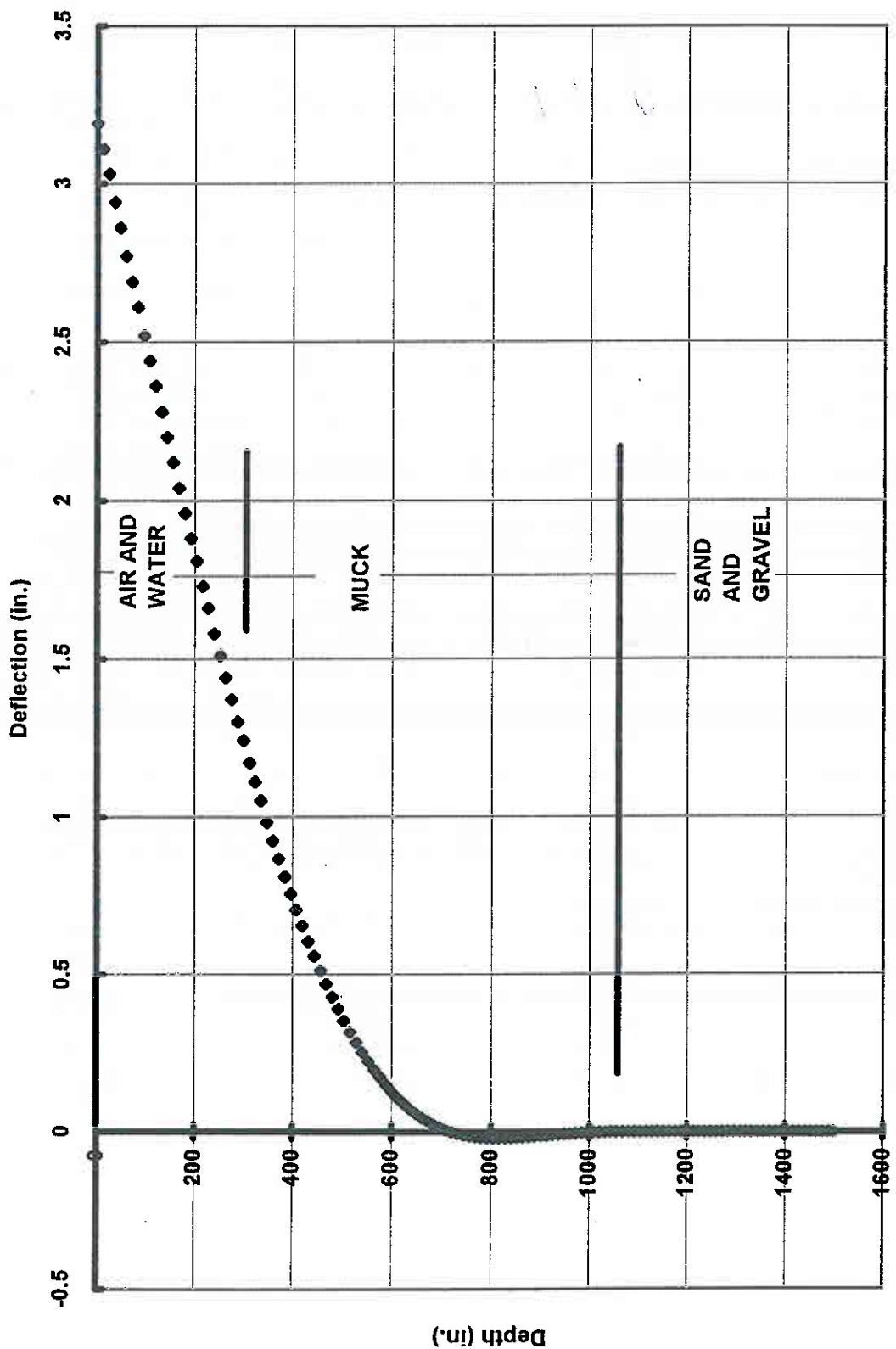


Fig. 41. Lateral Pile Head Deflection Diagram at 300 T Load

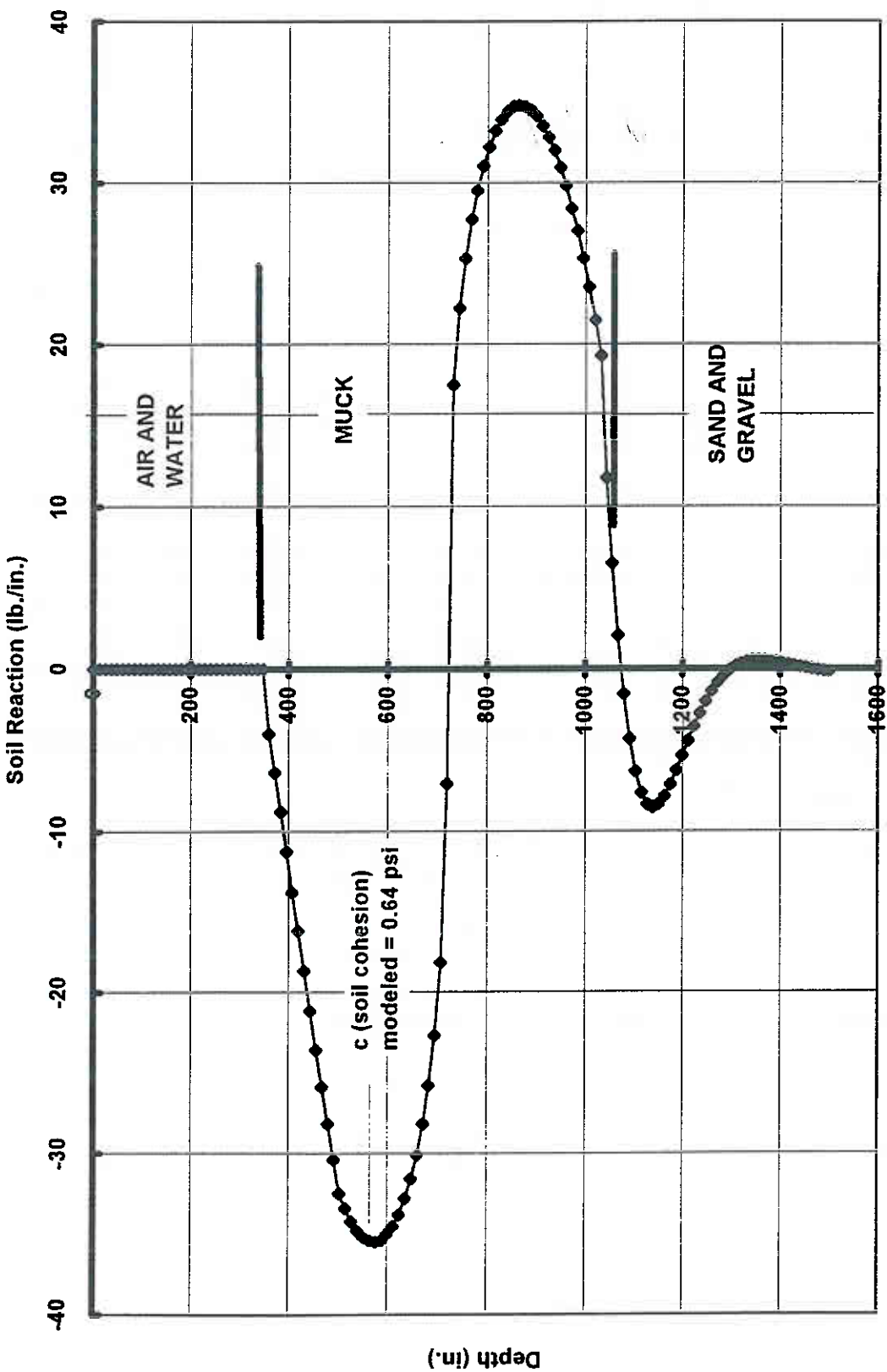


Fig. 42. Soil Reaction Vs. Depth at 300 T Load

Table 6. Computed depths to point of fixity for elastic buckling analysis of 24-inch concrete filled steel pipe pile from LPILEPLUS analyses

Head condition	Computed buckling load (P_{cr}) (lb)	Elastic buckling formula	Depth to fixity L_f (ft)	Distance below top of muck to fixity (ft)
Pinned-free	650 000	$L_f = \sqrt{\frac{\pi^2 EI}{4P_{cr}}}$	62.8	33.3
Pinned-restrained	6 980 000	$L_f = \sqrt{\frac{20.2EI}{P_{cr}}}$	54.9	25.4

Note: $EI = 14.97 \times 10^{10}$ lb-in²

Wall thickness of pile = 0.75 in.

Appendix

MINNESOTA DEPARTMENT OF TRANSPORTATION - GEOTECHNICAL SECTION

LABORATORY LOG & TEST RESULTS - SUBSURFACE EXPLORATION

UNIQUE NUMBER 56327
SI Units



Index Sheet Code 1.0m

State Project 8217		Bridge No. or Job Desc. 82011	Trunk Highway/Location TH 36	Boring No. T-20	Ground Elev. 217.5	Code S				
Location Prop. EB TH 36, 39 + 243.0, 55.8m LT Washington Co. Coordinate: X = 155729 Y = 62853				Lat. = 45°02'13.589"	SHEET 1 of 7					
DEPTH	Drilling Operation	Elev.	Classification	Samp	SPT	MC (%)	COH (kPa)	δ (kN/m ³)	Soil	Other Tests Or Remarks
				Core	REC (%)	RQD (%)	ACL (m)	Core Breaks	Rock	Formation or Member
0.8 216.7			S w/ some G; brn to 0.2 m, red-brn, 0.2 m-0.8 m; damp			7				
1	X		slpl SL w/ some pebbles, red-brn & moist		90.4	8				
2	X	PD			55	7				
2.1 215.4	X	PD			13	23				
3	X	PD	pl SL w/ some pebbles, some ashes; 58 mm CL seam at 2.65 m; dk gray w/ dk brn; wet							
3.4 214.2	X		S & G, dk gray-brn & vmoist			17				
3.8 213.7	X		S w/ some seams of FS & org L; brn w/ lt brn & blk; wet		15	11				
4.3 213.2	X	PD	FS, red-brn & sat							
4.9 212.6	X		Driller's Notes: boulder		62.3	21				
5.0 212.5	X	PD	Sst S, F w/some CR rounded grains, predominantly quartz, dk yel orange to very pale orange							
5.8 211.7	X		Top of Bedrock		45	18				
6	X	PD			50/.5	18				
7	X	PD	WEATHERED SANDSTONE, VF to F grain, silty, subangular to subrounded, extremely soft, white		50/.4	NSR				Jordan Sandstone Norwalk Member
7.6 209.9	X	WS			50/.3	NSR				

(Continued Next Page)

Soil Class: DB Rock Class: NMW Edit: JLD Date: 7/26/95

MINNESOTA DEPARTMENT OF TRANSPORTATION - GEOTECHNICAL SECTION
LABORATORY LOG & TEST RESULTS - SUBSURFACE EXPLORATION

UNIQUE NUMBER 56327
SI Units



Mn/DOT GEOTECHNICAL SECTION - LOG & TEST RESULTS

SHEET 2 of 7

State Project 8217		Bridge No. or Job Desc. 82011	Trunk Highway/Location TH 36			Boring No. T-20		Ground Elev. 217.5	Code S
Depth DEPTH	Drilling Operation Elev.	Classification	Samp	MC (%)	COH (kPa)	δ (kN/m ³)	Soil Type	Other Tests Or Remarks Formation or Member	
			Core	REC (%)	RQD (%)	ACL (m)	Core Breaks		
8.6 208.9	WS PD	SANDSTONE, slightly weathered, VF to F, silty, subangular to subrounded, extremely soft, white to greyish orange	50/2	28					
9			0						
10		SANDSTONE, as above w/ a few thin shaly lenses (to 1mm thick)	0						
11			100						
11.7 205.8		SANDSTONE, as above except very soft	78					friable	
12									
12.6 204.9		SILTSTONE to VF SANDSTONE, slightly weathered, IOS common, occasional hard iron rich laminae, very soft to soft, dk yel orange	93	27	0.06			St. Lawrence Formation Lodi Member	
13.5 204.0		SILTSTONE and VF SST, gen fresh w/sl wx, dolomitic, shaly laminae, slightly fissile, soft to moderately hard w/very soft zones, very thin beds, dk yel orng to lt grn gry							
14		14.1 to 14.2 m - extremely soft 14.25 m - sm flat intraclasts (to 10 mm)							
14.3 203.2									
15		DOLOSTONE, sl wx, intraclasts and very thin beds of VF Sst, silty, occasional shale laminae, mottled, crossbedded, IOS, soft to moderately hard, dk yel orange to yel grey	92	84	0.09				
16									

(Continued Next Page)

Soil Class: DB Rock Class: NMW Edit: JLD Date: 7/26/95

MINNESOTA DEPARTMENT OF TRANSPORTATION - GEOTECHNICAL SECTION
LABORATORY LOG & TEST RESULTS - SUBSURFACE EXPLORATION

UNIQUE NUMBER 56327
SI Units



SHEET 3 of 7

Mn/DOT GEOTECHNICAL SECTION - LOG & TEST RESULTS

State Project 8217		Bridge No. or Job Desc. 82011	Trunk Highway/Location TH 36	Boring No. T-20		Ground Elev. 217.5	Code S			
DEPTH	Depth Elev.	Drilling Operation	Classification	Samp	SPT	MC (%)	COH (kPa)	δ (kN/m ³)	Soil	Other Tests Or Remarks
				Core	REC (%)	RQD (%)	ACL (m)	Core Breaks	Rock	Formation or Member
17	17.3									
17.3	200.3		SANDSTONE, fresh, VF grain, slightly glauconitic, siltstone laminae, soft, lt grn grey	100	85	0.08		8		
17.9	18-199.6		SANDSTONE and DOLOSTONE interbedded, sl wx, shaly laminae, very iron rich, occasional pits & vugs (to 20 mm), soft to moderately hard, mottled, crossbedded but becoming more laminar with depth, dk yel orange to moderate yel bwn	100	95	0.09		4		
19	19.4 to 19.7 m		- grey zone, mostly dolostone	91	61	0.04		9		
20	20.2							7		
20.2	197.3		DOLOSTONE, fresh, silty, vug (10 mm) and pyrite rare, moderately hard, lt grey	97	82	0.08		6		(Splitting Tensile Strength of Intact Rock Core specimens - ASTM D-3967)
21	21.3 to 21.8 m		- zone of shaly and sandy laminae					12		(Unconfined Compressive Strength of Intact Rock Core specimens - ASTM D-2938)
22	22.2 to 22.5 m		- zone of pits and vugs (to 30 mm), Sst intraclasts, and rubble w/ shaly laminae	99	70	0.06		7		Splitting Tensile Strength - 18140 kPa @ 23 m, air-dried sample
23	23.3 to 23.5 m		- zone of interbedded Sst, Siltstone, Dolo, and traces of Shale, very thin laminar bedding							Unconfined Compressive Strength - 54990 kPa @ 23.75 m, air-dried sample
24	24.0									

(Continued Next Page)

Soil Class: DB Rock Class: NMW Edit: JLD Date: 7/26/95

MINNESOTA DEPARTMENT OF TRANSPORTATION - GEOTECHNICAL SECTION
LABORATORY LOG & TEST RESULTS - SUBSURFACE EXPLORATION

UNIQUE NUMBER 56327
SI Units



Mn/DOT GEOTECHNICAL SECTION - LOG & TEST RESULTS

SHEET 4 of 7

State Project 8217		Bridge No. or Job Desc. 82011	Trunk Highway/Location TH 36	Boring No. T-20		Ground Elev. 217.5	Code S			
DEPTH	Depth	Drilling Operation	Classification	Samp	SPT	MC (%)	COH (kPa)	δ (kN/m ³)	Soil	Other Tests Or Remarks
	Elev.			Core G	REC (%)	RQD (%)	ACL (m)	Core Breaks	Rock	Formation or Member
193.5					100	91	0.05		6	Unconfined Compressive Strength - 39460 kPa @ 24.3 m-24.38 m, air-dried sample
25			DOLOSTONE and SILTSTONE very thinly interbedded w/ occasional sandstone, fresh, crossbedded and mottled w/ occasional zones of more laminar bedding, intraclasts common, occurrence of glauconite increasing with depth, moderately hard, grn gr to lt olive grn		100	77	0.04		9	
26									6	Unconfined Compressive Strength - 45780 kPa @ 26.11 m-26.19 m, air-dried sample
27					98	80	0.07		7	
27.4	190.1									
28			SANDSTONE, gen fresh w/ sl wx, fine to medium grain, silty, highly glauconitic, dolomitic, soft to moderately hard, gr green		99	80	0.05		10	Franconia Formation
29	29.1									
29.1	188.4		SANDSTONE, gen fresh w/ sl wx, fine grain, dolomitic, glauconitic, occasional very thin beds of dolostone, moderately hard, dk grn gr to dk yel bwn							
30					100	27	0.04		10	
30.7	186.8									
31			SANDSTONE dolomitic, to sandy DOLOSTONE, sl wx, fine grain, occasional pits and vugs (to 15 mm), some crossbedding and intraclasts, IOS common, soft to moderately hard, dk yel orange		93	79	0.07		7	Unconfined Compressive Strength - 9920 kPa @ 31.6 m-31.7 m, air-dried sample
31.6	185.9									
32										

(Continued Next Page)

Soil Class: DB Rock Class: NMW Edit: JLD Date: 7/26/95

MINNESOTA DEPARTMENT OF TRANSPORTATION - GEOTECHNICAL SECTION
LABORATORY LOG & TEST RESULTS - SUBSURFACE EXPLORATION

UNIQUE NUMBER 56327
SI Units



Mn/DOT GEOTECHNICAL SECTION - LOG & TEST RESULTS

SHEET 5 of 7

State Project 8217		Bridge No. or Job Desc. 82011	Trunk Highway/Location TH 36			Boring No. T-20		Ground Elev. 217.5	Code S	
DEPTH	Drilling Operation	Elev.	Classification	Samp	SPT	MC (%)	COH (kPa)	δ (kN/m ³)	Soil	Other Tests Or Remarks
				Core	REC (%)	ROD (%)	ACL (m)	Core Breaks	Rock	Formation or Member
			SANDSTONE, gen fresh w/ sl wx, VF grain, silty, some glauconite and IOS, intraclasts and very thin beds of silty dolostone, soft to moderately hard, yel grey					7		
32.6 185.0										
33			SANDSTONE, gen fresh w/ sl wx, fine grain, somewhat silty, dolomitic, soft to very soft, some pits and vugs (to 25 mm), occasional very thin beds of dolostone, grey orange		88	35	0.05		>15	
33.9 183.6	PD									
34			SANDSTONE, fresh, fine grain to silty, very dolomitic, glauconite rare, small zones and very thin beds of dolostone, moderately hard w/ very soft zones from 34.5-34.7 m and 35.0-35.1 m, very pale orange		95	53	0.08	8		Splitting Tensile Strength - 18140 kPa @ 34.5 m, air-dried sample
35			zone of extremely soft VF SST w/ very thin bed of soft siltstone (35.3 - 35.4 m)					10		Splitting Tensile Strength - 14170 kPa @ 34.6 m-34.62 m, air-dried sample
35.4 182.1										
36			SANDSTONE, gen fresh w/sl wx, F to VF grain, somewhat silty, dolomitic, glauconitic, occasional laminae of siltstone, soft to moderately hard w/ occasional very soft zones, slightly bioturbated, grey orange highly glauconitic w/sst intraclasts at 35.75m and 36.33m		95					Unconfined Compressive Strength - 12650 kPa @ 34.65 m-34.8 m, air-dried sample
36			very soft to extremely soft at 36.6-36.9m and 37.4m occasional small (2mm) rounded quartz sst intraclasts from 36.9 m							
37										
38			bedding becoming more laminar from 37.95 - 38.41 m					3		
38.4 179.1										
39			SANDSTONE, gen fresh w/ sl wx, fine to medium predominantly quartz grains, slightly dolomitic, glauconite rare, soft to very soft, yellowish grey		98	93	0.11		7	
39			very iron rich carbonate beds (40-100mm thick) at 38.6m, 38.9m, 39m and 39.3m, moderately hard, dk yel orange							
40			(Continued Next Page)							
										Soil Class: DB Rock Class: NMW Edit: JLD Date: 7/26/95

MINNESOTA DEPARTMENT OF TRANSPORTATION - GEOTECHNICAL SECTION
LABORATORY LOG & TEST RESULTS - SUBSURFACE EXPLORATION

UNIQUE NUMBER 56327
SI Units



Mn/DOT GEOTECHNICAL SECTION - LOG & TEST RESULTS

SHEET 6 of 7

State Project 8217		Bridge No. or Job Desc. 82011	Trunk Highway/Location TH 36			Boring No. T-20			Ground Elev. 217.5	Code S
DEPTH Elev.	Depth Drilling Operation		Classification	Samp	SPT	MC (%)	COH (kPa)	δ (kN/m ³)	Soil Rock	Other Tests Or Remarks
				Core C3	REC (%)	RQD (%)	ACL (m)	Core Breaks		
41			very thin bed of Dolo, grn gr, w/ pyrite rich Sst lamina, 40.74 - 40.77 m		93					Unconfined Compressive Strength - 8360 kPa @ 40.14 m-40.22 m, air-dried sample
42			becoming slightly glauconitic and occasional IOS, soft to very soft, lt olive grey		72					Splitting Tensile Strength - 1526 kPa @ 41.7 m- 41.76 m, air-dried sample
43										
43.7 173.8			SANDSTONE, fresh, fine grained, dolomitic, glauconitic, somewhat silty, moderately hard, mottled, greenish grey		96					
44			Becoming highly glauconitic, occasional pits (to 6 mm), pyrite rare							
45		PD	occasional very thin beds of soft siltstone and shale associated w/ zones of more laminar bedding		91					
46										
46.2 171.3			SANDSTONE, fresh, fine grained, occasional laminae of siltstone and sandy dolostone, glauconitic to highly glauconitic, some cross-bedding, soft to moderately hard, greyish green		96	40	0.06	11		
47										
48									14	Unconfined Compressive Strength - 7200 kPa @

(Continued Next Page)

Soil Class: DB Rock Class: NMW Edit: JLD Date: 7/26/95

MINNESOTA DEPARTMENT OF TRANSPORTATION - GEOTECHNICAL SECTION
LABORATORY LOG & TEST RESULTS - SUBSURFACE EXPLORATION



UNIQUE NUMBER 56327
SI Units

Mn/DOT GEOTECHNICAL SECTION - LOG & TEST RESULTS

SHEET 7 of 7

State Project 8217		Bridge No. or Job Desc. 82011	Trunk Highway/Location TH 36			Boring No. T-20			Ground Elev. 217.5	Code S
DEPTH	Depth	Drilling Operation	Classification	Samp	SPT	MC (%)	COH (kPa)	δ (kN/m ³)	Soil	Other Tests Or Remarks
	Elev.			Core	REC (%)	RQD (%)	ACL (m)	Core Breaks	Rock	Formation or Member
49	49.2 168.3		Siltstone and Shale laminae common from 48.0 to 48.3 m moderately hard and mottled from 48.4 m to bottom		87	68	0.05	9		45.59 m-47.67 m, air-dried sample
			Bottom of Hole - 49.2 m Water measurements taken while drilling are not conclusive							"

Soil Class: DB Rock Class: NMW Edit: JLD Date: 7/26/95

MINNESOTA DEPARTMENT OF TRANSPORTATION - GEOTECHNICAL SECTION

LABORATORY LOG & TEST RESULTS - SUBSURFACE EXPLORATION



UNIQUE NUMBER 56350
SI Units

Index Sheet Code 1.0m

MINNESOTA DEPARTMENT OF TRANSPORTATION - GEOTECHNICAL SECTION
LABORATORY LOG & TEST RESULTS - SUBSURFACE EXPLORATION



UNIQUE NUMBER 56350
SI Units

Mn/DOT GEOTECHNICAL SECTION - LOG & TEST RESULTS

SHEET 2 of 5

State Project 8217		Bridge No. or Job Desc. 82011	Trunk Highway/Location TH 36			Boring No. T-43		Ground Elev. 206.6	Code	
DEPTH	Depth	Drilling Operation	Classification	Samp	SPT	MC (%)	COH (kPa)	δ (kN/m ³)	Soil	Other Tests Or Remarks
	Elev.			Core	REC (%)	RQD (%)	ACL (m)	Core Breaks	Rock	Formation or Member
9	PD		org SiCL w/ 102 mm wood piece at 9.7 m, brn & wet				NSR			(UU Triaxial c - cohesion, Unconsolidated Undrained triaxial compression test.)
10	10.4				150			11.4		
10.4	196.2				127			12.5		%org-12 UU Triax c - 4.8 kPa Wet Density-12.2 kN/m ³
11	PD		org pl SiL w/ some wood at 12.2 m, dk brn & Vmoist							
12					125	2.9	12.7			%org-10
13					139		12.5			UU Triax c - 8.2 kPa Wet Density - 12.6 kN/m ³
14	14.1				139	0.5	12.6			UU Triax c - 6.7 kPa Wet Density - 12.0 kN/m ³
14	192.5				160	1.9	11.9			%org-12 UU Triax c - 8.2 kPa
15			org SiCL w/ "organic scum" to 15.2 m dk gray w/ lt brn to 15.2 m, dk gray-brn 15.2-15.8 m moist to 14.6 m, Vmoist 14.6-15.2 m, Vwet 15.2-15.7 m, wet 15.7-15.8 m		134	2.9	12.6			
15					156					
16	15.8									

(Continued Next Page)

Soil Class: DB Rock Class: NMW Edit: JLD Date: 11/14/95

MINNESOTA DEPARTMENT OF TRANSPORTATION - GEOTECHNICAL SECTION
LABORATORY LOG & TEST RESULTS - SUBSURFACE EXPLORATION

UNIQUE NUMBER 56350
SI Units



Mn/DOT GEOTECHNICAL SECTION - LOG & TEST RESULTS

SHEET 3 of 5

State Project 8217		Bridge No. or Job Desc. 82011	Trunk Highway/Location TH 36			Boring No. T-43		Ground Elev. 206.6	Code	
DEPTH	Depth	Drilling Operation	Classification	Samp	SPT	MC (%)	COH (kPa)	γ (kN/m ³)	Soil	Other Tests Or Remarks
	Elev.			Core	REC (%)	RQD (%)	ACL (m)	Core Breaks	Rock	Formation or Member
190.7			crumbly org SiCL, dk brn & wet		190	4.3	12.0			UU Triax c - 11.8 kPa Wet Density - 12.1 kN/m ³
16.5										
190.1					172	4.8	12.1			UU Triax c - 13.2 kPa Wet Density - 12.4 kN/m ³
17								NSR		
18			org SiCL, dk brn moist to 17.1 m, Vwet 17.1-18.1 m, moist 18.1-20.2 m							
19					165					
20					138					
20.2					153					
186.4			slorg LFS, brn & sat		134	8.6	13.1			UU Triax c - 14.6 kPa Wet Density - 12.9 kN/m ³
20.6					34	5.3	18.1			UU Triax c - 23.2 kPa Wet Density - 12.3 kN/m ³
186.0					34					UU Triax c - 16.0 kPa Wet Density - 12.5 kN/m ³
21					34					UU Triax c - 12.4 kPa Wet Density - 16.2 kN/m ³
22			S w/ shells, some LS layers; brn & sat		33					UU Triax c - 18.2 kPa Wet Density - 17.2 kN/m ³
22.6		PD								
184.0										
23										
		X	Sst S w/sst chips, F to medium grained, glauconitic, silty, dolomitic, gray orange		90/.4	20				
23.7		PD			100/.4	NSR				Driller's Notes: Small flowing artesian at 23.3 m
182.8										
24										

(Continued Next Page)

Soil Class: DB Rock Class: NMW Edit: JLD Date: 11/14/95

MINNESOTA DEPARTMENT OF TRANSPORTATION - GEOTECHNICAL SECTION
LABORATORY LOG & TEST RESULTS - SUBSURFACE EXPLORATION



UNIQUE NUMBER 56350
SI Units

Mn/DOT GEOTECHNICAL SECTION - LOG & TEST RESULTS

SHEET 4 of 5

State Project 8217		Bridge No. or Job Desc. 82011	Trunk Highway/Location TH 36			Boring No. T-43		Ground Elev. 206.6	Code	
DEPTH	Depth	Drilling Operation	Classification	Samp	SPT	MC (%)	COH (kPa)	δ (kN/m ³)	Soil	Other Tests Or Remarks
	Elev.			Core	REC (%)	RQD (%)	ACL (m)	Core Breaks	Rock	Formation or Member
24.5	182.0		Sst and Sst S, F grained, extremely soft, lt gry (probably not in place) Top of Bedrock	65	0			friable		
25			SANDSTONE, gen fresh w/ sl wx, F grained, very slightly dolomitic and glauconitic, very soft, lt gry extremely soft zones at 24.7m and 25.9m	36	0				(Unconfined Compressive Strength of Intact Rock Core specimens - ASTM D-2938.)	Franconia Formation
26								friable		Mazomanie Member
27	27.2			50	10	0.05			(Splitting Tensile Strength of Intact rock Core specimens - ASTM D-3967)	
28	179.3		SANDSTONE, gen fresh w/sl wx, VF to F grained, silty, dolomitic, slightly glauconitic, very soft to soft, yel orange					7		Splitting Tensile Strength - 1020 kPa @ 27.74 m
			becoming more dolomitic and moderately hard from 28.4m	86	57	0.07		rubble		
29		PD						5		
29.9	176.7								Unconfined Compressive Strength - 2860 kPa, representing 28.76 m-28.85 m, @ 12.7% moisture.	
30									(medium hard drilling started at 29 m)	
31			SANDSTONE, gen fresh w/ sl wx, F grained, highly glauconitic, dolomitic, minor siltstone and shale, predominantly very thin laminar bedding, soft to moderately hard, grn	68	0			> 15		Reno Member
32								> 15		

(Continued Next Page)

Soil Class: DB Rock Class: NMW Edit: JLD Date: 11/14/95

MINNESOTA DEPARTMENT OF TRANSPORTATION - GEOTECHNICAL SECTION
LABORATORY LOG & TEST RESULTS - SUBSURFACE EXPLORATION



UNIQUE NUMBER 56350
SI Units

Mn/DOT GEOTECHNICAL SECTION - LOG & TEST RESULTS

SHEET 5 of 5

State Project 8217		Bridge No. or Job Desc. 82011	Trunk Highway/Location TH 36			Boring No. T-43		Ground Elev. 206.6	Code	
DEPTH	Depth	Drilling Operation	Classification	Samp	SPT	MC (%)	COH (kPa)	γ (kN/m ³)	Soil	Other Tests Or Remarks
	Elev.			Core	REC (%)	RQD (%)	ACL (m)	Core Breaks	Rock	Formation or Member
33	33.2	(as above)			92	14	0.03	> 15		
	173.3		Bottom of Hole - 33.2 m							

Soil Class: DB Rock Class: NMW Edit: JLD Date: 11/14/95

MINNESOTA DEPARTMENT OF TRANSPORTATION - GEOTECHNICAL SECTION
LABORATORY LOG & TEST RESULTS - SUBSURFACE EXPLORATION



UNIQUE NUMBER 56355
SI Units

Mn/DOT GEOTECHNICAL SECTION - LOG & TEST RESULTS

SHEET 2 of 6

State Project 8217		Bridge No. or Job Desc. 82011	Trunk Highway/Location TH 36	Boring No. T-48		Ground Elev. 207.4	Code S			
DEPTH	Depth	Drilling Operation	Classification	Samp	SPT	MC (%)	COH (kPa)	δ (kN/m ³)	Soil	Other Tests Or Remarks
	Elev.			Core	REC (%)	RQD (%)	ACL (m)	Core Breaks	Rock	Formation or Member
			(See previous page)							
9	9.0 198.4		Bottom of River - 9.0 m							
9.8 197.7		PD	Driller's Notes: soft & sat							
10										
11										
12			peaty pl SiL w/ some pieces of wood, dk brn & Vwet							
13										
14										
14.2 193.2		PD								
15			(See next page)							
16		PD								

(Continued Next Page)

Soil Class: DB Rock Class: NMW Edit: JLD Date: 11/14/95

MINNESOTA DEPARTMENT OF TRANSPORTATION - GEOTECHNICAL SECTION
LABORATORY LOG & TEST RESULTS - SUBSURFACE EXPLORATION



UNIQUE NUMBER 56355
SI Units

Mn/DOT GEOTECHNICAL SECTION - LOG & TEST RESULTS

SHEET 3 of 6

**MINNESOTA DEPARTMENT OF TRANSPORTATION - GEOTECHNICAL SECTION
LABORATORY LOG & TEST RESULTS - SUBSURFACE EXPLORATION**



UNIQUE NUMBER 56355
SI Units

Mn/DOT GEOTECHNICAL SECTION - LOG & TEST RESULTS

SHEET 4 of 6

MINNESOTA DEPARTMENT OF TRANSPORTATION - GEOTECHNICAL SECTION

LABORATORY LOG & TEST RESULTS - SUBSURFACE EXPLORATION

UNIQUE NUMBER 56355
SI Units



Mn/DOT GEOTECHNICAL SECTION - LOG & TEST RESULTS

SHEET 5 of 6

MINNESOTA DEPARTMENT OF TRANSPORTATION - GEOTECHNICAL SECTION
LABORATORY LOG & TEST RESULTS - SUBSURFACE EXPLORATION

UNIQUE NUMBER 56355
SI Units



Mn/DOT GEOTECHNICAL SECTION - LOG & TEST RESULTS

SHEET 6 of 6

State Project 8217		Bridge No. or Job Desc. 82011	Trunk Highway/Location TH 36			Boring No. T-48		Ground Elev. 207.4	Code S	
DEPTH	Depth	Drilling Operation	Classification	Sample	SPT	MC (%)	COH (kPa)	γ (kN/m ³)	Soil	Other Tests Or Remarks
	Elev.			Core	REC (%)	RQD (%)	ACL (m)	Core Breaks	Rock	Formation or Member
			SANDSTONE, sl wx, F grained, dolomitic, slightly glauconitic, soft, very thin bedding, some very soft shale laminae, yel gry, thin iron rich beds, dk yel orange							
41	41.0 166.5								15	
42			SANDSTONE, fresh, VF to F grained, moderate to highly glauconitic, pyrite nodules rare, moderately hard, grn occasional very soft shale laminae to 42.4m soft shale from 42.1m - 42.2m		96	37	0.04		13	Reno Member
43			low angle joint at 43m shows possible evidence of faulting		100	27	0.03		5	
44					100	100	0.12		5	
44.9 162.5			Bottom of Hole - 44.9 m		100	97	0.15		0	

Soil Class: DB Rock Class: NMW Edit: JLD Date: 11/14/95